

Archiv EURO MEDICA



2-2014

H III H
EUROPÄISCHE
WISSENSCHAFTLICHE
GESELLSCHAFT

EDITORIAL

Dear Colleagues!

In your hands, you are holding the second volume of the journal for 2014. This year we have suffered a great loss: Doctor Wolfgang Fischer — our colleague and friend, who has done a lot for the development of the journal and medical forum "Euromedica Hannover", is gone. Thanks to Dr. Fischer our journal not only proved its endurance and substantiality but also was strongly transformed. These changes were made to its structure, strengthening the editorial board, topics and the design.

As a next stage of development, we are planning to set up a separate website of the journal as well as its subscription in a quotation index.

A real problem of the world scientific experience that the principles of evidence-based medicine widely used in the clinical practice of Western countries should find an honourable place in the world medicine. Therefore, a priority direction of our journal becomes acquaintance with the world tendencies and their evaluation from the point of view of the evidence based medicine.

To achieve this we welcome specialists from various countries to cooperate, thus building a joint intellectual forum for doctors with different specializations and origins on the pages of the journal and in the frame of our medical event.

During the last years, the journal has affirmed itself as a truly international edition: it comprises works of the authors from Germany, Russia, Ukraine, the USA, Lithuania, Kazakhstan, Armenia and Tajikistan, which opens up perspectives for additional professional and social competence of specialists and our authors.

We hope on further fruitful cooperation and wish you interesting and productive reading!

Editor-in-Chief

*Dr. med. Georg Tyminski
Dr. med. Wolfgang Fischer*

Associate Editors

*Prof. Khalil Galymzyanov
Dr. med. Siegfried Schink
Prof. Dr. Jörg Schulz*

Editorial Advisory Board

*Prof. Vadim Astashev
Prof. Tatiana Belousova
Prof. Stephan Heymann
Prof. Habibullo Ibodov
Prof. Gayane Khachatryan
Prof. Sergey Kolbasnikov
Prof. Vladimir Krestyashin
Prof. Ants Peetsalu
Prof. Urij Peresta
Prof. Natalia Shnayder
Prof. Rudolf Yuy Tsun-Shu
Dr. Will Nelson Vance
Prof. Mikhail Zaraiski
Prof. Aleksei Zhidovinov*

ARCHIV EUROMEDICA
ISSN 2193-3863

Disclaimer

Europäische Wissenschaftliche
Gesellschaft e.V. Hannover

Sutelstr. 50A
30659 Hannover
Deutschland

Tel. 49(0)5113908088
Fax 49(0)511 3906454

Vorstand Dr. G. Tyminski, Vorsitzender
Eingetragen ins Vereinsregister
am Amtsgericht Hannover: VR 7957

Design & layout by
Tří barvy, s.r.o.
Mariánské Lázně,
Česká Republika

Printed by
Tiskárna POLYGRAF, s.r.o.
Turnov, Česká Republika
www.tisk.cz

C O N T E N T S

<p><i>I.F. Barinsky</i> LEUKOCYTIC CULTURES IN ISOLATION AND STUDY OF VIRUSES AT ACUTE LEUCOSIS AND CHRONIC MYELOEUCOSIS IN HUMANS 2</p> <p><i>Dr. S. Edeling, S. Pokupic</i> INTRAKORPORALE HARNABLEITUNG BEI DER ROBOTERASSISTIERTEN RADIKALEN ZYSTEKTOMIE (RARC) 7</p> <p><i>S.V. Dmitrienko, D.A. Domenyuk, A.S. Kochkonyan, A.G. Karslieva, D.S. Dmitrienko</i></p> <p>INTERRELATION BETWEEN SAGITTAL AND TRANSVERSAL SIZES IN FORM VARIATIONS OF MAXILLARY DENTAL ARCHES 10</p> <p><i>S.V. Dmitrienko, D.A. Domenyuk, A.S. Kochkonyan, A.G. Karslieva, D.S. Dmitrienko</i></p> <p>MODERN CLASSIFICATION OF DENTAL ARCHES 14</p> <p><i>G.H. Khachatryan, N.S. Qamalyan, A.G. Karapetyan, K.V. Khondkaryan</i></p> <p>COMPARATIVE CHARACTERISTICS OF RADIODIAGNOSTICS IN CARDIOLOGY AND CARDIOSURGERY 17</p> <p><i>D.U. Kenessary, U.I. Kenessariyev, A.U. Kenessary</i></p> <p>HUMAN HEALTH COST OF HYDROGEN SULFIDE AIR POLLUTION FROM AN OIL AND GAS FIELD 22</p> <p><i>R. Klopp, W. Niemer, J. Schulz, O. Marksteder, N. Abdulkerimova</i></p> <p>UNTERSUCHUNGEN ZU WIRKUNGEN AD- JUVANTER BEHANDLUNGSMÄßNAHMEN (BIOKORREKTUR UND PHYSIKALISCHE GEFÄßTHERAPIE) AUF DEN FUNKTIONS- ZUSTAND DER MIKROZIRKULATION BEI PATIENTEN MIT DIABETES MELLITUS TYP II. ERGEBNISSE EINER PLACEBOKONTROL- LIERTEN STUDIE 27</p>	<p><i>A.G. Loginov, V.N. Gorchakov</i></p> <p>EFFECT OF NICKELIDE TITANIUM IMPLANT ON THE DEHYDRONENASE ACTIVITY OF LYMPHOCYTES OF REGIONAL LYMPHATIC NODE 38</p> <p><i>I.M. Lopanova, A.N. Nikolaeva, N.L. Khmarhaya</i></p> <p>MEDICAL NURSE STAFF EMOTIONAL INTELLIGENCE QUOTIENT STUDY 42</p> <p><i>O.V. Marzoeva, E.D. Bespalova, R.M. Gasanova, M.N. Bartagova, O.A. Pitirimova</i></p> <p>EVALUATION OF BLOOD FLOW IN THE MEDIAL CEREBRAL ARTERY IN FETUSES WITH HYPOPLASTIC LEFT HEART SYNDROME 44</p> <p><i>V.A. Myshkin, D.A. Enikeyev, D.V. Srubilin</i></p> <p>ANTITOXIC PROTECTION OF THE BODY USING ANTIDOTES, ANTIOXIDANTS AND OTHER MEMBRANE PROTECTORS 50</p> <p><i>N.S. Qamalyan, G.H. Khachatryan, A.G. Karapetyan, K.V. Khondkaryan</i></p> <p>COMPLEX RADIATION DIAGNOSTICS OF MYOCARDIAL PERFUSION IN CIVIL AVIATION FLIGHT PERSONNEL WITH THE EXPERIENCE ABOVE 20 YEARS 56</p> <p><i>G.A. Tussupbekova, S.T. Tuleukhanov, N.T. Ablaikhanova, E.N. Kuandykov</i></p> <p>EPIDEMIOLOGICAL ASPECTS OF THE PUBLIC HEALTH IN THE ZONE OF ECOLOGICAL DISASTER OF THE ARAL SEA REGION 59</p> <p><i>E.A. Shliakhtunou</i></p> <p>EXPRESSION OF GLYCERALDEHYDE-3- PHOSPHATE DEHYDROGENASE IN THE TUMOR TISSUE OF BREAST CANCERS 62</p>	<p><i>N. Shnayder, T. Popova, M. Petrova, T. Nikolaeva, E. Chesheiko, S. Dyuzhakov, A. Semenov, E. Kantimirova, A. Dyuzhakova, K. Gazenkampf, Yu. Panina</i></p> <p>DIAGNOSIS OF SENSORY-PREDOMINANT CHRONIC INFLAMMATORY DEMYELINAT- ING POLYNEUROPATHY: THE EXPERIENCE OF OUR CLINIC 66</p> <p><i>W.N. Vance</i></p> <p>MIKTIONSSTÖRUNGEN BEI M. PARKINSON 72</p> <p><i>A.A. Zhidovinov, P.E. Permjakov, A.V. Pirogov</i></p> <p>ENDOSCOPIC CORRECTION OF THE MOUTH OF THE URETER WHEN VESICOURETERAL- REFLUX IN CHILDREN 79</p> <p><i>A.P. Chuprikov, A.M. Vayserman, L.V. Mekhova, E.S. Galchin</i></p> <p>DEVIATIONS OF THE SEASONAL PREVALENCE OF BIRTHS IN THE GENERAL POPULATION AND AT CHILDREN WITH AUTISM 83</p> <p><i>E.G. Fokina</i></p> <p>LABORATORY ESSENCE OF ADAPTIVE CHANGES ERYSIPelas ON THE FACE 83</p> <p><i>V.A. Kartashov, L.G. Sidelnikova, G.P. Chepurnaya, L.V. Chernova</i></p> <p>EXTRAKTIONSUNTERSUCHUNG VON EINIGEN ANTIPSYCHOTISCHEN ARZNAIST- OFFEN UND SCHLAFMITTELN 84</p> <p><i>A. Korchounov</i></p> <p>BEWEGUNGSREGULATION BEI GESENDET UND IHRE STÖRUNGEN BEIM PARKINSON 85</p> <p><i>A.N. Serkova, N.V. Glazova</i></p> <p>THE NANOSTRUCTURED MEDICINES IN THE FORM OF GEL AND CREAM INCLUDING THE PEROXIDASE OF THE BLACK RADISH 86</p> <p>A TRIBUTE TO DR. MED. WOLFGANG FISCHER 88</p>
--	--	---

LEUKOCYTIC CULTURES IN ISOLATION AND STUDY OF VIRUSES AT ACUTE LEUCOSIS AND CHRONIC MYELOLEUCOSIS IN HUMANS

I.F. Barinsky MD

D.Ivanovski Institute of Virology, Moscow, Russia

INTRODUCTION

Previously, human leucocyte cultures derived from the blood of healthy donors stimulated with PHA were successfully used for isolation of human hepatitis C virus from the blood of patients [1]. In the present study, the same cultures were used for isolation and cultivation of oncoviruses at acute leukosis and chronic myeloleukosis. This work was carried out in collaboration with A.K. Shubladze, E.P. Ugriumov, A.F. Bocharov.

MATERIALS AND METHODS

The method of *cultured leukocytes* was based on the technique by Moorhead et al. [see in refs. [1, 2]]. Venous blood was collected into sterile tubes containing 1 or 2 drops of concentrated heparin. Blood samples were centrifuged at 1000 rpm 10 min or left for 18 hrs at 40°C. The plasma was removed, and the leukocyte film was collected off the surface of erythrocytes. Leukocytes were then suspended in cultural medium 199 containing 25–30% of the autologous plasma to a final concentration of 2–3 or 6–7 million cells per 1 ml. An equal amount of leukocytes from healthy donors was added followed by PHA to a final concentration of 0.1–0.2 mg per 10 ml of cell suspension. The cells were incubated in an atmosphere with 2.5–5.0 CO₂ at 37°C. For a long-term culturing of leukocytes from patients with leucosis, leukocytes from healthy donors and PHA were not added.

For EM studies, cells were taken off the glass mechanically or with versene solution and washed off by centrifuging in medium 199 (1500 rpm). After that cells were fixed either with 1.6% glutaraldehyde for 1 hr followed by 1% osmium at 40°C for 45 min, or with 3% glutaraldehyde in 0.1 M cacodylate buffer (pH 7.2). (Osmium fixator was prepared in acetate-veronal buffer, pH 7.2) [1, 2]. Slices were prepared using LKB-8800 A microtome and contrasted with 1% uranyl acetate in 70% methanol for 15 min at room temperature followed by 1.5 % lead citrate for 10 min at room temperature. For negative contrasting, concentrated virus was placed on a net with a formvar underlayer dusted with coal and exposed to electric field. Con-



Igor F. Barinsky
Chief of the lab of
comparative virology

trasting was achieved by 3% phosphone-tungsten acid (pH 7.2). A 5EM-7A microscope was used. The density of the oncovirus was defined in a linear density gradient sucrose solutions [2, 3, 4].

The virus activity was measured in the reverse transcriptase (RT) assay by Spiegelman et al. [2, 4]. The proteins of the leucosis-like virus were fingerprinted [1, 4]. In serological studies, a rabbit serum against the virus isolated from leukocytes of a chronic myeloleukosis donor was used [2, 3, 4, 5].

An indirect immunofluorescence on blood or bone marrow smears was used. A total of 101 samples of bone marrow from patients were studied [1, 2, 3, 4]. Patients were diagnosed based on the clinical survey data and the results of morphologic research of blood and bone marrow samples.

RESULTS

The oncovirus was isolated through cocultivation of short-living PHA-stimulated leukocytes from patients with acute leucosis and from healthy donors. The virus was passaged in PHA-stimulated cultured leukocytes from healthy donors. For passage of the isolated virus, healthy leukocytes were inoculated before adding PHA. For the inoculate, destroyed infected leukocytes suspension free from cell debris, was used. For passage of the oncovirus isolated from long-living cultures from patients with chronic myeloleukosis, primary human embryo fibroblasts and human embryo kidney cells were used. The clarified cultural suspension from the previous passage was used inoculate for the next passage.

The comparative study of the two types of leukocyte cultures from leucosis patients (short-living

PHA-stimulated and long-living) showed an extreme difficulty of isolation and culturing of the human leucosis agent. In our opinion, use of primary leukocytes is a helpful approach to solve this problem. Leukocytes upon stimulation by PHA transform into blastocytes, which produce morphologically formed biologically active virus passaged on in cultured PHA-stimulated leukocytes.

Another approach is obtaining passageable lymphoblastoid cultures from white elements of the peripheral blood from leucosis patients. From patients with acute leucosis, we isolated three strains of the virus named 'leukocytic human leucosis virus'. In EM studies of ultrathin slices, C and A types particles typical for oncoviruses in size and structure were observed over 15 passages. Particles of the same types were also detected in the cultural fluid and infected leukocytes homogenates (Fig. 1). In control PHA-stimulated leukocyte cultures, no viral or virus-like particles were detected. The isolated leukocyte leucosis virus strains proved apathogenic for laboratory animals and chicken embryos and did not show cytopathic activity after inoculation of various primary and pasaged cultures. They did not cause chromosome alterations in infected leukocytes, but in a number of cases they stimulated the mitotic activity of the leukocytes, which was the direct indication of the presence of the virus. Leukocytic leucosis virus is instable to high temperature and is completely inactivated with ether. Its buoyant density is 1.16 g/cm^3 [2, 4, 5]. The reverse transcriptase activity of the virus was shown by using exo- and endogenous templates, the latter being the virion RNA with a sedimentation constant of 70 S. Similar viral particles were detected also in the cultural fluid.

The obtained results were used in our further studies on etiopathogenesis of human leucosis. We attempted to derive passageable cell lines from the blood of leucosis patients whose cells would contain morphologically formed oncovirus. Out of 74 assays conducted, only 5 cases proved successful. Those cells were from a patient with chronic myeloleucosis [3]. The observation showed that only few cells or groups of cells preserved vitality and attached to the glass (or plastic) as transparent cells with protrusions. Besides, some cells in the cultures had rounded shape. In the process of culturing they might enlarge transforming into giant cells with perinuclear graining. In some cases, giant and polynuclear cells formed clusters, from which cells with protrusions stemmed and that event was a good prognostic feature. The cultures began growing as cells with protrusions forming first foci (islets), then colonies followed by a mololayer. The histological studies showed that cultures were made up of large cells with big oval nuclei containing a few visible

nucleoli with a thin cytoplasm, sometimes vacuolized. The cultures metabolized actively, acidifying the medium rapidly. Cells of some patients were passaged for as long as 7 months [3]. Ultrathin slices of the cultured cells in EM studies revealed viral particles of type C with characteristic morphology. Particles were spheric or ellipsoid in shape, 87 to 130 nm in diameter, with a 65 to 70 nm nucleoid. Type C particles were observed in EPR channels and intracellular space (Fig. 2). We did not observe big clusters of particles. The characteristic budding of virions occurred on the plasma membrane or inside vacuoles formed by enlarges sites of the EPR. The cells looked viable and possessed all the typical organoids. The cytoplasm was partially vacuolized.

Thus using long-lived leukocyte cultures we showed that cultured cells contained oncovirus-like particles even without PHA stimulation.

We paid a special attention to the leukocyte leucosis virus as its isolation and passageing were based on use of human leukocytes and serum only, so contamination with any bovine oncoviruses from bovine serum was excluded. As it was shown, the oncovirus

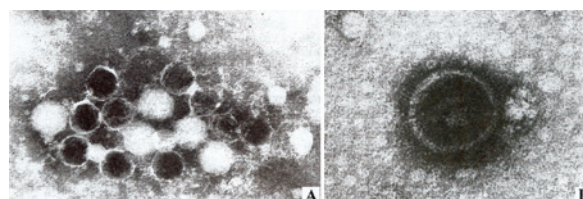


Fig. 1. Leukocytic leucosis virus (oncovirus type C) isolated in human leukocyte culture. Negative contrasting. A – multiple particles in a PHA-stimulated culture. B – single particle. $\times 100,000$



Fig. 2. Oncovirus type C in intracellular space and budding off cells. Leukocytic culture from a chronic myeloleucosis patient. $\times 250,000$

from leucosis patients was propagated in the leukocytes from healthy donors.

Human embryo fibroblasts and human embryo kidney cells were used in further passageing of the oncovirus. The virus' capability to replicate in primary human embryo cell subcultures was studied by radio-isotopes and EM. In 6 studied cultural fluid samples an RNAase-resistant fraction labeled with ^{3}H -uridine was detected in the density range of $1.15\text{--}1.18 \text{ g/cm}^3$, which corresponds to the density of the known oncoviruses. Such particles did not replicate in the presence of actinomycin D and were absent from non-inoculated control leukocyte cultures (Fig. 3).

In the cytoplasm of inoculated cells studied by EM, osmophilic clusters of fibrillar and membrane structures contained viral particles of type A with a diameter of 87 nm (nucleoids 45 nm). Virions of type C were also detected budding from the cell membrane. Some type C particles were found outside cells. Inside cells, condensed mitochondrial matrix and enlarged lamellar complex were observed [1, 2, 3]. RNA extracted from particles of 1.16 g/cm^3 was analysed by centrifuging in sucrose gradient [1, 2, 4, 5]. It is a 70 S molecule characteristic for oncoviruses. A reverse transcriptase assay detected 70 S RNA molecules marked with small fragments of newly synthesized DNA. In non-inoculated cultures, such structures were never found.

Long-living cells from 5 chronic myeloleucosis patients also supported replication of the oncovirus. Cells that began growing into a culture were the most likely producers of the virus. It is remarkable that the progeny of those cells preserved virus-producing capacity. Type C virions formed on the outer cytoplasm membrane, occurred outside the cells and had centered optically dense nucleoids. Type A particles were found inside the cells in fibrillar osmophilic clusters. Viral particles synthesized after inoculation of embryonic cells also had a buoyant density of 1.16 g/cm^3 [1]. The active reproduction of this virus in human embryonic cells did not cause either transformation or cytoplasmic changes in the clusters.

In the next series of experiments, we studied the structure of the oncovirus and compared it with other mammalian oncoviruses. The previously described technique Gautsch et al., 1978 [4, 6] allows to study individual protein structures, e.g. the major inner virion protein product of the gag gene. This protein accounts for roughly 25 % of the total virion proteins of oncoviruses, so it can be easily obtained by PAAGE. The peptide mapping of it is very informative for typing of novel isolates as has been shown in a number of cases [2, 3, 4, 6].

On Figure 4, the main proteins of the virus isolated form leucosis patients is presented. (The virus was concentrated from 400 ml of cultural fluid by cen-

trifuging followed by purification in sucrose density gradient). After PAAGE the proteins p15, p24 and gp70 characteristic for mammalian oncoviruses can be clearly seen. The major inner p24 protein was studied in collaboration with J. Elder, J. Gautsch and R. Lerner from the Oncovirus Lab, Scripps Institute, San Diego, CA. The p24-containing band was cut out of the slab, iodated with NaI125 and treated with either trypsin or chymotrypsin. The obtained polypeptides were separated by two dimensional elecrophoresis on cellulose sheets [2, 4]. The migration pattern of the obtained peptides differed from those obtained previously for p24 of the all known oncoviruses (Fig. 5).

The further concentration and purification of the virus allowed to use it in experiments. The specificity of the isolated virus was studied using immunomorphological and serological approaches. Ouchterloni gel precipitation was applied initially. Hyperimmune sera against (i) mouse leucosis virus, (ii) feline leukemia virus and (iii) type D virus from HE-p2 cells did not give any precipitation. Out of 12 sera from rabbits immunized with purified virus, only two contained specific antibodies. This fact indicated to a low antigenicity of the virus. In further studies by IF these sera were used in a 1:4 dilution. The immune rabbit sera preliminary were adsorbed with human (healthy donors) and bovine sera in order to get rid of non-specific rabbit antibodies against serum components.

Human embryo fibroblasts infected with leukocytic leucosis virus, showed a cytoplasmic fluorescence for 24 hrs p.i. onwards. First, the fluorescence granular, later it grew confluent. The dynamics and morphology of the fluorescence corresponded to the data obtained for the other vertebrate oncoviruses [2, 3, 4, 5].

After these experiments, the immune rabbit sera were used to survey of smears of bone marrow and blood autopsies from leucosis patients. 73 individuals were surveyed. A specific fluorescence of the bone marrow cells cytoplasm analogous to that of the inoculated fibroblast cultures was detected in 19 out of 31 patients with various forms of leucosis and in 9 of 42 control group individuals. The difference was statistically highly reliable ($p < 0.01$).

The cytoplasmic fluorescence was observed in 15 out of 25 cases of acute leucosis and in 4 out of 6 cases of chronical myeloleucosis. The control group consisted of 42 patients with so called 'border conditions': plasmacytosis, reticulosclerodermia, myelomice disease, Werlhof disease and others. Only 1 person was healthy donor of the bone marrow sample.

The blood samples studied from 70 of the total of the 73. Fluorescence of the leucocyte cytoplasm in the smears was detected in 10 out of 12 patients with acute and chronic forms of leucosis and in 5 out

of 58 control group individuals: 2 blood donors and 3 patients with rheumatoid arthritis. The difference between the two groups was statistically reliable ($p < 0.01$). The results of the conducted survey are presented in Table 1.

The next step of our study was examination of the virus in complement fixation test (CFT) for detection of antibodies against this virus in human blood sera.

In total, 128 blood sera from healthy donors and 74 sera from patients with acute and chronic myeloleucosis were surveyed by CFT with leukocytic leucosis viral antigen. The results are shown in Table 2. These results indicate that antibodies against the studied virus widely occur in sera of leucosis patients. The specific fluorescence of the cell cytoplasm and the nature of the fluorescence agree with the data on the other oncoviruses. This similarity was observed in both bone marrow and blood smears from patients with acute leucosis and chronic myeloleucosis as well as from some patients with reticulosclerodermia, myelom disease, rheumatoid arthritis and even some clinically healthy persons. The observed similarity appears fairly explicable given the wide spread of oncoviruses in humans and animals.

DISCUSSION

The conducted research has shown a successful application of cultured leukocytes from human blood for isolation of oncoviruses from patients with acute leucosis and myeloleucosis alike. Our data suggest that the two approaches in studying the viral nature of human leucosis, (i) primary PHA-stimulated leukocyte cultures for isolation of new viral strains and (ii) passaged lymphoblastoid cultures from white blood of patients for studies of virus persistence in the cells in the long run. These two approaches supplement rather than exclude each other.

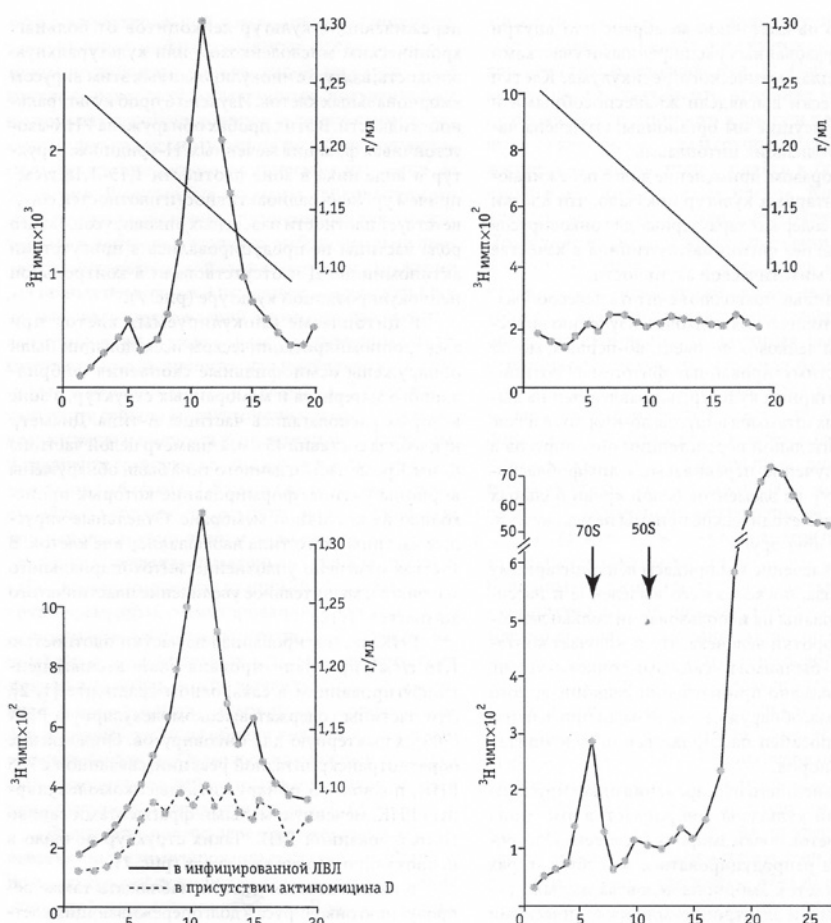


Fig. 3. Buoyant density of leukocytic leucosis virus and its RNA in sucrose gradient
A – Density of the oncavirus under study in the sucrose gradient; B – Same, uninfected culture; C – Oncovirus under study, grown in the presence of actinomycin D in the cultural medium: broken line; Same virus, grown in the absence of actinomycin D in the cultural medium: solid line; D – Density of the viral RNA in the sucrose gradient

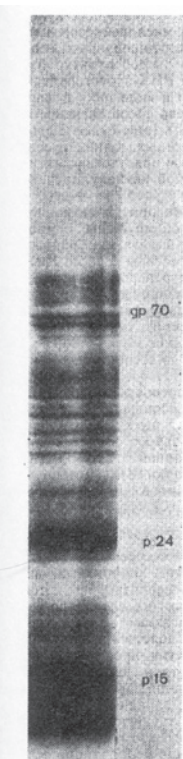


Fig. 4. Proteins of the oncovirus isolated from a leucosis patient, studied in PAAGE

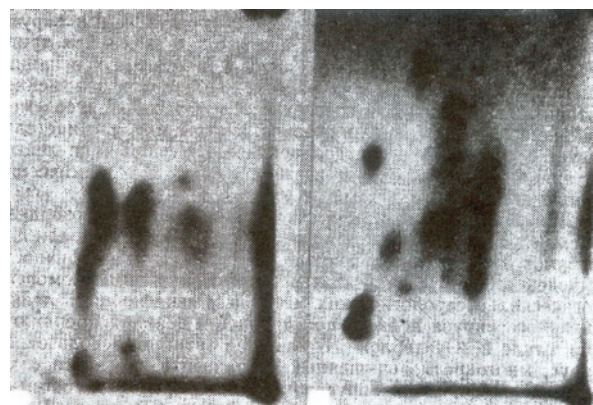


Fig. 5. Tryptic (A) and chemotryptic (B) peptides of the oncovirus p24 protein

Table 1. Detection of the oncoviral antigen in the bone marrow and blood smears using the immunofluorescence technique

Source	Patients with leucosis			Control group		Reliability of the difference
	Acute leucosis	Chronic myeloleucosis	Chronic lympholeucosis	Healthy donors	Patients with other conditions	
Bone marrow smears	15/25	4/6	0/1	0/1	9/41	$\chi^2=11.119$ ($p<0.01$)
Total	19/32			9/42		
Blood smears	2/2	5/6	3/4	2/28	3/30	$\chi^2=24.140$ ($p<0.01$)
Total	10/12			5/58		

Fractions: the numerator is the number of positive samples, the denominator is the number of samples studied.

Table 2. Antibodies against human embryo fibroblasts infected with the virus under study in blood sera from leucosis patients and healthy donors

Serum samples	Studied	Antibodies titers in CFT with the studied oncovirus antigen				Total and % of the positive samples	Reliability of the difference
		Negative	1:10	1:20	1:40		
Leucosis patients	74	29	12	24	9	45(68.81%)	$p<0.01$
Healthy donors	128	104	10	4	10	24(18.75%)	$p<0.01$

CFT: Complement fixation test.

The leukocytic cultures technique proved efficient in isolation of oncoviruses. Passageing of the isolated viruses in leukocytic cultures as well as in primary fibroblasts and embryo kidney cells allows to grow the virus in amounts sufficient for further studies.

In our study, both immunologic techniques, immunofluorescence and complement fixation, detected the examined viral antigen or antibodies against it reliably more frequently in samples from leucosis cases compared with samples from control groups. This fact is a strong indication to the etiologic role of the studied virus in human leucosis [2, 4, 5, 7].

REFERENCES

1. BARINSKY IF, SHUBLADZE AK. Leukocytic cultures in virological research. Moscow: Medicina; 1980.
2. BARINSKY IF, SHUBLADZE AK, BOCHAROV AF. Leukocytic human leucosis virus. Voprosy Virusologii (Problems of virology) 1970; 5:729–730.
3. UGRUMOV EP, FILATOV FP, DELIMBETOVA GA, BARINSKY IF. Isolation of virus from patients with chronic myeloleucosis. Voprosy Virusologii (Problems of virology) 1974; 29:152–156.
4. SHUBLADZE AK, BARINSKY IF, BOCHAROV AF. Use of leukocyte cultures in isolation of viruses in human leucosis. Voprosy Virusologii (Problems of virology) 1973; 28: 719–724.
5. BARINSKY IF. Human leucocyte culture in investigation of the hepatitis C etiology and etiology of human

acute leucosis and chronic myeloleucosis. In: XIth International Congress of Virology, IUMS, Abstract Book. Sydney: Darling Harbour; 1999: 343–344.

6. SHUBLADZE AK, BYCHKHOVA EN, BARINSKY IF. Viremia in acute and chronic infections. Moscow: Medicina; 1974.
7. SHUBLADZE AK, BARINSKY IF, BOCHAROV AF. Isolation of virus in human leucosis. The Bulletin of the Academy of Medical Science 1974; 3:27–31.

The article is devoted to the investigation of human leucocyte cultures derived from the blood of healthy donors stimulated with PHA were successfully used for isolation of human hepatitis C virus from the blood of patients. The same cultures were used for isolation and cultivation of oncoviruses at acute leukosis and chronic myeloleukosis. The research was conducted in a *careful* and *objective* way and can be recommended for publishing in the medical Journal *Archiv Euromedica*.

PROF. V.A. ZUEV,
RANS, Moscow, Russia

INTRAKORPORALE HARNABLEITUNG BEI DER ROBOTERASSISTIERTEN RADIKALEN ZYSTEKTOMIE (RARC)

Dr. Sebastian Edeling, Dr. Sasa Pokupic

edeling

ABSTRACT

Die radikale Zystektomie beim muskelinvasiven Urothelkarzinom ist ein großer operativer Eingriff, der in drei Teileingriffe gegliedert werden kann: radikale Zystoprostatektomie bzw. radikale Zystektomie bei der Frau, ausgedehnte Lymphadenektomie, Anlage einer Harnableitung (z.B. Ileumconduit oder Neoblase). Onkologisch ist eine R0-Resektion und die ausgedehnte Lymphadenektomie bis auf Höhe der Aorta entscheidend. Durch die Dauer und Ausdehnung des Eingriffs besteht ein hohes Risiko für intra- und postoperative Komplikationen. Durch den Einsatz des da Vinci®-Operationssystems sollen die Komplikationen minimiert werden.



Das da Vinci®-System hat sich bei der radikalen Prostatektomie in den USA durchgesetzt. Dort werden ca. 95% der radikalen Prostatektomien roboterassistiert durchgeführt. Vorteile bei der roboterassistierten Prostatektomie (RARP) sind neben den allgemeinen Vorteilen einer minimalinvasiven Operation wie geringerer intraoperativer Blutverlust, weniger postoperative Schmerzen, weniger Wundheilungsstörungen, kürzerer Krankenhausaufenthalt und schnellere Rückkehr in das normale Leben auch bessere funktionelle (Kontinenz und Erektionsraten) und onkologische Ergebnisse (geringere R1-Raten).

Bei der radikalen Zystektomie konnten die onkologischen Ergebnisse durch Veränderungen der offenen Operationstechnik in den letzten Jahren nicht wesentlich verbessert werden. Dies liegt vor allem daran, dass das rezidivfreie und Gesamtüberleben weniger von der OP-Technik als vom Tumorstadium und dem nodalen Status abhängig ist.

Die roboterassistierte Zystektomie (RARC) wird seit 2005 zunehmend in den USA durchgeführt.

Zunächst wurde die Zystektomie und die Lymphadenektomie roboterassistiert, die Anlage der Harnableitung über einen ca. 10 cm Hautschnitt operiert (extrakorporale Harnableitung). Seit 2013 wird auch die Harnableitung (Ileumconduit / Neoblase) ohne zusätzlichen Hautschnitt (intrakorporale Harnableitung) komplett roboterassistiert durchgeführt.

Die Daten des IRCC (International Radical Cystectomy Consortium) von 2013 zeigten, dass 77%

(n=698) mittels extrakorporaler Harnableitung und 23% (n=208) mittels intrakorporaler Harnableitung versorgt wurden. Hierbei erhielten 68% (n=613) ein Ileumconduit, 32% (n=294) eine kontinente Harnableitung. (1)

Die ersten Daten zeigten keine Unterschiede in den onkologischen und funktionellen Ergebnissen zwischen RARC und der offenen Operation. (2) (3) (4)

Unterschiede bestanden jedoch sowohl beim intraoperativen Blutverlust (RARC 460 ml vs. Offen 1172 ml), der Krankenhausverweildauer (5,5 vs 8,0 Tage) und den Komplikationen.

Ng konnte 2009 in einer der ersten RARC-Serien mit extrakorporaler Harnableitung in einem direkten Vergleich von 187 Patienten (83 RARC, 104 offen) eine deutliche Reduktion der Komplikationen beobachten (41% vs. 59%). Vor allem die high-grade-Komplikationen (Clavien 3–5) konnten innerhalb der ersten 30 Tage reduziert werden (10% vs. 30%). (2)

Die Daten des IRCC zeigen außerdem einen Vorteil der intrakorporalen verglichen zur extrakorporalen Harnableitung. Die Wiederaufnahmerate innerhalb von 30 Tagen nach der Operation unterschied sich signifikant (n=10 (5%) vs n=95 (15%)). (3)

OP-TECHNIK

Seit Mitte 2013 wird ein großer Teil der radikalen Zystektomien an unserer Klinik roboterassistiert mit intrakorporaler Harnableitung (Ileumconduit / Neoblase) durchgeführt.

Wir übernahmen hierfür die Operationstechnik von Prof. P. Wiklund aus Stockholm.

Die Patienten werden nach dem fast-Track-Schema behandelt. Antibiotisch erfolgt lediglich ein Single-Shot mit Tazobac 4g, der nach 4 Stunden OP-Dauer erneut gegeben wird.

Das Port-Placement unterscheidet sich nur leicht von dem Standardplacement bei der RARP: Der Kameratrocark wird etwas weiter kranial (4 cm oberhalb des Nabels) gesetzt. Die restlichen Trokare werden dann in den üblichen Abständen platziert. Der 8mm-da Vinci®-Trocark für Arm 3 im linken Unterbauch wird in einen 12mm-Trocark gesteckt über den später das Stapeln des Dünndarms erfolgt. Wir stapeln die Dünndarm Anastomose in seit-zu-seit-Technik.

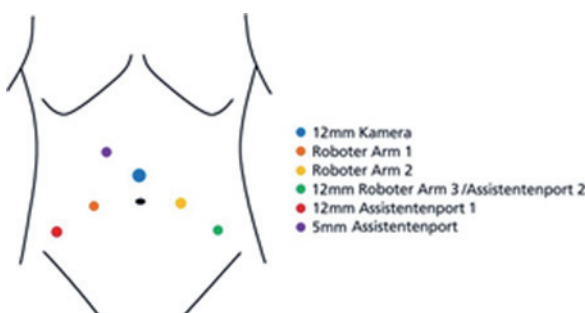


Abb.1: Port-Placement bei der RARC

Die Neoblase nach Wiklund ist eine modifizierte Studer-Neoblase bei der im ersten Schritt die Anastomose zwischen Dünndarm und Harnröhre genäht wird. Erst dann wird der Dünndarm antimesenterial eröffnet und die Neoblase vernäht.

Die Harnleiter werden spatuliert und zu einer Wallace-Platte adaptiert. Diese wird an das Ende des Conduits oder an den Dünndarm-Schornstein der Neoblase genäht.

Das Präparat wird in einen großen Bergebeutel gelegt und bei der Frau transvaginal entfernt. Beim Mann wird der Schnitt des Kameratrocars am Ende der OP erweitert und so der Bergebeutel geborgen.

ERGEBNISSE

Wir versorgten 14 Patienten mit einem Ileumconduit, 7 Patienten mit einer Neoblase und 5 Patienten erhielten eine Harnleiter-Haut-Fistel bei Einzelniere.

Trotz zunächst langer Operationszeiten, die sich schnell reduzierten, gab es intraoperativ keine Komplikationen. Die OP mit Anlage eines Ileumconduits dauerte durchschnittlich 352 Minuten (241–475 min), bei Anlage einer Neoblase betrug die OP-Zeit 443 Minuten (350–525 min).

Orientierend dauerte hierbei die Zystektomie ca. 1,5 Stunden, die Lymphadenektomie ca. 1,0–1,5 Stunden, die Harnableitung ca. 2–4 Stunden.

Bei der Lymphadenektomie, die standardmäßig bis zur Aorta durchgeführt wird, wurden durchschnittlich 21,1 Lymphknoten (8–40) entfernt.

Der intraoperative Blutverlust betrug durchschnittlich 305 ml (50–800 ml), sodass keine Erythrozytenkonzentrate verabreicht werden mussten.

Eine R0-Resektion konnte bei 25 der 26 Patienten erreicht werden. Der R1-Befund bestand an einem Ureter, der in der endgültigen Histologie trotz mehrmaliger Nachresektion ein pTis aufwies. Hier wurde beschlossen, eine BCG-Spülung der Niere mit anschließender URS und Stufenbiopsien durchzuführen. Bei dann weiterhin positivem Befund sollte zweizeitig eine Nephroureterektomie erfolgen.

Der unmittelbare postoperative Verlauf zeigte eine schnelle Erholung der Patienten. Fast alle Patienten lagen nur die postoperative Nacht auf der Intensivstation und wurden am Morgen des ersten postoperativen Tages auf die Normalstation verlegt und dort mobilisiert.

Wundheilungsstörungen traten bis auf eine verlängerte Sekretion aus einer Trokar-Stelle keine auf.

Die Krankenhausverweildauer konnte gegenüber unseren offenen Zystektomien gesenkt werden: Für Patienten, die ein Ileumconduit erhielten betrug die postoperative Liegezeit 10,0 Tage (6–16 Tage) (InEK-Kalkulation: mittlere VWD 17,6 Tage), für Patienten mit Neoblase 13,2 Tage (6–33 Tage) (InEK mittlere VWD 22,3 Tage). Die Patienten, die lediglich eine Ureter-Haut-Fistel bekamen lagen 8,0 Tage (5–17 Tage) postoperativ.

An Komplikationen, die prospektiv erfasst wurden, zeigten sich hauptsächlich Grad 1–2 Komplikationen. Grad 3-Komplikationen traten nur bei den Patienten mit Neoblase auf.

Der zunächst häufig auftretende postoperative paralytische Ileus kam nach Anpassung der prophylaktischen abführenden Medikation nur noch selten vor.

ZUSAMMENFASSUNG

Die RARC mit intrakorporaler Harnableitung ist sehr gut durchführbar. Die Operationszeiten unterscheiden sich nach einer kurzen Lernkurve kaum von denen der offenen Operation.

In bisher durchgeföhrten Studien kann sich das OP-Verfahren sowohl onkologisch als auch funktionell mit der offenen Operation messen.

Vorteile des robotischen Vorgehens sind: geringe intra- und postoperative Komplikationsraten, geringer intraoperativer Blutverlust, kürzere Liegezeit auf der ITS und kürzere Krankenhausverweildauer.

Im Vergleich zu den Patienten, die eine RARC mit intrakorporalem Ileumconduit erhielten, zeigten sich im weiteren stationären Verlauf mehr und höhergradige Komplikationen bei den Patienten, die mittels Neoblase versorgt wurden.

Art der Harnableitung	Anzahl der Patienten mit Komplikationen	Komplikation	Clavien-Grad	Therapie
Neoblase (n=7)	7	Paralytischer Ileus	2	Abführende Maßnahmen
		Metabolische Azidose	2	Orale Alkalisierung
		Anastomoseninsuffizienz Neoblase (n=3)	2	DK belassen
		II° Nierenstau bds.	2	Abschwellende Medikation
		Harnwegsinfekt (n=4)	2	Antibiotische Therapie
		Sekretion aus Trokarstelle	3a	Naht
		Blasen-Scheiden-Fistel	3b	Vaginale Naht
Ileumconduit (n=14)	6	Nierenstau links	3b	Perkutane Nierenfistel
		SJK-Dislokation in Abdomen	3b	Laparoskopische Bergung
		Sekretion aus Vagina	1	
		Flüssigkeitsabgang Urethra	1	
		Asymptomat. Nierenstau rechts	1	
Ureter-Haut-Fistel (n=5)	1	Paralytischer Ileus (n=3)	2	Abführende Maßnahmen
		Fieber bei HWI	2	Antibiotische Therapie
		Pseudomembranöse Kolitis	2	Antibiotische Therapie
		Paralytischer Ileus	2	Abführende Maßnahmen
		Harnwegsinfekt	2	Antibiotische Therapie

Entscheidend für eine Reduzierung der Komplikationen ist neben der operativen Qualität das prä-, peri- und postoperative Management (fast-Track, Antibiotika-Regime, frühzeitige Mobilisation,...) das wir weiter zu verbessern versuchen.

LITERATUR

- 1 JOHAR, R., HAYN, M., ET AL. Complications After Robot-assisted Radical Cystectomy: Results from the International Robotic Cystectomy Consortium. Eur. Urol 2013
- 2 NG, C., ET AL. A Comparison of Postoperative Complications in Open versus Robotic Cystectomy. Eur. Urol 2009
- 3 NIX J., ET AL. Prospective Randomized Controlled Trial of Robotic versus Open Radical Cystectomy for Bladder Cancer: Perioperative and Pathologic Results. Eur Urol. 2009
- 4 WIKLUND, P., ET AL. Robotic radical cystectomy and diversion in 2013: Where do we stand? 2013

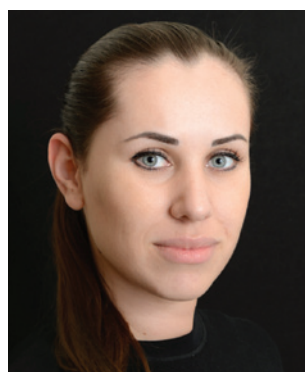
INTERRELATION BETWEEN SAGITTAL AND TRANSVERSAL SIZES IN FORM VARIATIONS OF MAXILLARY DENTAL ARCHES

**S.V. Dmitrienko¹, D.A. Domenyuk², A.S. Kochkonyan²,
A.G. Karslieva, D.S. Dmitrienko³**

¹*Department of Dentistry, Pyatigorsk Medical-Pharmaceutical Institute,
Pyatigorsk, Russia*

²*Department of general practice dentistry and child dentistry, Stavropol
state medical university, Stavropol, Russia*

³*Department of dentistry of Child Age, Volgograd State Medical University,
Volgograd, Russia*



Numerous experts for more than a hundred years now have offered description of the shapes and the sizes of maxillary dental arches [1, 5, 6, 7, 8]. The first classification for dental arch forms proposed three main forms – narrowed, square and oval [2]. At the same time, research data and clinical observations suggest that maxillary dental arch forms in humans can be described with considerable diversity. Most researchers evaluated the biometrics of maxillary arches and detected their relation to the size of the teeth and the craniofacial complex [3, 4, 9].

In the literature available, we did not find any data on the relationship between the sagittal and the transversal sizes of maxillary dental arches in view of the variety of their shapes, namely mesognathia, dolichognathia, and brachygnathia, which has stood to be

the objective of the present study.

There has been an analysis conducted regarding the sagittal and transversal sizes in maxillary dental arches in 287 patients (both sexes; in their early adulthood) with physiological occlusion of permanent teeth.

Three types of maxillary dental arches have been proposed – the vestibular dental arch, the alveolar

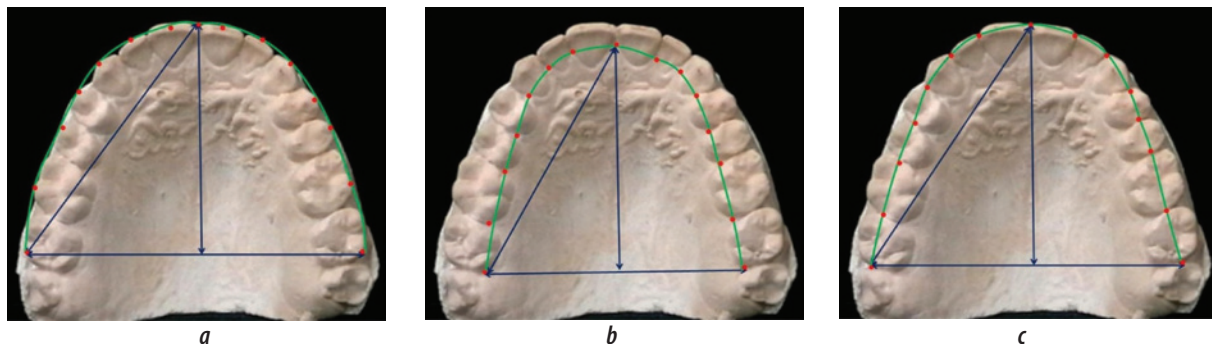


Fig. 1. Maxillary cast models with the contours of the dental arch (a), the alveolar arch (b), and the dentoalveolar arch (c).

lingual (palatal) arch, and the dentoalveolar arch. The cast models of the upper jaw were dotted in order to constructing and morphometric measurements in the maxillary dental arches. When studying the dental arch, the main points were set in the middle of the vestibular surface of the incisors, canines and premolars' occlusal contour (the most prominent part in the vestibular contour of the tooth crown' occlusal surface); the most protruding points on the vestibular contour' occlusal surface of the vestibular distal cusps were marked on the molars. The alveolar lingual (palatal) arch was formed through connecting the dots located at the lingual surface of the dental arch in the interdental spaces. When studying the dental arch the dots were set in the middle of the teeth crowns' distal surface in proximity of the occlusal contour (Fig. 1).

The key parameters for measuring the maxillary dental arches included the arch length, width, and depth as well as the frontal distal diagonal. The longitudinal length of the dentition was detected through the Nance method as a sum of the mesial distal diameters of the compounding teeth. The third molars were not included in the measurements due to being the most variable ones.

When measuring the dental arch and the dentoalveolar arch, the frontal vestibular point was arranged amidst the medial incisors. The width of the maxillary arches (dental arch, dentoalveolar arch, and alveolar arch) was measured between the second molars (W_d^{7-7} , W_{da}^{7-7} and W_a^{7-7}). The depth of the arch (D_d^{1-7} , D_{da}^{1-7} and D_a^{1-7}) was determined as a distance from the frontal vestibular point to the line connecting the corresponding points of the second molars along the projection of the median palatal suture.

The arch form was defined through the arch index (the ratio between its depth and width). The maxillary dental arch form was defined as mesognathic in the cases where the dental arch index was 0.74 ± 0.03 ,

that of the dentoalveolar the alveolar arch – 0.9 ± 0.05 , regardless of the teeth size (macrodontia, microdontia or normal teeth size). For the brachygnathic form the dental arch index was below 0.7, the indices of the dentoalveolar and the alveolar arches being less than 0.85. In the event the dental arch index went beyond 0.77, that in the dentoalveolar and the alveolar arches exceeding 0.95, the form was classified as dolichognathic.

To estimate the size of the teeth we used the mean module of the molar crowns (half-sum of the first and second molar crowns modules). The crown module was calculated employing the A.A. Zubov method, taken as half-sum of the vestibular lingual and the mesial distal diameters of the tooth crown. The mean module of the molar crowns residing in the range of 10.6 – 11 mm was viewed as normal teeth size. A reduced value was typical of microdontia, while the value's increase was indicative of macrodontia in the permanent molars.

The outcomes suggest that in case of physiological occlusion of permanent teeth there were nine major types of maxillary dental arches to be found. Individuals with the mesognathic, brachygnathic, and dolichognathic arch forms revealed variants of microdontia, normal teeth size, and macrodontia of the permanent molars. There also has been an investigation into the parameters of the dental, the alveolar, and the dentoalveolar arches in patients with the above-mentioned forms of maxillary dental arches.

The study has shown that, regardless of the form of the maxillary arches and the teeth size, the matching index for the teeth size in relation to the frontal distal diagonal (the ratio between the sum of the mesial distal diameters of the seven teeth on one side to the length of the frontal distal diagonal) was stable, and for the dental arches it was 1.06 ± 0.01 , for the dentoalveolar arches – 1.07 ± 0.01 , while for the alveolar arches it was 1.14 ± 0.01 . This index is of high pragmatic value

and allows determining whether or not the size of teeth conforms to the size of the jaws, as well as it allows predicting a deficit or an excess of space in the jaw bones for permanent teeth. Mention to be made here that the dental arch length (which is the sum of the mesial distal diameters of 14 teeth) in case of normal teeth size in the permanent teeth averaged 115.11 ± 4.21 mm. In case of macrodontia the dental arch length was over 120 mm with an average of 124.14 ± 4.37 mm. For microdontia it was typical to have the dental arch length less than 110 mm with its value being 105.34 ± 4.64 mm.

We have studied the main parameters in the dental, the alveolar and the dentoalveolar arches also evaluating the interrelation between the major points.

Table 1 contains the results obtained through a study of the dental arches.

The outcomes have shown that under macrodontia of permanent teeth virtually all the measurements in the dental arches were significantly higher than in case of microdontia. The major indicator for the teeth size was the frontal distal diagonal (FDDd1-7).

During that, the key indicator for the dental arch form was the dental arch index, and the ratio between the depth of the dental arch (D_{d1-7}) and the width between the second permanent molars in those with mesognathic dental arch was 0.75 ± 0.03 for normal teeth size, 0.74 ± 0.03 – for macrodontia, and 0.73 ± 0.03 – under microdontia. Thus, the dental arch index in case of mesognathia averaged 0.75 ± 0.03 , depended on the ratio of sagittal and transversal dimensions, and revealed absolutely no dependence on the actual sizes of the teeth. The dental arch index for dolichognathic form was, on average, 0.81 ± 0.02 , while in case of brachygnathic form it averaged 0.68 ± 0.02 . Note to be made here of the ratio of the dental arch depth (D_{d1-7}^{1-7}) to the depth of the anterior part of the arch (D_{d1-3}^{1-3}), which in case of mesognathia was 4.81 ± 0.03 , for dolichognathia – 3.73 ± 0.03 , while under brachygnathia it was 4.97 ± 0.04 .

Table 2 contains the results of the study in relation to the alveolar arches measurements.

The results showed that the absolute values of the alveolar arches' parameters were significantly lower if compared to the dental ones. However, the comparative measures revealed the same proportional relationships. The ratio of the depth of the alveolar arch (D_{a1-7}^{1-7}) to the width between the second permanent molars (W_{a1-7}^{7-7}) in those with the mesognathic arch was 0.93 ± 0.02 for the normal teeth size, 0.9 ± 0.03 – for macrodontia, and 0.89 ± 0.03 – in case of microdontia of the permanent teeth. The ratio of the depth of the alveolar arch (D_{a1-7}^{1-7}) to the depth of the anterior part of the arch (D_{a1-3}^{1-3}) under mesognathia was 4.3 ± 0.03 , while

for dolichognathia it was 3.6 ± 0.04 , and for brachygnathia – 4.95 ± 0.04 , coinciding with the similar dental arch indices.

Table 3 offers the study results regarding the dentoalveolar arches.

The dentoalveolar arch index in people with mesognathic arch form was 0.93 ± 0.02 for normal teeth size, 0.92 ± 0.03 – for macrodontia, and 0.91 ± 0.03 – for microdontia. Therefore, the dentoalveolar arch index under mesognathia averaged 0.91 ± 0.03 and depended on the ratio of the sagittal and the transversal dimensions, while being virtually irrespective of the actual sizes of the teeth. The dentoalveolar arch index in case of the dolichognathic form was, on average, 0.97 ± 0.02 , while for the brachygnathic form it was 0.79 ± 0.03 . The fact that stands out here is the ratio of the depth of the dentoalveolar arch (D_{d1-7}^{1-7}) to the depth of the anterior part of the arch (D_{d1-3}^{1-3}), which under mesognathia was 3.53 ± 0.03 , under dolichognathia – 3.01 ± 0.03 , being equal to 3.99 ± 0.04 for brachygnathia.

Hence, each of the maxillary arch forms has typical major parameters, which may prove useful when determining the size of the metal arcs implemented at various stages of orthodontic treatment.

REFERENCES

1. BRADER A.C. Dental arch form related to intra-oral forces // American Journal of Orthodontics. – 1972. – № 61. – P. 541-561.
2. CHUCK G.C. Ideal arch form. Angle Orthodontist. – 1932. – 116. – P. 1-12.
3. DMITRIENKO S.V., DMITRIENKO D.S., KLIMOVA N.N., SEVASTYANOV A.V. On constructing the Hawley arch // Orthodontics. – 2011. – № 2 (54). – P. 11-13.
4. DOMENYUK, D.A. Study of dentition adaptive reactions in children and adolescents when using removable orthodontic appliances / D.A. Domenyuk, IV. Zelenskiy, E.N. Ivancheva // Child dentistry and prevention. – 2012. – Vol. XI. – № 4 (43). – P. 41-46.
5. FISHCHEV S.B., DMITRIENKO D.S., SEVASTYANOV A.V., EGOROVA A.V., RTISHCHEVA S.S. Algorithm for detecting teeth sizes, arches' parameters, craniofacial complex, and occlusion relationships // Institute of Dentistry. – № 3 (48). – 2010. – P. 58-62.
6. HAWLEY C.A. Determination of the normal arch and its application to orthodontia // Dental Cosmos. – 1905. – № 47. – P. 541-552.
7. McLAUGHLIN, R., BENNETT, J., TREVISI, H. Systemized Orthodontic Treatment Mechanics. Translated from Eng. – Lvov: GalDent, 2005. – 324 p. – 950 fig.
8. SCOTT J.H. The shape of dental arches // Journal of Dental Research. – 1957. – № 36. – P. 996-1003.
9. TUGARIN V.A., PERSIN L.S., POROKHIN A.YU. Modern fixed-type orthodontic appliances Edgewise. – M., 1996. – 220 p.

Table. 1. The main parameters of the dental arches in case of their form variations

Forms of the dental arches	Main measurements in dental arches (mm)				
	W _d ⁷⁻⁷	D _d ¹⁻⁷	W _d ³⁻³	D _d ¹⁻³	FDD _d ¹⁻⁷
Mesognathic, normal teeth size	57.48 ± 1.54	43.11 ± 0.93	36.08 ± 0.67	9.22 ± 0.36	52.12 ± 1.42
Mesognathic macrodontia	64.28 ± 1.61	47.45 ± 1.08	35.96 ± 1.14	10.85 ± 0.55	57.42 ± 1.63
Mesognathic microdontia	55.17 ± 1.39	40.16 ± 0.87	36.03 ± 0.78	7.46 ± 0.32	48.73 ± 1.38
Dolichognathic, normal teeth size	59.83 ± 1.69	47.45 ± 1.29	37.04 ± 0.92	11.32 ± 0.68	56.09 ± 1.54
Dolichognathic macrodontia	61.17 ± 1.82	50.78 ± 1.93	38.41 ± 1.16	15.03 ± 1.51	59.28 ± 1.97
Dolichognathic microdontia	55.07 ± 1.33	43.47 ± 1.12	36.67 ± 0.72	12.01 ± 1.24	51.08 ± 1.23
Brachyggnathic, normal teeth size	61.98 ± 1.95	42.02 ± 1.09	35.81 ± 0.91	7.98 ± 0.41	51.98 ± 1.39
Brachyggnathic macrodontia	66.32 ± 2.04	44.52 ± 1.25	35.04 ± 1.08	9.37 ± 0.74	56.06 ± 1.73
Brachyggnathic microdontia	57.54 ± 1.43	38.68 ± 0.86	32.42 ± 0.59	7.92 ± 0.41	48.31 ± 1.29

Table. 2. The main parameters of the alveolar arches in case of their form variations

Arch forms	Main measurements in alveolar arches (mm)				
	W _a ⁷⁻⁷	D _a ¹⁻⁷	W _a ³⁻³	D _a ¹⁻³	FDD _a ¹⁻⁷
Mesognathic, normal teeth size	46.21 ± 2.03	43.12 ± 0.59	33.79 ± 1.34	9.56 ± 0.74	48.31 ± 0.86
Mesognathic macrodontia	54.03 ± 2.36	48.51 ± 1.24	32.47 ± 0.95	11.84 ± 1.22	52.96 ± 1.75
Mesognathic microdontia	44.52 ± 1.99	39.03 ± 0.82	31.21 ± 0.96	9.09 ± 0.57	44.82 ± 1.31
Dolichognathic, normal teeth size	49.02 ± 1.36	48.02 ± 1.12	31.03 ± 0.89	13.03 ± 1.14	52.04 ± 1.48
Dolichognathic macrodontia	50.48 ± 1.94	49.53 ± 1.67	36.01 ± 1.23	14.48 ± 1.54	55.11 ± 1.76
Dolichognathic microdontia	44.51 ± 1.13	43.04 ± 1.09	31.97 ± 0.91	12.04 ± 1.11	47.29 ± 1.42
Brachyggnathic, normal teeth size	52.04 ± 1.19	40.47 ± 1.05	32.96 ± 1.45	9.48 ± 0.47	48.47 ± 1.35
Brachyggnathic macrodontia	54.49 ± 1.88	44.95 ± 1.21	33.01 ± 1.15	9.51 ± 0.88	52.19 ± 1.65
Brachyggnathic microdontia	46.52 ± 1.21	38.93 ± 0.81	32.38 ± 0.62	7.89 ± 0.38	44.72 ± 1.07

Table. 3. The main parameters of the dentoalveolar arches in case of their form variations

Arch forms	Main measurements in dentoalveolar arches (mm)				
	W _{da} ⁷⁻⁷	D _{da} ¹⁻⁷	W _{da} ³⁻³	D _{da} ¹⁻³	FDD _{da} ¹⁻⁷
Mesognathic, normal teeth size	49.51 ± 1.52	46.03 ± 1.13	38.48 ± 1.03	13.02 ± 0.78	51.71 ± 1.54
Mesognathic macrodontia	56.49 ± 1.82	50.98 ± 1.53	38.61 ± 1.44	14.39 ± 1.03	56.68 ± 1.69
Mesognathic microdontia	48.03 ± 1.55	43.31 ± 1.21	33.47 ± 1.07	12.41 ± 1.01	48.29 ± 1.13
Dolichognathic, normal teeth size	51.49 ± 1.92	50.02 ± 1.34	36.61 ± 1.12	17.04 ± 1.09	56.11 ± 1.66
Dolichognathic macrodontia	54.53 ± 1.73	53.96 ± 1.88	38.48 ± 1.12	18.02 ± 1.57	59.19 ± 2.08
Dolichognathic microdontia	48.51 ± 1.42	46.22 ± 1.23	36.19 ± 1.08	14.99 ± 1.22	51.03 ± 1.12
Brachyggnathic, normal teeth size	55.04 ± 1.89	43.33 ± 1.17	37.51 ± 1.19	11.48 ± 1.04	52.01 ± 1.13
Brachyggnathic macrodontia	58.68 ± 1.84	46.48 ± 1.29	38.49 ± 1.27	11.51 ± 1.05	55.29 ± 1.54
Brachyggnathic microdontia	50.96 ± 1.31	41.52 ± 1.18	35.52 ± 1.15	10.02 ± 1.11	48.04 ± 1.32

MODERN CLASSIFICATION OF DENTAL ARCHES

S.V. Dmitrienko¹, D.A. Domenyuk², A.S. Kochkonyan²,
A.G. Karslieva, D.S. Dmitrienko³

¹Department of Dentistry, Pyatigorsk Medical-Pharmaceutical Institute, Pyatigorsk, Russia

²Department of general practice dentistry and child dentistry, Stavropol state medical university, Stavropol, Russia

³Department of dentistry of Child Age, Volgograd State Medical University, Volgograd, Russia

ABSTRACT

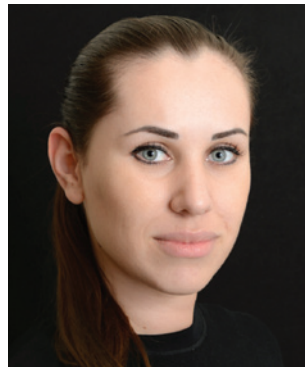
The authors put forward a classification for maxillary dental arch forms, which includes nine major clinical variants. Individuals with mesognathic, brachygнатic, and dolichognathic arch forms demonstrated microdontia, normal teeth size, and macrodontia in permanent molars. Each of the maxillary dental arch forms were characterized by the main biometric parameters, which may prove useful when determining the size of metal arcs implemented at various stages of orthodontic treatment.

Orthodontic literature has studied the shapes and sizes of dental arches for ages now, and a vast number of scientific papers offer the description of ideal arch forms [2, 7, 11, 12].

G.C. Chuck (1932) was the first one to propose a classification for the arch forms, specifying them as narrowed, square and oval ones [4]. At the same time, the classification holds terms referring, on the one hand, to the arches' sizes (narrowed), while on the other – to their similarity with geometric figures, which, above that, do not actually reflect the true shape of the arches (square).

The classifications describing the shape of the dental arches through various mathematical expressions utilize definitions like chain curves, elliptic curves, parabolical, mixed models (ellipse and parabola), conic sections, spline curves, and beta functions [1, 3, 6, 10].

Scientific studies and clinical observations confirm the fact that dental arch forms in humans vary a lot [5, 9]. This diversity does not allow making a search for the ideal arch shape. E.H. Angle proposed that the concept of the ideal arch form should be related to the facial types, namely dolichocephalic, mesocephalic and brachycephalic. During that, it has been proven that the dolichocephalic facial type, more often than not, comes along with narrow and long arches, while in case of the brachycephalic type short and wide arches dominate [8]. Yet, the author offers no morphometric data just like shows no parameters for determining the arch shapes.



This reveals a need for a system-wide approach to ascertaining arch forms, both when diagnosing their shape and size abnormalities and through orthodontic treatment, which prompted this present study.

There has been an analysis conducted regarding the sagittal and transversal sizes in maxillary dental arches in 287 patients (both sexes; in their early adulthood) with physiological occlusion of permanent teeth.

To construct dental arch we used the main points that were set in the middle of the vestibular surface of the incisors' occlusal contour; canines and premolars were used to set the most prominent part in the vestibular contour of the tooth crown' occlusal surface; the most protruding points on the vestibular contour' occlusal surface of the vestibular cusps were marked on the molars (Fig. 1).

The key parameters for dental arches measurement included the arch width, depth and the frontal distal diagonal. When measuring the dental arch, the frontal vestibular point was set amidst the medial incisors on the vestibular surface. The width of the dental

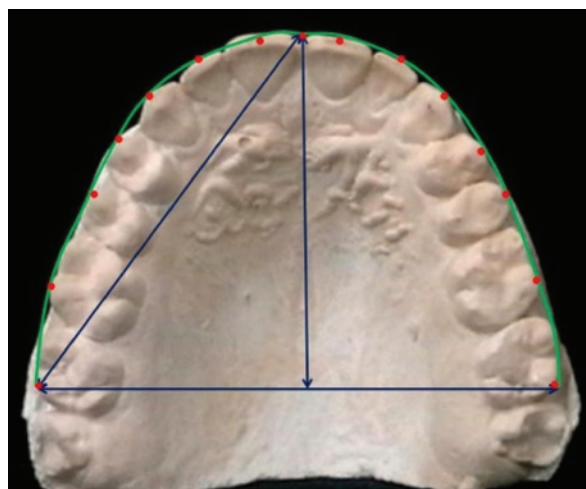


Fig. 1. Maxillary cast model bearing the dots and contours of the dental arch

arch was measured between the second molars at the most protruding points on the vestibular contour' occlusal surface of the vestibular distal cusps. The depth of the dental arch was measured from the frontal vestibular point located on the vestibular surface between the medial incisors of the upper or lower jaw, and up the line connecting the vestibular distal points of the second molars along the projection of the median palatal suture. The arch form was defined through arch index (the ratio between its depth and width).

Estimation of the teeth size implied using the mean module of the molar crowns (half-sum of the first and second molar crowns modules). The crown module was calculated as half-sum of vestibular lingual and mesial distal diameters of the tooth crown. The mean module of the molar crowns of 10.6 to 11 mm was accepted as normal teeth size. Reduced value was

typical of microdontia, while an increase in the same value revealed macrodontia of the permanent molars.

The outcomes have shown that physiological occlusion of permanent teeth came along with three major forms of dental arches identified in accordance with the arch index.

With the dental arch index of 0.74 ± 0.03 the arch form was defined as mesognathic. In case of an index below 0.71, the arch form was viewed as brachygnathic, while an index going beyond 0.77 pointed at the dolichognathic form (Fig. 2).

Individuals with physiological occlusion of permanent teeth mostly demonstrated the mesognathic type of the dentoalveolar arch, which was found in $56 \pm 4.5\%$. The dolichognathic type was found in $36 \pm 4.5\%$, while the brachygnathic type in $28 \pm 4.5\%$ of all the patients studied.

In the cases with the normal size of the permanent teeth combined with the mesognathic arch, the length of the dental arch (the sum of mesial distal diameters of 14 teeth) averaged 112.6 ± 3.62 mm, the width of the arch between the second permanent molars was 57.5 ± 2.8 mm, while the depth of the arch was as long as 43.1 ± 2.8 mm. The arch index was 0.75 ± 0.03 . The mean module of the molar crowns was 0.8 ± 0.2 mm. The average measure of the frontal distal diagonal was 51.8 ± 2.8 mm. In the brachygnathic type combined with the normal size of the permanent teeth, the dental arch length (which is the sum of the mesial distal diameters of 14 teeth) averaged 110.2 ± 2.87 mm, the width of the dental arch between the second permanent molars being 62.23 ± 2.8 mm, and the depth of the arch was 42.1 ± 2.8 mm. The arch index proved to be significantly lower than that in patients with mesognathic type of the dental arch and was equal to 0.68 ± 0.03 . The mean module of the molar crowns was 10.75 ± 0.15 mm. The frontal distal diagonal was, on average, 52.2 ± 2.8 mm. The dolichognathic dental arches typically revealed enlarged sagittal sizes, and reduced transversal sizes, if compared with the mesognathic type of the arch. The width of the dental arches was 59.83 ± 2.8 mm, the depth being 47.45 ± 2.8 mm. Given that, the arch index was 0.82 ± 0.03 .

In microdontia of the permanent teeth, the typical point making it different from normal sized arches was that the arch length (the sum of the mesial distal diameters of 14 teeth) was significantly lower in all forms of the dental arches surveyed. In mesognathic type the arch length was 103.22 ± 2.8 mm, in the brachygnathic type – 100.78 ± 2.8 mm, while in the dolichognathic it was 105.3 ± 2.8 mm. Due to that, there was a significantly smaller size in the frontal distal diagonal, which in case of mesognathia was equal to

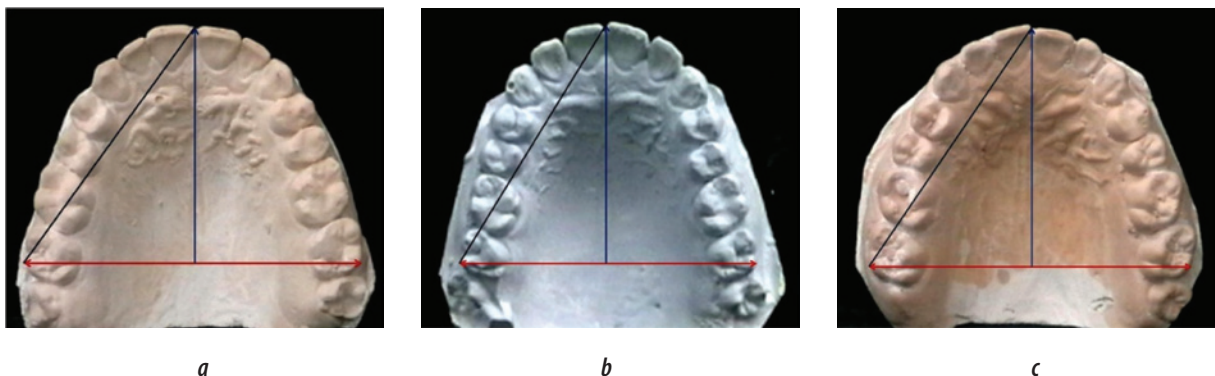


Fig. 2. Major types of dental arches: mesognathic (a), dolichognathic (b), and brachygnathic (c)

48.72 \pm 2.8 mm, in brachygnathia – 48.21 \pm 2.8 mm, and in dolichognathia – 51.15 \pm 2.8 mm. At the same time, the arch index was basically not different from that in people with a normal teeth size and was typical of mesognathia, brachygnathia, and dolichognathia.

People with macrodontia of the permanent teeth manifested significant elongation of the dental arch and the frontal distal diagonal. In the mesognathic type of the arch its length was 103.22 \pm 2.8 mm, in the brachygnathic type – 100.78 \pm 2.8 mm, and in the dolichognathic type – 105.3 \pm 2.8 mm. The frontal distal diagonal in mesognathia made up to 48.72 \pm 2.8 mm, in case of brachygnathia – 48.21 \pm 2.8 mm, while in case of dolichognathia it was 51.15 \pm 2.8 mm.

Therefore, physiological occlusion of permanent teeth demonstrated nine major variants of the dental arches. Individuals with the mesognathic, brachygnathic, and dolichognathic types of the dental arches revealed microdontia, normal teeth size, and macrodontia of the permanent molars. Each dental arch form had its typical biometric parameters, which could help detect the size of metal arcs, used through various stages of orthodontic treatment.

REFERENCES

1. BEGOLE E.A., FOX D.L., SADOWSKY C. Analysis of change in arch form with premolar expansion // American Journal of Orthodontics and Dentofacial Orthopedics. – 1998; 113: 307–315.
2. BRADER A.C. Dental arch form related to intra-oral forces // American Journal of Orthodontics. – 1972. – № 61. – P. 541–561.
3. BRAUN S., HNAT W.P., FENDER D.E., LEGAN H.L. The form of the dental arch // Angle Orthodontist. – 1998; 68: 29–36.
4. CHUCK G.C. Ideal arch form. Angle Orthodontist. – 1932. – 116. – P. 1–12.
5. DOMENYUK, D.A. Study of dentition adaptive reactions when using removable orthodontic appliances in children / D.A. Domenyuk, V.A. Zelenskiy // Child dentistry and prevention. – 2013. – Vol. XII. – № 1 (44). – P. 50–57.
6. FERRARIO V.F., SFORZA C., MIANI JR. A., Tartaglia G. Mathematical definition of the shape of dental arches in human permanent healthy dentitions // European Journal of Orthodontics. – 1994; 16: 287–294.
7. HAWLEY C.A. Determination of the normal arch and its application to orthodontia // Dental Cosmos. – 1905. – № 47. – P. 541–552.
8. KHOROSHILKINA F.YA., PERSIN L.S., OKUSHKO-KALASHNIKOVA V.P. Orthodontics. Prevention and treatment of functional, morphological and aesthetic disturbances in the dentofacial area. Book IV. M., 2005. – 460 p.
9. McLAUGHLIN, R., BENNETT, J., TREVISI, H. Systemized Orthodontic Treatment Mechanics. Translated from Eng. – Lvov: GalDent, 2005. – 324 p. – 950 fig.
10. SAMPTON P.D. Dental arch shape: a statistical analysis using conic sections // American Journal of Orthodontics. – 1981; 79: 535–548.
11. SCOTT J.H. The shape of dental arches // Journal of Dental Research. – 1957. – № 36. – P. 996–1003.
12. TUGARIN V.A., PERSIN L.S., POROKHIN A.YU. Modern fixed-type orthodontic appliances Edgewise. – M., 1996. – 220 p.

COMPARATIVE CHARACTERISTICS OF RADIODIAGNOSTICS IN CARDIOLOGY AND CARDIOSURGERY

**G.H. Khachatrian, N.S. Qamalyan, A.G. Karapetyan,
K.V. Khondkaryan**

*Department of Radiological Diagnostics, Mkhitar Heratsi Yerevan State Medical University, Yerevan, Republic of Armenia
Scientific Center of Radiation Medicine and Burns, Ministry of Health, Yerevan, Republic of Armenia*

Radiation methods for studies of various organs and systems continue to be one of the decisive factors in setting the final clinical diagnosis at the earliest stages possible. The latter acquires particular importance when the pathology deals with such a multifunctional organ like the heart.

The task of a clinician is to select the desired set of diagnostic approaches that best reflect the state of the test body both in the anatomical and functional meaning.

The entire arsenal of modern methods used in cardiology is divided into ionizing (x-ray computed tomography with all varieties, coronary angiography, radionuclide methods of research) and non-ionizing (echocardiography and magnetic resonance imaging).

The selective coronary angiography (CAG) is still considered the only reliable method for studying the anatomy of the coronary bed to quantify the degree of stenosis, and myocardial revascularization [1, 25, 18, 10].

Nevertheless, the method has several limitations: invasiveness, radiation exposure, the risk of complications and high costs. However, the negative side of the CAG is purely anatomical and methodological feature: the method is limited only by the assessment of the intraluminal loop of the coronary vessels, not allowing to study the condition of the walls and the functional significance of the stenosis. This fact contributes to inadequate assessment and diagnosis of early manifestations of atherosclerosis.

The following clinical situation occurs: atherosclerosis plaque that does not cause narrowing of the vessel lumen, leads to underestimation or overestimation of the extent and / or severity of atherosclerotic lesions. In these cases, the results of intravascular ultrasound are much more demanded, especially in patients with multiple, but intermediate stenoses [42].

The most reasonable way is to combine the capabilities of modern radiation diagnosis — from the

visualization of the coronary arteries to detection of hidden perfusion abnormalities or acute myocardial infarction with *silent* clinic. In recent clinical situations in tandem CAG and echocardiography (ECHO CG) the third method, radionuclide imaging (SPECT or PET), is added.

However, there are certain inherent difficulties of conducting any diagnostic procedure, especially for ECHO CG. They include: anatomy peculiarities of the coronary arteries (CA), small diameter, hyperkinesis, respiratory excursions of the lungs and chest. [7].

But the method of ECHO CG has undeniable advantages: non-invasive, low cost, availability, the possibility of dynamic studies. In turn, the variety of technologies and techniques allow us to study various functions of the heart (hemodynamics, contractility) and the state of the coronary arteries. From a clinical point of view, the following methods: are mostly demanded direct visualization of atherosclerotic plaque, determination of the rate and nature of coronary blood flow evaluation of coronary reserve in the main vessels, state of hemodynamics in the central circulation, the state inotropic function of the heart muscle, the presence of zones of akinesia and hypokinesia.

However, even with these multifunctional capabilities of the method, there are some difficulties in evaluating each of these advantages.

For example, direct imaging of atherosclerotic plaque in CA is possible with considerable calcium component [1], more frequent at the mouths of the left and right coronary arteries. Naturally, the diagnosis of stricture formation or stenosis is primarily based on the use dopplerographic color mapping methods [3, 31].

Without going into details of technical and methodological conditions of ECHO CG, it should be noted that there are 2 access pathways: the transthoracic and transdermal.

If we consider percutaneous ECH CG, this technique allows to qualitatively visualize the proximal and middle portions of the main coronary arteries [4], but with the damage of the middle and distal parts of the coronary bed, it becomes impossible, because they do not fall into the plane of the ultrasound slice.

Sensitivity and specificity of transesophageal ECHO CG in the diagnosis of proximal coronary stenoses and occlusions, according to different authors, ranges between 32 and 91% at stenosis, and from 76 to 100% — at occlusions [4, 3, 31, 30].

In recent years, for non-invasive study of coronary blood flow and coronary reserve, the method of transthoracic ECHO CG is used [32,33].

In contrast to transesophageal ECHO CG, the transthoracic approach allows visualization of the middle and distal portions [32–36]. For clinicians, of the greatest interest is the opportunity to study coronary flow reserve in the distal parts, as the latter occurs not only in the area of constriction, but also along the distal vessel. A limitation of the method is the duration of the investigation, qualification of a radiologist, variability of location window in individual patients.

Another extensive branch of radiation diagnostics used in cardiosurgical practice is presented by methods of computed tomography (CT), especially the multislice spiral computed tomography (MSCT).

The dynamics of development and CT research findings, which had the following trends and directions, are extremely interesting. In particular, if at the early stages of studying the role of CT in the diagnosis of coronary artery atherosclerosis the presence and degree of calcification were considered, the results of further investigations showed the opposite. The presence, localization and degree of calcification do not always correspond to the location and degree of stricture formation or stenosis revealed during invasive coronary angiography.

The most interesting one was the clinical observation that acute coronary complications more frequently occur due to spontaneous rupture of non-calcified plaque that are not visible on the native images.

Identifying non-calcified (*tender*) plaques is possible using CT angiography. At intravenous bolus of nonionic iodine-containing contrast there is an opportunity to study coronary bed anatomy, malformations, aneurysms of the coronary arteries, to diagnose and evaluate the degree of stenosis, as well as to assess the patency of aortocoronary mammocoronary shunts.

The sensitivity and specificity of the method for diagnosis of stenosis and occlusion of shunts reaches 83-100 and 88-98%, respectively [9, 29, 38].

The disadvantage of the method is radiation load dose to the patient and the possibility of allergic reactions [8, 37].

To our mind, another more significant disadvantage is the fact that it is impossible to study at multislice spiral CT (MSCT) the flow velocity characteristics of the coronary flow and, therefore, only anatomical but not functional assessment of stenoses and occlusions significance is conducted. The presence of causal artifacts (pronounced calcification, heart rate greater than 65 beats/min, arrhythmias) also decreases both the use and quality of the obtained images [28, 17, 23, 24].

Another modern imaging technique for coronary vessels visualization is a magnetic resonance imaging (MRI).

A technical advantage of the method is the lack of exposure to the patient, not using iodinated contrast agents [2].

The method allows to estimate the structure of the atherosclerotic plaque with the determination of lipid and fibrous components, to conduct angiography. However, the ability of MRI for detection of coronary calcification is limited [37].

Visualization of the coronary arteries, taking into account the new generations of MRI, is of higher quality, but limited by the size of visible vessels. Upon the study for the detection of stenoses and occlusions contrast material - gadolinium chelates is injected intravenously.

The sensitivity and specificity of this method in detecting coronary artery stenosis ranges between 65–82% (sensitivity) and 82–89% (specificity) [14].

Disadvantages of MRI include: due to the complexity of the implementation, diagnosis and assessment of stenotic coronary artery remains unsatisfactory for practical medicine. Unlike MSCT these circumstances are linked to the complexity of cardiac and respiratory movements suppression, inadequate suppression of the signal from epicardial fat and myocardium, limited spatial resolution and overlapping of layers in the research area of the heart [43].

There are also relative and absolute contraindications to MRI: as absolute ones pacemakers, hemostatic clips on the vessels are considered, metal brackets on the sternum, stents and artificial heart valves are ranked to be relative contraindications. The investigation is also limited by the risk of the implant displacement, its dysfunction and heating at the investigation [1].

Another large group of radioisotopic research methods are radionuclide methods of research: myocardial tomography imaging to determine myocardial perfusion and metabolism. Currently, two methods - SPECT and PET imaging — are widely used.

SPECT, or single photon emission computed tomography has expressed functional tendency as non-alternative method for the study of myocardial perfusion and the possibility of reversibility of these changes; most commonly such radiopharmaceuticals as radioactive ^{99m}Tc with a set of MIBI (technetium sestamibi) or radioactive thallium-citrate as analog of sodium are used.

Effective and timely reperfusion contributes to the restoration of myocardial contractility, reversibly injured cardiomyocytes, but this process is only possible after the normalization of energy production and

reduction of the intracellular calcium concentration. This recovery occurs more slowly in later periods after the direct reduction of the coronary bed.

Such a situation is possible at hibernating (*stunned*) myocardium (Sokolova R. et al., 2002; Bolli R., 1990; Braunwald E, Kloner RA, 1982). The phenomenon of “stunned” myocardium, especially in the last 10-15 years, is the subject of intense studies [5, 22, 15, 16, 21, 26, 27].

Myocardial scarring is not the only outcome of coronary stenosis and subsequent myocardial ischemia (cardiomyocytes).

In some cases disorder of the inotropic function is accompanied with the preserved viability of cardiomyocytes. Clinical manifestation of such states is ventricular dysfunction (systolic and diastolic).

By the early 1980s, Rahimtoola described a syndrome characterized by reversible damage of the local myocardial contractility at rest with signs of severe prolonged silent ischemia and suggested that the term *hibernation* or *hibernating myocardium* [39, 40] for the characterization of foci of reduced contractility, located in the basin of the stenotic artery [41].

In our opinion, these studies have had revolutionary significance in cardiology and cardiac surgery, as well as other disciplines, especially in terms of radiation diagnostics.

The author and his followers showed that a decrease of contractile function even though it is a major factor in predictions of deteriorating condition of the patient, may be temporary transient. Hibernating myocardium state may be asymptomatic both clinically and paraclinically.

Diagnosis of *stunned* myocardium is possible only upon using radionuclide techniques — SPECT and PET tomography.

PET investigations allow studying metabolic processes in myocardium, especially the metabolism of fatty acids (FAs) and glucose.

Although the first studies were carried out in 1954. [11], especially for the FAs metabolism, they are invaluable till now. It was shown that FAs are a major source of energy in cardiomyocytes.

Another important source of energy for the heart is glucose, which is metabolized through glycolysis [19]. Under normal physiological conditions, the FAs and glucose utilization is balanced and depend on their delivery. It is believed that the contribution of glycolysis to the total amount of energy production in the myocardium under aerobic conditions is no more than 10%. Ischemia of the heart muscle increases the efficiency of the process.

Compared with glucose FAs are less *profitable*: upon their oxidation for the production of the same

amount of ATP by 10% more oxygen is necessary (required) [11]. About 60–70% of oxygen consumed by a man is used for FAs oxidation.

But this proportion might change dramatically during different pathological processes [20]. The authors noted that during hypoxia there occurs inhibition of both glucose and lactate oxidation, as well as the FAs with the simultaneous formation and alteration of energetic process and its deficiency. This is precisely what happens in myocardial ischemia.

To assess glucose and FAs metabolism ^{11}C acetate radiopharmaceutical is used; to study metabolism of glucose — ^{11}R -fluorodeoxyglucose.

The opportunity to study energetic processes in the myocardium by tracing the FAs and glucose is provided by PET imaging method. We have presented the fundamentals and the *basics* of this radiation diagnostics method in detail, as it has no alternative.

In conclusion, we should like to note that the comparative analysis of radiological methods of examinations in cardiology and cardiac surgery indicates that each method has its place in the whole complex of surveys, however, international protocols clearly indicate to the triad of methods: coronary angiography, echocardiography, SPECT/PET tomography.

REFERENCES

1. VRUBLEVSKI A.V., BOSHCHENKO A.A. Modern methods for noninvasive imaging of the coronary arteries in the diagnosis of coronary atherosclerosis. Cardiology. 2007, 7: 83–93 (in Russian).
2. BELENKOV Yu.N., TERNOVOY S.K., SINITSIN V.E. Magnetic resonance tomography of the heart and blood vessels. Moscow. Vidar, 1997; 142p. (in Russian).
3. VRUBLEVSKI A.V. Complex ultrasound assessment of coronary blood flow, coronary reserve, latent myocardial ischemia and structural and functional disorders of the thoracic aorta in patients with coronary heart disease: Author's Abstract of Dissertation for Dr.Med. Sciences. Tomsk, 2006; 53p. (in Russian).
4. VRUBLEVSKI A.V., BOSHCHENKO A.A., KARPOV R.S. Noninvasive ultrasound coronary artery Dopplerography: methodological and diagnostical aspects. Visualization in clinics. 2001; 19: 50–60 (in Russian).
5. KOSTENIKOV N.A., FADEEV N.P., TYUTIN L.A. et al. Comparative evaluation of the diagnostic capabilities of PET with ^{18}F -FDG and ^{1-11}C -sodium butyrate when examining patients with volumic lesions of the brain and impaired cerebral perfusion (results semi-quantitative estimates of data). Bulletin of Rentgenology and radiology. 2002, № 4, pp 4–8 (in Russian).
6. SOKOLOVA R.I., ZHDANOV B.C. Hibernation and stunning as a manifestation of ischemic myocardial dysfunction. Archives of Pathology, 2002, 64, №. 1, pp 50–54 (in Russian).

7. TERNOVOY S.K., SINITSIN V.E.. Spiral CT and electron angiography. Moscow. Vidar. 1998; 144p. (in Russian).
8. TERNOVOY S.K., SINITSIN V.E., GAGARIN H.V. Noninvasive diagnosis of atherosclerosis and coronary artery calcification. Moscow. Atmosphere. 2003, 141p. (in Russian).
9. ACHENBACH S., ROPERS D., POHLE K. ET AL. Clinical results of minimally invasive coronary angiography using computed tomography. *Cardiol Clin* 2003; 21:4:549–559.
10. ACHENBACH S., UHLZHEIMER S., BAUM V. ET AL. Noninvasive coronary angiography by retrospectively ECG-gated multislice spiral CT. *Circulation* 2000; 102: 2823–2828.
11. BING R.J. The metabolism of the heart. *Harvey*. 1954, 55, P. 27–70.
12. BOLLI R. Mechanism of myocardial stunning. *Circulation*, 1990, 82, P. 723–738
13. BRAUNWALD E., KLONER R.A. The stunned myocardium: prolonged, postischemic ventricular dysfunction. *Circulation*, 1982, 66, P. 1146–1149.
14. BUNCE N.H., JHOOTI P., KEEGAN J. ET AL. Evaluation of free-breathing three-dimensional magnetic resonance coronary angiography with hybrid ordered phase encoding (HOPE) for the detection of proximal coronary artery stenosis. *J Magn Res Imaging* 2001; 14: 677–684.
15. CARLSON E., COWLEY M., WOLFGANG T. Acute changes in global and regional rest left ventricular function after coronary angioplasty: comparative results in stable and unstable angina. *J. Am. Coll. Cardiol.*, 1989, 13, P. 1262–1269.
16. CHATTERLEE K., SWAN H., PAMLEY W. Influence of direct myocardial revascularization on left ventricular asynergy and function in patients with coronary heart disease with and without previous myocardial infarction. *Circulation*, 1973, 47, P. 276–286.
17. CORDERIO M.A.S., MILLER J.M., SCHMIDT A. ET AL. Non-invasive half millimetre 32 detector row computed tomography angiography accurately excludes significant stenoses in patients with advanced coronary artery disease and high calcium scores. *Heart* 2006; 92:589–597.
18. DE BONO D. Complications of diagnostic cardiac catheterization: results from 34041 patients in the United Kingdom confidential enquiry into cardiac catheter complications. *Br Heart J* 1993; 70: 297–300.
19. DEPRE Ch., VANOVERSCHELDE J.L., TAEGTMAYER H. Glucose for the heart. *Circulation*, 1999, 99 P. 578–588.
20. DRAKE A.J., RAINES JR., NOBLE MIM. Preferential uptake of lactate by the normal myocardium in dogs. *Cardiovasc. Res.*, 1980, 14, P. 65–72.
21. FALESCHOT G., FARAGGI M., DROBINSH G. Myocardial viability in patients with Q wave myocardial infarction and no residual ischemia. *Circulation*, 1992, 86, P. 47–55.
22. FERRARI R. The new ischemic syndromes — an old phenomenon disguised with a new glossary? *Cardiovasc. Res.*, 1997, 36, P. 298–300.
23. GARSIA M.J., LESSICK J., HOFFMAN M.H.K. Accuracy of 16-row multidetector computed tomography for the assessment of coronary artery stenosis. *JAMA* 2006; 296: 403–411.
24. GHERSIN E., LITMANOVICH D., DRAGY R. 16-MDCT coronary angiography versus invasive coronary angiography in acute chest pain syndrome: a blinded prospective study. *Am J Roent* 2006; 186: 177–184.
25. HABERL R., BECKER A., LEBER A. ET AL. Correlation of coronary calcification and angiographically documented stenoses in patients with suspected coronary artery disease: results of 1764 patients. *J Am Coll Cardiol* 2001; 37: 451–457.
26. HEUSCH G. Hibernating myocardium. *Physiol. Rev.*, 1998, 78, P. 1055–1085.
27. HEUSCH G., SCHUZ R. Hibernating myocardium: a review. *J. Mol. Cell. Cardiol.*, 1996, 28, P. 2359–2372.
28. HEUSCMID M., KUETTNER A., SCHROEDER S. ET AL. ECG-gated 16-MDCT of the coronary arteries: assessment of image quality and accuracy in detecting stenoses. *Am J Roent* 2005; 184: 1413–1419.
29. HONG C., CHRYSANT G.S., WOODARD P.K., BAE K.T. Coronary artery stent patency assessed with in-stent contrast enhancement measured at multi-detector row CT angiography: initial experience. *Radiology* 2004; 233: 286–291.
30. ISAAZ K., DA COSTA A., DE PASQUALE J.P. ET AL. Use of the continuity equation for transesophageal Doppler assessment of severity of proximal left coronary artery stenosis: a quantitative coronary angiography validation study. *J Am Coll Cardiol* 1998; 32: 42–48.
31. KASPRZAK J.D., KRZEMINSKA-PAKULA M., DROZDZ J. ET AL. Definition of normal flow parameters in proximal coronary arteries using transesophageal Doppler echocardiography. *Echocardiography* 2000; 17: 141–150.
32. KORCARZ C.E., STEIN J.H. Noninvasive assessment of coronary flow reserve by echocardiography: technical considerations. *J Am Soc Echocardiogr* 2004; 17: 6: 704–707.
33. KRZANOMKI M., BODZON W., BRZOSTEK T. ET AL. Value of transthoracic echocardiography for the detection of high-grade coronary artery stenosis: prospective evaluation in 50 consecutive patients scheduled for coronary angiography. *J Am Soc Echocardiogr* 2000; 13: 1091–1099.
34. KRZANOMKI M., BODZON W., PETKOW DIMITROW P. Imaging of all three coronary arteries by transthoracic echocardiography. An illustrated guide. *Cardiovascular Ultrasound* 2003; 1: 16:1–51.
35. LAMBERTZ H., TRIES H.P., STEIN T., LETHEN H. Noninvasive assessment of coronary flow reserve with transthoracic signal-enhanced Doppler echocardiography. *J Am Soc Echocardiogr* 1999; 12: 186–195.

36. LETHEN H., TRIES H. P., BRECHTKEN J. ET AL. Comparison of transthoracic Doppler echocardiography to intracoronary Doppler guidewire measurements for assessment of coronary flow reserve in the left anterior descending artery for detection of restenosis after coronary angioplasty. *Am J Cardiol* 2003; 91: 4: 412–417.
37. PHAN M.L. STATE-OF-THE-HEART IMAGING: The current state of noninvasive cardiac imaging. Applications in imaging. *Cardiac Intervent* 2004; 22–27.
38. MAINTZ D., JUERGENS K.U., WICHTER T. Imaging of coronary artery stents using multislice computed tomography: in vitro evaluation. *Eur. Radiol.* 2003; 13: 830–835.
39. RAHIMTOOLA S.A. Perspective on the three large multi-center randomized clinical trials of coronary bypass surgery for chronic stable angina. *Circulation*. 1985, 72. P. 123–135.
40. RAHIMTOOLA S. Importance of diagnosing hibernating myocardium: how and in whom? *J. Am. Coll. Cardiol.*, 1997, 30, P. 1701–1706.
41. RAHIMTOOLA S.H. The hibernating myocardium. *Am. Heart J.*, 1989, 117, P. 211–221.
42. RODENWALDT J. Multislice computed tomography of the coronary arteries. *EurRadiol* 2003; 13: 748–757.
43. RUMBERGER J. A., SHEEDY P.F, BREEN J.F., SCHWARTZ R.S. Coronary calcium, as determined by electron beam computed tomography, and coronary disease on arteriogram: effect of patient's sex on diagnosis. *Circulation* 1995; 91: 1363–1367.

HUMAN HEALTH COST OF HYDROGEN SULFIDE AIR POLLUTION FROM AN OIL AND GAS FIELD

D.U. Kenessary*, U.I. Kenessariyev, A.U. Kenessary

Kazakh National Medical University, Almaty,
Republic of Kazakhstan

ABSTRACT

INTRODUCTION AND OBJECTIVE: The Karachaganak oil and gas condensate field (KOGCF) is one of the largest in the world, located in the Republic of Kazakhstan (RoK), Central Asia, and is surrounded by 10 settlements with total population of 9,000 people. Approximately 73% of this population constantly mention a specific rotten eggs odor in the air that is typical for hydrogen sulfide emissions and the occurrence of low-level concentrations of hydrogen sulfide around certain industrial installations (ex.: oil refineries) is a well known fact. Therefore human health impact, as well as economic damage to the country due to H₂S emissions were determined.

MATERIALS AND METHODS: Dose-response dependency between H₂S concentrations in the air and cardiovascular morbidity using multiple regression analysis was applied in this research. Economic damage from morbidity was derived with a newly developed method with Kazakhstani peculiarities taken into account.

RESULTS: Hydrogen sulfide air pollution due to the KOGCF activity cost the state almost \$60,000 per year. Moreover, this is the reason for over 40% rise of cardiovascular morbidity in the region.

CONCLUSION: The reduction of hydrogen sulfide emissions into the air is recommended, as well as successive constant ambient air monitoring in future. Economic damage evaluation should be made mandatory, on a legal basis, whenever an industrial facility operations result in associated air pollution.

KEYWORDS — hydrogen sulfide, human health, economic damage, air pollution, oil field, Kazakhstan

INTRODUCTION

Today, secondary to continuous industrialization of the society the anthropogenic environmental impact has increased manifold, which cannot help affecting the health of the exposed population. According to WHO reports, globally only 3.7 million deaths were attributable to ambient air pollution in 2012. About 88% of these deaths occurred in low and middle income countries [1]. Former Soviet republics, including the Republic of Kazakhstan (RoK, Central Asia), just can be attributed to those middle-income countries, where the health care services desperately need to harmonize the existing post-Soviet legal documentation with the international practices. In this connection, the main goal is to identify the main risk factors for



Dinara Kenessary

PhD in Public health

dku999@mail.ru

occurrence of additional morbidity and mortality in various environmentally disadvantaged areas, including oil and gas facilities, like the Karachaganak field (KOGCF) discovered in 1979 on the territory of the western Kazakhstan.

Being one of the largest oil and gas condensate fields in the world it has an estimated 1.2 billion tons of oil reserves. In view of continuous emissions of combustion products from the field, for more than 20 years the air quality and human health have been continuously monitored in the nearest villages (5-15 km) with a total population of 9,000 people. Moreover the health status of the exposed population was compared with that of Alexandrovka village which is similar to the exposed villages according to the climate, geographic position, socio-economic, gender and age parameters but is situated at a significant distance (50 km) from the field [2-4].

The sociological survey made by Alikeeva in 2009 in the nearest village Berezovka (5 km from the field) showed that over 90% of respondents have mentioned a specific odor in the air: oil products (12%), ammonia (12%), and especially rotten eggs (73%) [5]. As explained by Hirsch et al., rotten eggs odor is typical for hydrogen sulfide (H₂S). Inhalation of air containing a small amount of hydrogen sulfide causes dizziness, headache, and nausea whereas significant concentrations lead to coma, convulsions, pulmonary edema and even death [6].

In 2006 Erzhanova with the use of a multiple regression analysis between morbidity and concentrations of chemical elements in the air of Berezovka village confirmed the influence of hydrogen sulfide chronic exposure on appearance of additional cardiovascular morbidity cases [7].

Human health risk assessment from the KOGCF emission, based on modeled data (Kenessariyev et al. in 2011) did not include hydrogen sulfide into the air pollutants priority list due to insufficient share (less than 1%) from total emissions and low expected chronic concentrations of chemical that led to insignificant health risk ($HQ < 1$) [8]. However due to numerous complaints from the habitants of the nearby villages a decision was made to include hydrogen sulfide into the list of chemicals to be constantly monitored.

MATERIALS AND METHODS

The data on H_2S was collected using the environmental monitoring stations (EMS) installed in the above mentioned villages.

Brief description of the EMS

Continuous monitoring of ambient air was done with the help of 14 EMS that automatically collected data for every 10 seconds. The data from EMS may be averaged for any length interval. The minimum detection limit is less than 0.00056 mg/m^3 . The stations are connected to the emergency response services thus permitting timely alert of the local governments (akimats) and population when excessively high concentrations of pollutants, hazardous for health and life of population, are detected [9].

Determination of additional cardiovascular morbidity

According to Erzhanova A. [7] an increase in the daily average concentration of H_2S by 0.001 mg/m^3 increases by 1.1 times the cardiovascular morbidity (if by 0.002 mg/m^3 , then 2.2 times, respectively). In this case 2 times increase means that 50% of general morbidity (M) is an additional morbidity due to increased concentration of H_2S (Ma). Therefore additional morbidity in percentage ($Ma\%$) is a multiplication of quantity of times of increase (k) by 50% and divided by 2 times. So, additional cardiovascular incidence (Ma) was calculated with the next formula:

$$Ma = M * Ma\% / 100\% \\ Ma\% = k * 50\% / 2$$

Economic damage evaluation

Economic damage from morbidity is a sum of multiplication of a single case morbidity cost (Mc_y) and additional morbidity risk (Mr_y) calculated separately for each age group (y) – children, adolescents, adults, and seniors.

$$EDm = \sum Mc_y * Mr_y$$

Single case morbidity cost is a sum of a cost of a treated case (TC), sick-pay (SIC), disability benefits

(SSC) and loss of tax revenue to the budget and extra-budgetary funds (TRL):

$$Mc_y = TC + SIC + SSC + TRL$$

Treated case cost is equal to the medical-economic tariffs, officially approved by the state in 2011 [10].

Sick pay cost was calculated by multiplying the cost of one day of disability according to the sick list (s), number of lost days of work (d) and coefficient of employed people share in the study group (k_w).

Disability benefits cost was not calculated due to the lack of data on disability from the explored diseases.

Loss of tax revenue to the budget due to sickness was calculated by multiplying d to k_w and average value of the total income tax attributable to spent man-day (t). This t -value consists of corporate income tax revenues (t_{ci}), personal income tax revenues (t_{pi}) and single social tax revenues (t_{ss}) and is calculated in a next way:

$$t = (t_{ci} + t_{pi} + t_{ss}) / (d_w * Q_w)$$

where d_w — quantity of working days in a year; Q_w — quantity of working people in Kazakhstan for 2012.

RESULTS

Maximum average monthly concentrations of hydrogen sulfide in some of the selected villages exceeded the reference point concentrations in the range of 0.001 – 0.002 mg/m^3 , as shown in Table 1.

Therefore it became necessary to quantify the degree of negative health impact from excess H_2S . Calculated additional cardiovascular morbidity cases caused by the increase in the maximum monthly average concentrations of H_2S equaled 67.1 cases out of total 166, including 57.2 additional cases of diseases among the working population (out of 141), 8.8 cases among seniors (out of 23) and 1.1 cases among adolescents and children (out of 2). The results of the calculations are shown in Table 2.

Economic damage from additional cases of cardiovascular diseases due to excess concentrations of H_2S equaled \$59,610 and was highest among the Kiziltal habitants — \$37,613 (Table 3).

Although the economic damage evaluation methodology used in this study might have similarities all around the world, the peculiarities of Kazakhstani health care system, taken into consideration while designing this exact specific method, have a number of differences. In particular, we used medical and economic tariffs (MET) [11] to calculate the cost of treatment instead counting the price of one day of hospitalization multiplied by the length of staying as

Table 1. H₂S monthly average highest concentrations in selected villages

Selected rural ambulance (outpatient clinic)(RA), named by the location	Maximum monthly average concentration in 2012, mg/m ³	Over the reference point village concentration, mg/m ³
Berezovka (EMS 13-14)	0.002	0.001
Priuralny (EMS 8)	0.002	0.001
Zharsuat (EMS 7) (including Zhanatalap)	0.002	0.001
Kiziltal (EMS 10-11)	0.003	0.002
Alexandrovka RA (reference point)	0.001	

Table 2. Additional cardiovascular morbidity

Selected Rural ambulance	Berezovka	Priuralny	Zharsuat (including Zhanatalap)	Kiziltal
H ₂ S concentrations (C), mg/m ³	0.001	0.001	0.001	0.002
Dose-response dependence (k), times	1.1	1.1	1.1	2.2
Percentage of Ma out of M (Ma%), %	27.5	27.5	27.5	55
	Total	45	16	27
General morbidity (M), cases	adults	41	12	21
	seniors	4	4	6
	adolescents	0	0	0
	children	0	0	1
	Total	12.4	4.4	7.4
Additional morbidity (Ma), cases	adults	11.3	3.4	5.9
	seniors	1.1	1	1.5
	adolescents	0	0	0
	children	0	0	0.55

made in the Russian Federation. These tariffs already include the cost of payment for the medical workers, social taxes, nutrition and drugs. The cost of MET in our exact case is the arithmetic mean of the arterial hypertension and coronary heart disease MET, since in more than 90% of cases the above were diagnosed upon first visits of the Burlin district patients with cardiovascular diseases.

DISCUSSION

Although the negative impact of acute H₂S exposure is already known for decades, epidemiological

Table 3. Economic damage from additional cases of circulatory system disease due to excess concentrations of H₂S

Selected rural ambulance	Berezovka			
Age groups	1	2	3	4
Quantity of inhabitants, Q	1923	1359	132	52
Morbidity risk, Mry	12	11	1	0
Economic damage, EDm	11279	10679	599	0
Single case morbidity cost , Mcy	n/c	947	547	547
Cost of a treated case , TC	n/c	547	547	547
Medical-economic tariff	n/c	547	547	547
Sic-pay cost , SIC	733	367	n/c	n/c
Cost of one day of disability , s=3Π/dw	n/c	53	n/c	n/c
Number of lost days of work, d	n/c	10	n/c	n/c
Coefficient of employed people share , kw	n/c	0.7	n/c	n/c
Loss of tax revenue to the budget , TRL	66.05143	3.3E+01	n/c	n/c
Average value of the total income tax , t	9.480516	4.7E+00	n/c	n/c
Corporate income tax revenues, tci	n/c	6.94E+09	n/c	n/c
Personal income tax revenues, tpi	n/c	2.92E+09	n/c	n/c
Single social tax revenues, tss	n/c	2.27E+09	n/c	n/c
Quantity of working people in a studied group, qw	939	939	n/c	n/c
Quantity of working days in a year, dw	n/c	301	n/c	n/c
Quantity of working people in Kazakhstan , Qw	n/c	8.51E+06	n/c	n/c

Comments: 1—total number of people, 2—adults, 3—seniors, 4—adolescents, 5—children; n/c—no need to be calculated.

Total cost denominated in the national currency tenge (KZT) was converted into USD at the exchange rate set by of the National Bank of Kazakhstan: KZT150 / USD1. Source: references [9, 20–25]

data concerning longer-term exposures are still limited. Before the 1990s the main regulatory assumption was that if an exposure to H₂S is not fatal, there are few, if any, lasting health effects. But this view became medically outdated due to numerous investigations.

According to the research by Kilburn et al. symptoms of chronic exposure to H₂S include pronounced deficits in balance and reaction time, dizziness, insomnia, and overpowering fatigue [12]. These investigators stated that H₂S poisons the brain, and the poisoning is irreversible.

Legator et al. [13] determined that over 86% of the population under chronic exposure to H₂S experienced central nervous system impairment similar to that described by Kilburn et al. vs. only 26% of a reference point population (20 miles away from the plant). Tarver et al. also stated that people living near an industrial plant demonstrated attention deficits and an inability to process information quickly [14].

Teams of researchers at separate institutions have discovered evidence that H₂S even damages DNA [15–18].

The occurrence of low-level concentrations of H₂S around certain industrial installations is a well

	Priuralni					Zharsuat					Kizital				
5	1	2	3	4	5	1	2	3	4	5	1	2	3	4	5
380	1232	667	204	38	323	2001	1263	329	67	342	3768	2165	303	160	1140
0	4	3	1	0	0	7	6	2	0	0	43	37	5	1	1
0	3944	3381	564	0	0	6774	5934	840	0	0	37613	33994	2808	301	510
947	n/c	1003	547	547	1003	n/c	1007	547	547	1007	n/c	927	547	547	927
547	n/c	547	547	547	547	n/c	547	547	547	547	n/c	547	547	547	547
547	n/c	547	547	547	547	n/c	547	547	547	547	n/c	547	547	547	547
367	837	418	n/c	n/c	418	844	422	n/c	n/c	422	697	348	n/c	n/c	348
53	n/c	53	n/c	n/c	53	n/c	53	n/c	n/c	53	n/c	53	n/c	n/c	53
10	n/c	10	n/c	n/c	10	n/c	10	n/c	n/c	10	n/c	10	n/c	n/c	10
0.7	n/c	0.8	n/c	n/c	0.8	n/c	0.8	n/c	n/c	0.8	n/c	0.7	n/c	n/c	0.7
3.3E+01	7.5E+01	3.8E+01	n/c	n/c	3.8E+01	7.6E+01	3.8E+01	n/c	n/c	3.8E+01	6.3E+01	3.1E+01	n/c	n/c	3.1E+01
4.7E+00	9.5E+00	4.7E+00	n/c	n/c	4.7E+00	n/c	4.7E+00	n/c	n/c	4.7E+00	n/c	4.7E+00	n/c	n/c	4.7E+00
n/c	n/c	6.94E+09	n/c	n/c	n/c	n/c	6.94E+09	n/c	n/c	n/c	n/c	6.94E+09	n/c	n/c	n/c
n/c	n/c	2.92E+09	n/c	n/c	n/c	n/c	2.92E+09	n/c	n/c	n/c	n/c	2.92E+09	n/c	n/c	n/c
n/c	n/c	2.27E+09	n/c	n/c	n/c	n/c	2.27E+09	n/c	n/c	n/c	n/c	2.27E+09	n/c	n/c	n/c
n/c	526	526	n/c	n/c	n/c	1005	1005	n/c	n/c	n/c	1422	1422	n/c	n/c	n/c
301	n/c	301	n/c	n/c	301	n/c	301	n/c	n/c	301	n/c	301	n/c	n/c	301
n/c	n/c	8.51E+06	n/c	n/c	n/c	n/c	8.51E+06	n/c	n/c	n/c	n/c	8.51E+06	n/c	n/c	n/c

known fact. Low-level concentrations may occur continuously in certain industries, such as in viscose rayon and pulp production, in geothermal energy installations and at oil refineries, where there is a high risk of exposure for the general population. A large accidental release of H₂S into the air surrounding industrial facilities can cause very severe effects, as at Poza Rica, Mexico, where 320 people were hospitalized and 22 died [19].

As seen from the research on the impact of chronic H₂S exposure has been underestimated for a long period of time. People in countries with weak environmental protection regulations are constantly under chronic exposure to numerous chemicals, including H₂S that is an important chemical for Kazakhstan, since oil mining is one of the driving forces in the country's economy.

CONCLUSION

Hydrogen sulfide air pollution due to the KOGCF activity costs Kazakhstan budget almost \$60,000 per year. Moreover, this is the reason for over 40% rise of cardiovascular morbidity in the affected villages. In this regard the reduction of hydrogen sulfide emissions into the air is recommended, as well as successive constant ambient air monitoring in future.

We suggest that evaluation of economic damage should be made mandatory, on a legal basis, whenever

an industrial facility operations result in associated air pollution.

The results of this research should be included as determining an expense item in the statutory payments made by an enterprise to the government, in order to rehabilitate the health of the exposed population, within the framework of the Free Public Health Care system.

REFERENCES

- WHO databases. Burden of disease from Ambient Air Pollution for 2012. Summary of results. Available from: www.who.int/phe/health_topics/outdoorair/databases/FINAL_HAP_AAP_BoD_24March2014.pdf - 91k.
- KENESSARIYEV UI. Hygienic basis of assessment prognoses and development of environmental-health system at KOGCF. [dissertation]. Almaty (RoK); 1993.
- OMARKOJAEVA GN. Complex assessment of environment quality and risk-factors of oil fields [dissertation]. Almaty (RoK); KazNMU; 2006.
- KURMANGALIEV OM. Ecological and hygienic aspects of forming pathology of the genitourinary system in RoK oil and gas condensate regions (on an example of KOGCF). [dissertation]. Almaty (RoK); 2008
- ALIKEEVA GM. Hygienic assessment and prognoses of sanitary-demographic processes in KOGCF region [dissertation]. Almaty (RoK); KazNMU; 2001.

6. HIRSCH AR, ZAVALA G. Long-term effects on the olfactory system of exposure to hydrogen sulphide. *Occup Environ Med* 1999; 56:284–287. Available from: <http://oem.bmjjournals.com/content/56/4/284.full.pdf>
7. ERZHANOVA AE. Mathematical modeling of the air quality effect on public health (on the example of the Karachaganak oil and gas field). *Veda a vznik – 2009/2010: Proceedings of the 5th International scientific conference; 2009–2010; 27 December – 5 Jan; Prague; Czech Republic.* p. 7–9.
8. KENESSARIYEV UI, DOSMUKHAMEDOV AT, AMRIN MK, ERZHANOVA AE. Human health risk assessment in oil and gas condensate region. *Vestnik KazNNU.* 2012. №1: 334–336. Available from: <http://kaznmu.kz/press/>
9. GLADKIH AU, SHIRYAEVA T, PODORENKO EN, KAMAEVA TA, KAIDAKOVA NN ET AL. Established Karachaganak oil gas and condensate field sanitary protection zone; Volume-1; Kazakhstan Agency of Applied Ecology; Almaty, 2013. Project. pp. 19-20, pp. 131–135, p. 202. Contract No: AP/Y/13/0272. Sponsored by KPO b.v.
10. RoK Government Decree No1400. On the remuneration system for civil servants, employees of organizations financed from the state budget, workers of state enterprises. Dec 29, 2007. Available from: http://online.zakon.kz/Document/?doc_id=30155616
11. RoK Ministry of Health Decree No936 (30.12.2011). Appendix 11. Available from: http://www.03portal.kz/images/stories/prilozheniya_pr936_301211.pdf
12. KILBURN KH, THRASHER JD, GRAY MR. Low-level hydrogen sulfide and central nervous system dysfunction. *Environ Epidemiol Toxicol* 1999;1:207–17. Available from: <http://punapono.com/docs/Kilburn1.pdf>
13. LEGATOR MS, SINGLETON CR, MORRIS DL, PHILIPS DL. Health effects from chronic low-level exposure to hydrogen sulfide. *Arch Environ Health.* 2001 Mar-Apr; 56(2):123-31. Available from: <http://www.ncbi.nlm.nih.gov/pubmed/11339675>
14. TARVER GA, DASGUPTA PK. Oil Field Hydrogen Sulfide in Texas: Emission Estimates and Fate. *Environ Sci Tech* 1997;31:3669-3676.
15. MATIAS SA, ELIZABETH DW, MICHAEL JP, GASKINS HR. Evidence That Hydrogen Sulfide Is a Genotoxic Agent. *Molecular Cancer Research* 2006 4:9-14. Available from: <http://mcr.aacrjournals.org/content/4/1/9.abstract>
16. MATIAS SA, ELIZABETH DW, GASKINS HR, MICHAEL JP. Hydrogen Sulfide Induces Direct Radical-Associated DNA Damage. *Molecular Cancer Research.* May 1, 2007 5(5):455–459.
17. Available from: <http://mcr.aacrjournals.org/content/5/5/455.full?sid=eecd1bb4-0c98-493d-9655-baa48ca29a52>
18. BASKAR R, LI L, MOORE PK. Hydrogen sulfide-induces DNA damage and changes in apoptotic gene expression in human lung fibroblast cells. *FASEB J.* 2007 Jan;21(1):247–55. Epub 2006 Nov 20. Available from: <http://www.ncbi.nlm.nih.gov/pmc/articles/1711674/>
19. SAADAT M, ZENDEH-BOODI Z. Association between genetic polymorphism of GSTT1 and depression score in individuals chronically exposed to natural sour gas. *Neurosci Lett.* 2008 Apr 11;435(1):65-8. doi: 10.1016/j.neulet.2008.02.008. Epub 2008 Feb 9.
20. Hydrogen sulfide. Geneva, World Health Organization, 1981 (Environmental Health Criteria, No. 19). Available from: http://www.euro.who.int/__data/assets/pdf_file/0019/123076/AQG2ndEd_6_Hydrogensulfide.PDF
21. Statistical Annals. Kazakhstan in 2012. RoK statistics Agency. Astana. 2013. Available from: <file:///localhost/C:/Users/user/Downloads/1-Казахстан%20в%202012%20роы.pdf>
22. Health of the RoK and the Activities of Health Care Organizations in 2012. Statistical Book. The Ministry of Health (RoK). Astana. 2013.
23. Diagnostic and treatment protocols for diseases (intended for primary health care facilities). LBC 51.1 (2) 2. RoK Ministry of Health Decree No 655 (30.12.2005).
24. Diagnostic and treatment protocols for diseases (intended for hospitals of therapeutic type). LBC 53.5. RoK Ministry of Health Decree No 655 (30.12.2005).
25. RoK Labor Code (including amendments and additions). Art.159, paragraph 3 (04.07.2013).
26. Burlin central district hospital Statistics Division. Data on the primary morbidity and demographic indicators in 2012.

UNTERSUCHUNGEN ZU WIRKUNGEN ADJUVANTER BEHANDLUNGSMASSNAHMEN (BIOKORREKTUR UND PHYSIKALISCHE GEFÄSSTHERAPIE) AUF DEN FUNKTIONSZUSTAND DER MIKROZIRKULATION BEI PATIENTEN MIT DIABETES MELLITUS TYP II. ERGEBNISSE EINER PLACEBOKONTROLLIERTEN STUDIE

**R. Klopp¹, W. Niemer¹, J. Schulz², O. Marksteder³,
N. Abdulkirimova³**

¹Institut für Mikrozirkulation,
Campus Berlin-Buch / Bernau b. Berlin, D.

²ICP Health Care, Campus Berlin-Buch, D.

³Noventalis, Nem. Institut Systemnoi BioKorrekkii,
Saki, Rep. Krim i.d. Russ. Föderation



Dr.med. Rainer Klopp
Institut für Mikrozirkulation
Berliner Str. 25
16321 Bernau bei Berlin

Prof.Dr.med. Jörg Schulz
Campus Berlin-Buch
Robert-Rössle-Str. 10
13125 Berlin

EINLEITUNG

Ein absoluter oder relativer Insulinmangel führt zu Diabetes mellitus, wobei der relative Mangel an Insulin (Diabetes Typ II) sehr viel häufiger auftritt als der absolute Insulinmangel und in den heutigen Industriestaaten einen vorderen Platz in den Morbiditätsstatistiken einnimmt. Auswirkungen des relativen Insulinmangels sind Hyperglykämie und Hyperlipidämie und deren Folgen : Advanced Glycation Endproducts AGE, Gefäßwandschädigungen, Durchblutungsstörungen, Retinaschädigungen, diabetische Nephropathie, arterielle Hypertonie u.a.m. In sehr vielen Fällen leiden Patienten mit Diabetes Typ II an Fettstoffwechselstörungen und arterieller Hypertonie (Metabolisches Syndrom) mit den bekannten Folgen : myokardiale Effekte, Polyangioneuropathie, arteriosklerotische Gefäßwandschädigungen sowie diabetische Mikroangiopathie. Das Metabolische Syndrom sollte daher zutreffender Metabolisch-vaskuläres Syndrom genannt werden.

Körperliche Betätigung (Sport) ist eine wirksame Therapiemaßnahme bei Diabetikern mit ihrer erhöhten Blutglukosekonzentration, da bei körperlicher Aktivität Glukose auch ohne Insulin in die Muskelzellen zur Energiegewinnung im Zellstoffwechsel

gelangen kann, wodurch die Konzentration von Glukose im Blut gesenkt wird. Bei körperlicher Aktivität benötigen Diabetiker weniger Medikamente (orale Antidiabetika, Insulin), wobei Kohlenhydratzufuhr, körperliche Aktivität und Medikamentendosierung individuell aufeinander abgestimmt sein müssen, um eine Hypoglykämie zu vermeiden.

In Abhängigkeit vom Aktivitätszustand des Organismus erfolgt die Energiebereitstellung in den Zellen im Wesentlichen über die Oxydation von Kohlehydraten und Fetten. Ob im Organismus zu einem bestimmten Zeitpunkt eher Kohlehydrate oder Fette verbrannt werden, lässt sich aus den Verhältnis der Kohlendioxydabgabe und der Sauerstoffaufnahme bestimmen (respiratorischer Quotient RQ). Da bei der Verbrennung von Fetten bekanntlich mehr Sauerstoff benötigt wird als bei der Verbrennung von Kohlehydraten, ist der RQ bei der Fettverbrennung niedriger als bei der Kohlehydratverbrennung. Bei körperlicher Betätigung wird somit durch eine erhöhte Sauerstoffzufuhr (Bewegung unter hyperoxischen Bedingungen)

die Fettverbrennung begünstigt, was für die zumeist übergewichtigen Diabetiker von großer Bedeutung ist.

Basierend auf Erfahrungen und Untersuchungen der russischen Raumfahrtmedizin haben SCHULZ et al. [13] das adjuvante Behandlungsverfahren „BioKorrektur“ vorgeschlagen und erprobt, bei dem eine individuell angepaßte (RQ-gesteuerte) Bewegungsbehandlung mit definierten Belastungsbedingungen am Laufband unter hyperoxischen Umgebungsbedingungen (Raumluft mit 26 Vol.% Sauerstoff) Anwendung findet. Die Untersuchungsergebnisse von zwei Pilotstudien mit Stichproben aus Diabetes-Patienten Typ II wurden von SCHULZ et al. im Jahr 2013 mitgeteilt, wobei anhand systemischer laborklinischer Befunde therapierelevante Wirkungen insbesondere auf Parameter des Fettstoffwechsels nachgewiesen wurden. [13]

Eine therapeutisch wirksame Anwendung der BioKorrektur-Bewegungsbehandlung bei Patienten mit Metabolisch-vaskulärem Syndrom ist jedoch nur dann gegeben, wenn die Regulationsmechanismen der Organdurchblutung eine stoffwechseladäquate Realisierung der Transportphänomene des Stoffaustausches zumindest annähernd gewährleisten. Es ist davon auszugehen, daß bei Patienten mit Diabetes mellitus Typ II insbesondere verschiedene vaskuläre Schädigungen und mehr oder weniger eingeschränkte Regelbreiten lokaler und übergeordnet angesteueter Mechanismen der Organdurchblutung vorliegen. Es stellt sich die Frage : Ist unter den Bedingungen der definierten Bewegungsbehandlung eine weitgehend stoffwechseladäquate Durchblutungsregulation insbesondere der aktivierte Skelettmuskulatur gewährleistet ? Hierzu haben KLOPP et al. im Jahr 2014 [9] Meßdaten aus einer orientierenden Studie an einer kleinen Patientenstichprobe ($n = 8$) vorgelegt, bei der sich anhand repräsentativer Merkmale zum Funktionszustand der Mikrozirkulation ein Stimulierungseffekt der Durchblutungsregulation bei den behandelten Diabetes-Patienten zeigte.

Die biorhythmisch unterschiedlichen Vasomotionen in großkalibrigen Arteriolenabschnitten und in den nachgeschalteten kleinkalibrigen Arteriolenabschnitten, welche unmittelbar in die kapillären Netzwerke münden, determinieren die Entmischungsphänomene zwischen Blutzellen und Blutplasma im Bereich der Mikrogefäß und damit den Verteilungszustand des Plasma-Blutzell-Gemisches in den kapillären Netzwerken, wobei die Vasomotionen im großkalibrigen Arteriolenabschnitt übergeordnet, d.h. nerval und humorale, geregelt werden, die Vasomotionschwankungen im kleinkalibrigen Arteriolenabschnitt jedoch spontan, autorhythmisch erfolgen und einer lokalen Regulierung im Rahmen der schubspannungsabhängigen endothelvermit-

telteten Tonusregulation dienen [3, 4, 11, 12, 14]. Es ist bekannt, daß defizitäre arterioläre Vasomotionen, insbesondere die spontanen Vasomotionen, durch einen spezifischen biometrisch definierten Signalkomplex in einem gewissen Ausmaß stimuliert werden können (Physikalische Gefäßtherapie BEMER) [5, 6, 7, 8]. Ein gemeinsamer adjuvanter Einsatz von BioKorrektur und Physikalischer Gefäßtherapie erscheint daher erfolgversprechend.

Die Autoren der vorliegenden Studie haben sich die Aufgabe gestellt, im Rahmen einer placebokontrollierten, verblindeten Untersuchungsreihe an einer hinreichend großen Patientenstichprobe einen Beitrag zur Klärung folgender Fragen leisten :

1. Lassen sich die von SCHULZ et al. [13] und KLOPP et al. [9] mitgeteilten Untersuchungsergebnisse zu Wirkungen der BioKorrektur an einem größerem Patientengut bestätigen ?
2. Kann durch einen zätzlichen Einsatz der Physikalischen Gefäßtherapie BEMER eine Steigerung des Behandlungserfolges der BioKorrektur erzielt werden ?

AUFGABENSTELLUNG, MATERIAL UND METHODEN

Im Rahmen einer placebokontrollierten Untersuchungsreihe war an einer weitgehend homogenen Stichprobe aus 20 ambulanten Patienten mit Diabetes mellitus Typ II durch valide Messungen repräsentativer Merkmale des Funktionszustandes der Mikrozirkulation mit hochauflösenden Untersuchungsmethoden zu prüfen, ob und in welchem Ausmaß durch die Anwendung der adjuvanten Bewegungsbehandlung „BioKorrektur“ eine effektive stoffwechseladäquate Stimulierung mikrozirkulatorischer Durchblutungsregulationen realisiert wird und ob die von SCHULZ et al [13] erhobenen systemischen Stoffwechseldaten im Einklang mit den von KLOPP et al. [9] erhobenen mikrozirkulatorischen Befunden an einer größeren Patientenstichprobe funktionsdiagnostisch anhand von Merkmalen der Mikrohemodynamik in repräsentativen Targetgeweben bestätigt werden können. Des weiteren ist zu prüfen, ob und in welchem Ausmaß eine zusätzliche Anwendung der Physikalischen Gefäßtherapie BEMER den therapeutischen Erfolg der BioKorrektur zu steigern vermag.

In die Untersuchungen war eine Stichprobe aus 20 älteren männlichen und weiblichen Patienten mit Diabetes mellitus Typ II einbezogen (ambulante Rehabilitanden mit eingestelltem Diabetes, mäßig adipös, geringe arterielle Hypertonie, GCP-konforme Definition der Ein- und Ausschlusskriterien). Die Tabelle 1 informiert über die Konstitutionsdaten der untersuchten Patienten.

Tabelle 1. Konstitutionsmerkmale der Patienten
(Mittelwerte und Standardabweichungen)

Alter (Jahre)	Körpermasse (kg)	Körperlänge (cm)	Geschlecht
54,9 ± 2,91	79,8 ± 5,27	172,6 ± 4,13	10♀, 10♂

Alle 20 Patienten absolvierten 3 Behandlungsgänge (Kontrolle, Verum 1, Verum 2) mit je einer täglichen Behandlung von 60 Minuten in einem Zeitraum von 10 Tagen, wobei zwischen den drei 10-tägigen Behandlungsgängen ein Zeitintervall von 1 bis 2 Wochen lag. Die Reihenfolge der Absolvierung der drei Behandlungsgänge wurde für jeden Patienten durch einen Zufallsgenerator festgelegt. Die jeweilige Behandlungsmodalität war für die Patienten verblindet.

Die drei Behandlungsmodalitäten sind der Tabelle 2 zu entnehmen.

Tabelle 2. Behandlungsgänge

Kontrolle (Placebo) n = 20	Bewegungsbehandlung „BioKorrektur“ mit definierter Laufbandbelastung (Zeitdauer 60 min an den Behandlungstagen 1.d bis 10.d) unter <u>normoxischen Raumluftbedingungen</u> (Sauerstoffanteil der Raumluft 20,9 Vol.%). Vor Behandlung 2 x 10 min simulierte Physikalische Gefäßtherapie BEMER Classic (Matte) im Abstand von 90 min (Gerät nicht eingeschaltet).
Verum 1 n = 20	Bewegungsbehandlung „BioKorrektur“ mit definierter Laufbandbelastung (Zeitdauer 60 min an den Behandlungstagen 1.d bis 10.d) unter <u>hyperoxischen Raumluftbedingungen</u> (Sauerstoffanteil der Raumluft 26 Vol.%). Vor Behandlung 2 x 10 min simulierte Physikalische Gefäßtherapie BEMER Classic (Matte) im Abstand von 90 min (Gerät nicht eingeschaltet).
Verum 2 n = 20	Bewegungsbehandlung „BioKorrektur“ mit definierter Laufbandbelastung (Zeitdauer 60 min an den Behandlungstagen 1.d bis 10.d) unter <u>hyperoxischen Raumluftbedingungen</u> (Sauerstoffanteil der Raumluft 26 Vol.%). Vor Behandlung 2 x 10 min Physikalische Gefäßtherapie BEMER Classic (Matte, Stufe 3) im Abstand von 90 min.

Zur Laufbandbelastung : Dauer 60 Minuten am jeweiligen Behandlungstag, Laufbandneigung 5%, mittlere Laufbandgeschwindigkeit 0,8 bis 1,0 m/s (beginnend mit geringer

Laufbandgeschwindigkeit, im Verlauf der 60-minütigen Behandlung in Stufen alle 10 min um 0,1 bis 0,2 m/s gesteigert).

Zur Physikalischen Gefäßtherapie BEMER :

Eingesetzt wurde das handelsübliche, zertifizierte Gerät BEMER Classic der Fa. BEMER International (FL – Triesen), bei dem ein elektromagenisches Feld geringerer magnetischer Flussdichte zur Übertragung eines komplexen biometrisch definierten Stimulationssignals zur Anregung defizitärer arteriolärer Vasomotionen Anwendung findet. [5, 6, 7, 8]

Die Meßwerterhebungen erfolgten zu äquidistanten Zeitpunkten jeweils am 1., 2., 3., 4., 5., 6., 7., 8., 9. und 10. Behandlungstag unmittelbar unmittelbar nach dem Ende der 60-minütigen Laufbandbelastung. Die Ausgangswerte, auf die sich die Meßdaten vom 1. bis zum 10. Tag als prozentuale Änderungen beziehen, wurden am 0. Tag ermittelt.

Die Erhebung der Meßwerte erfolgte unter konstanten Randbedingungen:

bequemes Sitzen unter konstanten makrozirkulatorischen und temperaturregulatorischen Randbedingungen. Zwei Stunden vor den Untersuchungen kein Alkohol, kein Kaffee, Tee oder Cola-Getränk. Mindestens 6 Stunden Schlaf täglich, keine biotrope Wetterlage im Beobachtungsintervall.

Zur Erfassung von Funktionsmerkmalen der Mikrozirkulation wurde die Wadenmuskulatur als repräsentatives Targetgewebe ausgewählt :

Definierte Geweberegion am rechten dorsalen Unterschenkel in der Mitte der Projektionsfläche des Musculus gastrocnemius (Subkutis, Skelettmuskelatur).

Eindringtiefe ~ 8 mm.

Im begrenztem Umfang erfolgten vitalmikroskopische Referenzmessungen in der entsprechenden Subkutis (Eindringtiefe 2–3 mm).

Die Untersuchungen erfolgten nicht-invasiv mit einem hochauflösenden Untersuchungssystem zur kombinierten Laser-Doppler-Mikrofluss-Messung und Weißlicht-Spektroskopie (LEA, Gießen, Deutschland), welches die Bestimmung spektrometrischer und mikrohämodynamischer Merkmale in Mikrogefäßnetzwerken mit Gefäßdurchmessern $7\text{ }\mu\text{m} \leq d \leq 200\text{ }\mu\text{m}$ ermöglicht. Angaben zur Validierung und zu den Meßvorschriften sind der Literatur zu entnehmen. [2, 3, 4, 10, 14, 15, 16]

Technische Daten des angewendeten Meßsystems : Lightguide Separation 2000 μm und 8000 μm , Wavelengthrange 500–630 nm (Separation 1 nm) und 650–795 nm (Separation 1 nm), Laser Wavelength 830 nm.

Zusätzlich wurde in begrenztem Umfang eine Intravitalmikroskopische Untersuchungseinheit mit computergestützter Bildverarbeitung eingesetzt (OLYMPUS, ZEISS, KONTRON / Japan, Deutschland, USA). [3]

Die Erhebung der Meßdaten erfolgte zu jedem Meßzeitpunkt in der gleichen Geweberegion (exakte Markierung der Meßregion auf der Hautoberfläche und entsprechende Justierung der Meßsonde).

Am jeweiligen Behandlungstag wurden die Meßwerterhebungen kontinuierlich in einem Gesamtzeitintervall von 80 min (10 min Ausgangswerte vor Behandlung, 60 min Behandlung, 10 min nach Behandlung) alle 20 ms vorgenommen. Zur computergestützten Auswertung der Meßdaten dienten die international anerkannten Datenanalyse-Programme. Im Rahmen der vorliegenden Abhandlung sind von den Autoren jene Meßdaten ausgewählt worden, die einen Vergleich der Meßdaten vor Behandlungsbeginn und nach erfolgter Behandlung am jeweiligen Behandlungstag gestatten (Angabe jeweils als prozentuale Änderungen).

Im ausgewählten Targetgewebe wurden folgende Merkmale des Funktionszustandes der Mikrozirkulation gemessen :

- Relative Hb-Sättigung im Bereich des mikrovaskulären Netzwerkes, rHb.

Angegeben als prozentuale Änderung im Vergleich mit dem jeweiligen Ausgangswert, der gleich Null gesetzt wurde.

- Mittlerer Strömungsfluß der roten Blutzellen im mikrovaskulären Netzwerk, QRBC.

Angegeben als prozentuale Änderung im Vergleich mit dem jeweiligen Ausgangswert, der gleich Null gesetzt wurde.

- Venolenseitige Sauerstoffausschöpfung ΔpO_2 (Differenz der Sauerstoffsättigung des Hämoglobins in den zuführenden Arteriolen und abführenden Venolen des mikrovaskulären Target-Netzwerkes).

Angegeben als prozentuale Änderung im Vergleich mit dem jeweiligen Ausgangswert, der gleich Null gesetzt wurde.

- Anzahl der blutzellperfundierte Knotenpunkte nNP im mikrovaskulären Netzwerk eines definierten Gewebevolumens ($V = 1200 \mu m^3$).

Angegeben als prozentuale Änderung im Vergleich mit dem jeweiligen Ausgangswert, der gleich Null gesetzt wurde.

Die Definitionen und Meßvorschriften für die untersuchten Merkmale sind der Literatur zu entnehmen. [3, 10, 14]

Zur statistischen Auswertung der erhobenen Messdaten fand ein parameterfreies Prüfverfahrens für kleine Stichproben Anwendung. Eingesetzt wurde

der WILCOXON-Rangsummentest auf dem Signifikanzniveau $\alpha = 5\%$. Die kritischen Werte für T sind der Literatur zu entnehmen. [1]

Im Rahmen der vorliegenden Abhandlung werden die biometrischen Prüfresultate für jeden Meßtag zu jedem Merkmal betreffs Ausgangswerte vor Behandlungsbeginn versus Meßwerte nach Behandlung mitgeteilt. Ferner erfolgt ein Vergleich der Meßdaten zwischen den drei Behandlungsgängen (Kontrolle, Verum 1, Verum 2) zu gleichen Meßzeitpunkten.

ERGEBNISSE

Bei der Auswertung der erhobenen Meßdaten traten aussagefähige Resultate im Sinn der Aufgaben- und Zielstellung zutage, wobei vergleichsweise geringe Streuungen der Meßdaten um die Mittelwerte (Standardabweichungen) festgestellt wurden. Die Graphen in den Abbildungen 1 bis 4 zeigen die zusammengefaßten Meßergebnisse der untersuchten Merkmale.

Der Abbildung 1 sind die Meßdaten für das Merkmal „Relative Hb-Sättigung rHb“ bei den drei untersuchten Behandlungsgängen zusammenfassend vom 1. bis zum 10. Behandlungstag zu entnehmen. In der Kontrollgruppe treten nur geringe Merkmaländerungen auf, die am 5. Tag mit 2,1% ($\pm 3,8$) ihren höchsten Betrag erreichen und sich nur an diesem Tag signifikant von den Ausgangswerten am 0. Tag unterscheiden. Bei den Behandlungsgängen Verum 1 und Verum 2 unterscheiden sich die Meßdaten vom 1. bis zum 10. Tag signifikant von ihren jeweiligen Ausgangswerten und signifikant sowohl von der Kontrolle als auch signifikant untereinander. Bei beiden Behandlungsgängen werden am 10. Tag die größten Merkmaländerungen festgestellt (Verum 1 : 14,2% ($\pm 5,1$); Verum 2 19,4% ($\pm 7,1$)).

In der Abbildungen 2 veranschaulichen die Graphen das Merkmalverhalten „Mittlere Strömungsgeschwindigkeit der roten Blutzellen vRBC“, im Targetnetzwerk bei den drei Behandlungsgängen vom 1. bis zum 10. Behandlungstag. Vom 1. bis zum 10. Behandlungstag unterscheiden sich die Meßdaten bei allen drei Behandlungsgängen signifikant von ihren jeweiligen Ausgangswerten (0.d), jedoch mit unterschiedlichen Beträgen der Merkmaländerungen. Signifikante Unterschiede treten vom 1. bis zum 10. Tag auch zwischen den drei Behandlungsgängen auf. Die größten festgestellten Merkmaländerungen in den drei Behandlungsgängen sind : Kontrolle am 3. Tag 21,2% ($\pm 6,6$); Verum 1 am 4. Tag 40,6% ($\pm 7,2$); Verum 2 am 4. Tag 55,9% ($\pm 10,8$).

Das Verhalten des Merkmals „Venolenseitige Sauerstoffausschöpfung ΔpO_2 “ in den mikrovaskulären Netzwerken des Targetgewebes ist vom 1. bis zum 10. Behandlungstag für die drei Behandlungsgänge als

Abbildung 3 dargestellt. Im Vergleich mit den jeweiligen Ausgangswerten treten bei Kontrolle signifikante Merkmalunterschiede vom 1. bis zum 8. Tag auf, bei Verum 1 und Verum 2 vom 1. bis zum 10. Tag. Ein Vergleich der drei Behandlungsgänge untereinander läßt vom 1. bis zum 10. Tag signifikante Unterschiede erkennen. Die größten Beträge der ermittelten Merkmaländerungen in den drei Behandlungsgängen sind : Kontrolle am 1. Tag 9,5% ($\pm 2,7$); Verum 1 am 10. Tag 23,8% ($\pm 6,0$); Verum 2 am 10. Tag 37,6% ($\pm 7,4$).

Der Abbildung 8 ist das Verhalten des Merkmals „Anzahl der blutzellperfundierten Knotenpunkte nNP im definierten Targetnetzwerk“ für die drei Untersuchungsgänge vom 1. bis zum 10. Behandlungstag zu entnehmen. Die statistische Analyse der erhaltenen Meßdaten ergab beim Datenvergleich Ausgangswerte versus Meßdaten zu den Zeitpunkten 1. bis 10. Tag folgende signifikante Unterschiede : Kontrolle – signifikante Merkmalunterschiede zu den Ausgangswerten nur vom 1. bis 4. Tag und am 10. Tag ; Verum 1 und Verum 2 jeweils vom 1. bis zum 10. Tag. Die Meßdaten zu allen drei Behandlungsgängen unterscheiden sich vom 1. bis zum 10. Tag signifikant voneinander. Bei den einzelnen Behandlungsgängen waren die größten im Behandlungszeitraum festgestellten Merkmaländerungen : Kontrolle am 1. Tag 5,3% ($\pm 2,6$); Verum 1 am 10. Tag 19,3% ($\pm 5,4$); Verum 2 am 10. Tag 33,6% ($\pm 7,8$).

Zur Veranschaulichung einer Änderung des Verteilungszustandes des Blutes in den mikrovaskulären Netzwerken (Merkmal nNP) zeigt die Abbildung 5 ein vitalmikroskopisches Befundbeispiel als Pseudofarbtransformation von einem Patienten aus dem Behandlungsgang Verum 2 am 10. Tag aus einer tiefen subkutanen Gewebeschicht der Targetregion. In der Abbildung 5a ist der Ausgangszustand (0. Tag) dargestellt, Abbildung 5 b lässt die deutliche Zunahme blutzellperfunderter Mikrogefäße am 10. Tag in der gleichen Netzwerkregion erkennen.

Man beachte, daß die mikrovaskulären Netzwerke der tieferen Subkutis mit jenen der darunter liegenden Skelettmuskulatur kommunizieren.

Merkmalunterschiede zwischen männlichen und weiblichen Patienten konnten bei keinem Behandlungsgang festgestellt werden. Hinweise auf unerwünschte Wirkungen wurden bei keinem Behandlungsgang erhalten.

DISKUSSION

Eine gesteigerte körperliche Aktivität durch eine Laufbandbelastung hat eine höhere Energiebereitstellung, insbesondere in den Zellen der Skelettmuskulatur, zur Voraussetzung. Eine stoffwechseladäquate Regulation der Organdurchblutung mit

entsprechender Regelbreite (Mobilisierung mikrozirkulatorischer Reserven) ist für die notwendige Realisierung der Transportphänomene zwischen Blut und Gewebe hierfür unerlässlich. Patienten mit Diabetes Typ II verfügen jedoch über mehr oder weniger defizitäre mikrovaskuläre Regulationsmechanismen der Organdurchblutung, welche durch geeignete Konditionierungsbehandlungen und Stimulierungsmaßnahmen therapeutisch wirksam beeinflußt werden können.

Wie der Abbildung 1 zu entnehmen ist, tritt im Gegensatz zur Kontrolle bei der Laufbandbelastung unter hyperoxischen Raumluftbedingungen (Verum 1, Biokorrektur) eine deutliche Zunahme der Hämoglobin-Sättigung im Behandlungszeitraum auf. Dies bestätigt Untersuchungsergebnisse von SCHULZ et al. [13], die an einer kleineren Patientengruppe gewonnen wurden. Eine zusätzliche Anwendung der Physikalischen Gefäßtherapie BEMER (Verum 2) bewirkt eine weitere Erhöhung der Hämoglobin-Sättigung, die sehr wahrscheinlich auf eine wirksame Stimulierung defizitärer Regulationsmechanismen der Organdurchblutung, insbesondere der lokalen arteriären Vasomotion, zurückzuführen ist. [9, 14] Das Verhalten des Merkmals Mittlerer Strömungsfluß der roten Blutzellen im Targetnetzwerk Q_{RBC} (Abbildung 2) spricht für diese Annahme. Die Meßdaten zu Q_{RBC} zeigen, daß bei einer Bewegungsbehandlung unter normoxischen Raumluftbedingungen (Kontrolle) der anfänglichen leichten Steigerung der Mikroperfusion bis zum 3. Behandlungstag ab dem 4. Behandlungstag eine Verringerung der Beträge der Merkmaländerungen folgt, wobei am 10. Behandlungstag die Ausgangswerte nahezu wieder erreicht werden. Hieraus wird der Schluß gezogen, daß eine Bewegungsbehandlung der Patienten unter normoxischen Raumluftbedingungen eines weitaus längeren Behandlungszeitraumes bedarf, um therapeutisch effektiv zu sein (vergl. hierzu auch Abbildung 3 und 4).

Eine erhöhte Hb-Sättigung bedeutet nicht zwingend auch einen erhöhten Sauerstofftransport vom Blut in das Gewebe. Von herausragender Bedeutung ist daher das Verhalten des Merkmals „Venolenseitige Sauerstoffausschöpfung ΔpO_2 “ (Abbildung 3). Es zeigt sich, daß durch die BioKorrektur-Behandlung (Verum 1) eine deutliche Steigerung des Sauerstofftransports ins Gewebe bewirkt wird, wobei etwa ab dem 6. bis 7. Behandlungstag die Funktion des Merkmalverhaltens eine größere Steilheit (Anstieg der Funktion, tan a) annimmt. Die Funktion zum Merkmalverhalten von Verum 2 (BioKorrektur + Physikalische Gefäßtherapie BEMER) zeigt einen ähnlichen Verlauf wie Verum 1, jedoch mit deutlich höheren Merkmalbeträgen. Durch die zusätzliche Stimulierung vasomotorischer Regulationsmechanismen (BEMER-System) kann

eine Optimierung des therapeutischen Erfolges der BioKorrektur-Behandlung erzielt werden.

Frage man sich, worauf letztlich der erhöhte Sauerstofftransport ins Gewebe, wie er bei Verum 1 und Verum 2 festgestellt wurde, zurückzuführen ist, so kommt den Änderungen des Verteilungszustandes des Blutes in den mikrovaskulären Netzwerken die entscheidende Bedeutung zu. Ein Maß für den Verteilungszustand ist die „Anzahl der blutzellperfundierte Knotenpunkte im mikrovaskulären Targetnetzwerk nNP“ (Abbildung 4).

Störungen der Mikrozirkulation, Einschränkungen der lokalen Regelbreiten der Organdurchblutung und Verringerungen der mikrozirkulatorischen Reserven sind weniger durch Limitationen der Gesamtpfusion eines Gewebes oder eines Organes charakterisiert als vielmehr durch Einschränkungen der Verteilung des Plasma-Blutzell-Gemisches in den kapillären Netzwerken. Mikrozirkulationsstörungen stellen daher in der Regel Verteilungsstörungen dar, wofür die Diffusionsstörung geradezu ein Paradigma ist. Die Verteilung des Plasma-Blutzell-Gemisches in den kapillären Netzwerken wird durch verschiedene Entmischungsphänomene zwischen Plasma und Blutzellen im Bereich der Mikrogefäß determiniert, wobei regulativ die Mechanismen der arteriären Vasomotionen von entscheidender Bedeutung sind (lokal, spontan im kleinkalibrigen Teil der Arteriole sowie nerval und humorale angesteuert im großkalibrigen Arterienabschnitt). [3, 14] Hierdurch erklären sich die höheren Beträge der Merkmänderungen der mikrozirkulatorischen Funktionsgröße D_pO_2 bei der Verum 2-Behandlung (BioKorrektur + Physikalische Gefäßtherapie) im Vergleich zur Verum 1 –Behandlung.

Im Folgenden werden die Ergebnisse von Korrelationsanalysen gemäß $y = f(x)$ vorgestellt. Von besonderem Interesse sind die Korrelationen von Q_{RBC} und ΔpO_2 , Q_{RBC} und nNP, sowie nNP und ΔpO_2 . Ermittelt wurden die linearen und nicht-linearen Funktionen und ihre zugehörigen Regressionskoeffizienten R^2 . Die Ergebnisse sind in der Tabelle 3 dargestellt. Man erkennt, daß Q_{RBC} und ΔpO_2 sowie Q_{RBC} und nNP nicht-linearen Gleichungen mit Korrelationskoeffizienten $R^2 > 0,9$ folgen. Eine besondere Beachtung verdient der Zusammenhang von nNP und ΔpO_2 :

Sowohl bei der Kontrolle als auch bei Verum 1 und Verum 2 werden die Zusammenhänge von nNP und ΔpO_2 nicht-linear wie auch linear mit Korrelationskoeffizienten R^2 nahe dem Wert 1 beschrieben.

$$\text{Kontrolle: } y = -0,0115x^3 + 0,2x^2 - 0,2367x - 0,7277 \quad (R^2 = 0,9719).$$

$$\text{Verum 1: } y = 0,0112x^2 + 0,5577x - 0,0485 \quad (R^2 = 0,9991).$$

$$\text{Verum 2: } y = 0,0051x^2 + 0,7044x - 0,0193 \quad (R^2 = 0,9998).$$

In den Abbildungen 6 bis 14 sind die wichtigsten Ergebnisse der Korrelationsanalysen graphisch dargestellt.

Man beachte: Die angegebenen Gleichungen gelten streng genommen nur für das untersuchte Patientengut. Sie werden jedoch als prinzipiell gültig angesehen (Tabelle 3).

Die ermittelten Meßdaten und deren Analyse erlauben folgende zusammenfassende Einschätzung:

Die insbesondere bei älteren Diabetikern (nicht nur im dekompensierten Zustand) auftretenden Regulationsdefizite der Organdurchblutung betreffen im Wesentlichen die spontane autorhythmische arteriäre Vasomotion (Reduktionen der Schwingungsamplituden und Verringerungen der Anzahl der Schwingungsweiten pro Zeiteinheit im kleinkalibrigen Arteriolenteil) mit den Folgen mehr oder weniger ausgeprägter Restriktionen der Entmischungsphänomene zwischen Blutplasma und Blutzellen in den mikrovaskulären Netzwerken, wodurch eine stoffwechseladäquate Verteilung des Plasma-Blutzell-Gemisches und damit den Stoffaustausch zwischen Blut und Gewebezellen behindert wird (Diffusionswege!). Des Weiteren sind Veränderungen der Basalmembran, Permeabilitätsänderungen der Mikrogefäßwände und eine Reihe enzymatischer und metabolischer Veränderungen zu beachten (diabetische Mikroangiopathie). Je länger ein manifeste Diabetes besteht, umso ausgeprägter sind die vasomotorischen und die mikroangiopathischen Veränderungen. [3, 11, 14]

SCHULZ et al [13] wiesen anhand von spiroergometrischen Meßdaten und laborchemischen Untersuchungsergebnissen (Blutzucker, C-Peptid, HbAIC, Cholesterin, Triglyceride, HDL, LDL, Insulin, antioxydative Status, HOMA-Index, CgI) einen therapierelevanten metabolischen Effekt der Bewegungsbehandlung „BioKorrektur“ nach. Für den Fall, daß diese metabolischen Wirkungen durch eine extreme Belastung ohnehin defizitärer Regulationsmechanismen der Organdurchblutung zustande kämen, wäre ein gesteigertes Risiko hypoxischer Zustände im Gewebe, verursacht durch die Bewegungsbehandlung, die Folge. In diesem Fall ist mit Änderungen rheologische Merkmale und Hyperkoagulabilität zu rechnen, die sich letztlich als weiter verstärkte Mikrozirkulationsstörungen mit den bekannten Folgen auswirken. Im Rahmen einer orientierenden Studie an einer kleinen Patientenstichprobe konnte von KLOPP et al. [9] gezeigt werden, daß ein derartiges Risiko nicht besteht. Die Bewegungsbehandlung unter hyperoxischen Raumluftbedingungen (BioKorrektur) geht mit einer Stimulierung der körpereigenen vasomotorischen Durchblutungsregulation einher, wie anhand

Table. 3. Ergebnisse der Korrelationsanalysen

Korrelation	Behandlungs-gang	Gleichung	Korrelations-koeffizient
$Q_{RBC} - \Delta pO_2$	Kontrolle	linear $y = 1,3783x + 5,6131$	$R^2 = 0,4672$
		nicht-linear $y = -0,061x^3 + 0,3554x^2 + 2,8563x + 1,9334$	$R^2 = 0,9219$
	Verum 1	linear $y = 0,879x + 20,102$	$R^2 = 0,2684$
		nicht-linear $y = 0,0138x^3 - 0,6453x^2 + 8,9833 - 0,0284$	$R^2 = 0,9834$
	Verum 2	linear $y = 1,1693x + 17,061$	$R^2 = 0,6119$
		nicht-linear $y = -0,0679x^2 + 3,861x + 0,0175$	$R^2 = 0,9928$
$Q_{RBC} - nNP$	Kontrolle	linear $y = 1,6524x + 9,0701$	$R^2 = 0,331$
		nicht-linear $y = -0,333x^3 + 1,1034x^2 + 3,6259x + 7,4684$	$R^2 = 0,7769$
	Verum 1	linear $y = 0,8362x + 23,759$	$R^2 = 0,1757$
		nicht-linear $y = 0,0277x^3 - 1,0287x^2 + 11,298x - 0,0345$	$R^2 = 0,9859$
	Verum 2	linear $y = 1,2042x + 20,636$	$R^2 = 0,5372$
		nicht-linear $y = 0,0016x^3 - 0,173x^2 + 5,5256 - 0,1122$	$R^2 = 0,9938$
$nNP - DpO_2$	Kontrolle	linear $y = 0,6821x - 1,433$	$R^2 = 0,9438$
		nicht-linear $y = -0,0115x^3 + 0,2x^2 - 0,2367x - 0,7277$	$R^2 = 0,9719$
	Verum 1	linear $y = 0,8445x - 1,3934$	$R^2 = 0,9859$
		nicht-linear $y = 0,0112x^2 + 0,5577x - 0,0485$	$R^2 = 0,9991$
	Verum 2	linear $y = 0,907x - 1,3022$	$R^2 = 0,9939$
		nicht-linear $y = 0,0051x^2 + 0,7044x - 0,0193$	$R^2 = 0,9998$

repräsentativer Merkmale des Funktionszustandes der Mikrozirkulation zu erkennen ist. Diese Aussage wird durch die Resultate der vorliegenden Arbeit, die an einem umfangreicheren Patientengut gewonnen wurden, bestätigt. Die von SCHULZ et al erhobenen metabolischen Daten und die in der vorliegenden Arbeit mitgeteilten mikrozirkulatorischen Meßergebnisse bezeugen eine adjuvante therapeutische Wirkung der „BioKorrektur“.

Die Meßdaten, welche bei einer Bewegungsbehandlung unter normoxischen Raumluftbedingungen erhoben wurden (Kontrolle), lieferten im 10-tägigen Behandlungsintervall keine relevanten Hinweise auf eine Stimulierung vasomotorischer Regulationsmechanismen. Diese sind offenbar erst bei längerzeitiger Bewegungsbehandlung zu erwarten, wahrscheinlich mit geringeren Merkmalbeträgen.

Der therapeutische Erfolg einer BioKorrektur-Behandlung kann durch eine zusätzliche Stimulierung der arteriären Vasomotionen (Physikalische Gefäßtherapie BEMER) deutlich gesteigert werden.

ZUSAMMENFASSUNG

Untersucht wurde eine Stichprobe aus 20 ambulanten älteren Patienten mit Diabetes mellitus Typ II, an der mittels validier Messungen repräsentativer Merkmale des Funktionszustandes der Mikrozirkulation mit hochauflösenden Methoden geprüft wurde, ob die nachgewiesenen metabolischen Wirkungen einer Bewegungsbehandlung unter hyperoxischen Raumluftbedingungen („BioKorrektur“) mit einer entsprechenden stoffwechseladäquaten Stimulierung mikrozirkulatorischer Durchblutungsregulationen einhergehen.

Die Ergebnisse der Untersuchungen lassen den Schluß zu, daß durch die BioKorrektur-Bewegungsbehandlung eine weitgehende Stimulierung der vasomotorischen Durchblutungsregulation mit ihren therapierelevanten Auswirkungen auf den Verteilungszustand des Blutes in den mikrovaskulären Netzwerken und auf die venolenseitige Sauerstoffausschöpfung erzielt wird.

Eine zusätzliche Anwendung der Physikalischen Gefäßtherapie BEMER bewirkt im Bereich der Mikrozirkulation eine deutliche Steigerung des therapeutischen Erfolges der BioKorrektur-Behandlung.

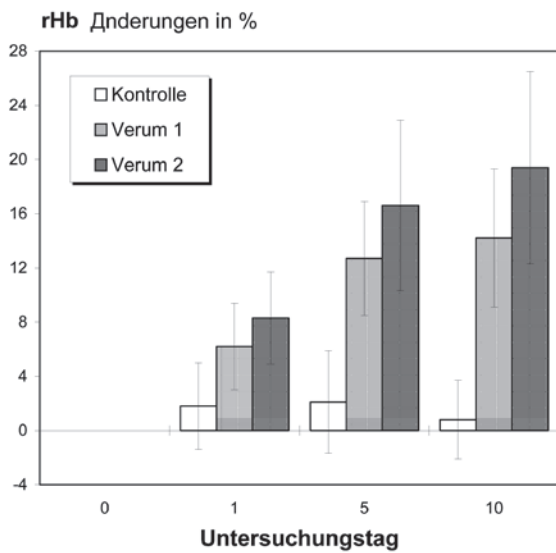


Abb. 1. Meßwerte zum Merkmal „Relative Hb-Sättigung rHb“ (Mittelwerte und Standardabweichungen) im muskulären Targetgewebe bei Kontrolle, Verum 1 und Verum 2. Ordinate: Prozentuale Änderungen im Vergleich mit den Ausgangswerten. Abszisse: Meßzeitpunkte; 0. Tag (Ausgangswerte gleich Null gesetzt); 1., 5. und 10. Behandlungstag.

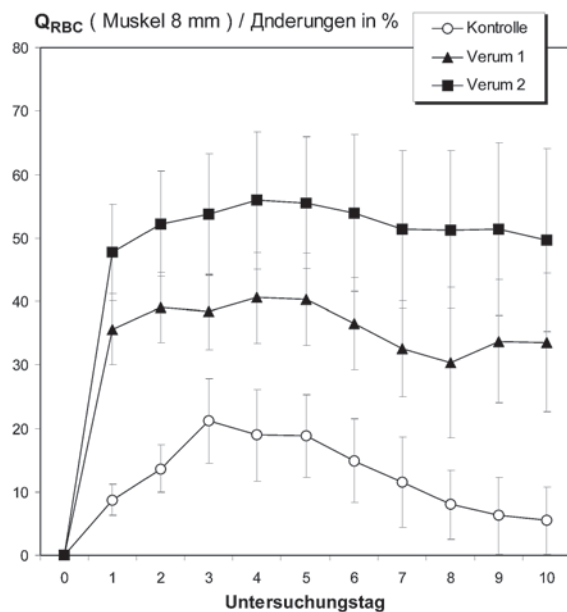


Abb. 2. Meßwerte zum Merkmal „Mittlerer Strömungsfluß der roten Blutzellen im mikrovaskulären Netzwerk, QRBC“ (Mittelwerte und Standardabweichungen) im muskulären Targetgewebe bei Kontrolle, Verum 1 und Verum 2. Ordinate: Prozentuale Änderungen im Vergleich mit den Ausgangswerten. Abszisse: Meßzeitpunkte; 0. Tag (Ausgangswerte gleich Null gesetzt); 1. bis 10. Behandlungstag.

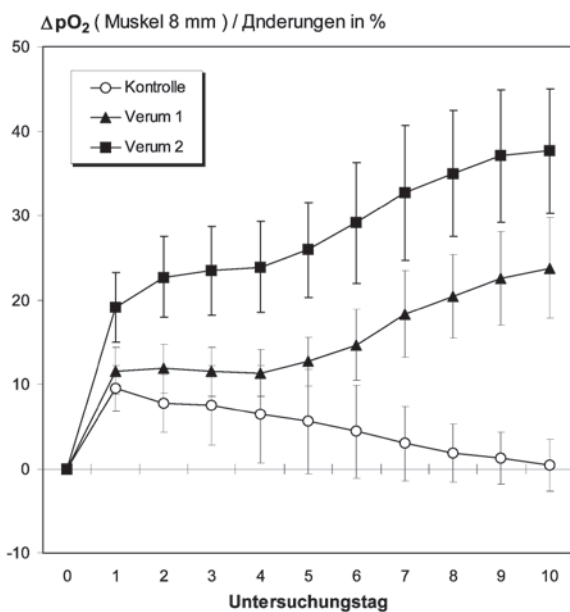


Abb. 3. Meßwerte zum Merkmal „Venolenseitige Sauerstoffausschöpfung ΔpO₂“ (Mittelwerte und Standardabweichungen) im muskulären Targetgewebe bei Kontrolle, Verum 1 und Verum 2. Ordinate: Prozentuale Änderungen im Vergleich mit den Ausgangswerten. Abszisse: Meßzeitpunkte; 0. Tag (Ausgangswerte gleich Null gesetzt); 1. bis 10. Behandlungstag.

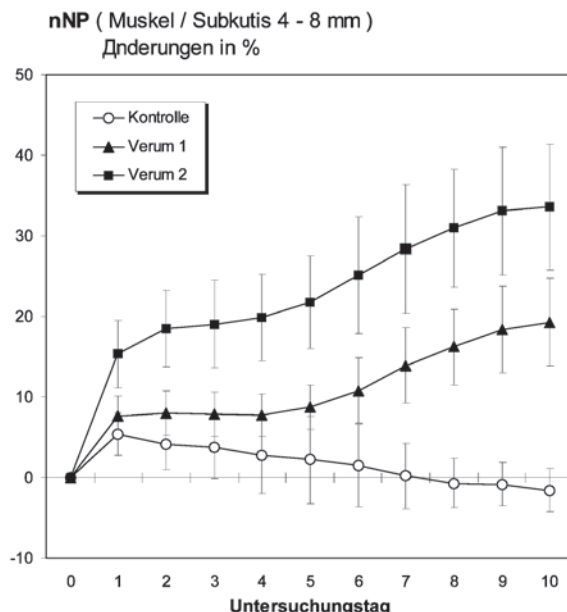


Abb. 4. Meßwerte zum Merkmal „Anzahl der blutzellperfundierten Knotenpunkte im definierten Targetnetzwerk nNP“ (Mittelwerte und Standardabweichungen) im muskulären Targetgewebe bei Kontrolle, Verum 1 und Verum 2. Ordinate: Prozentuale Änderungen im Vergleich mit den Ausgangswerten. Abszisse: Meßzeitpunkte; 0. Tag (Ausgangswerte gleich Null gesetzt); 1. bis 10. Behandlungstag.

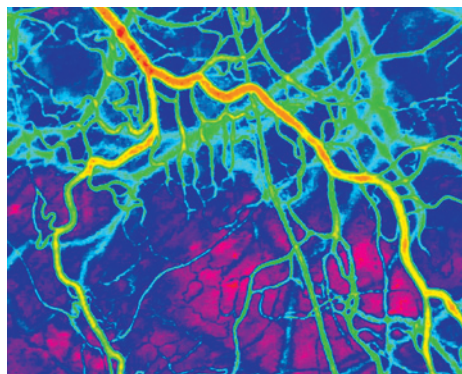
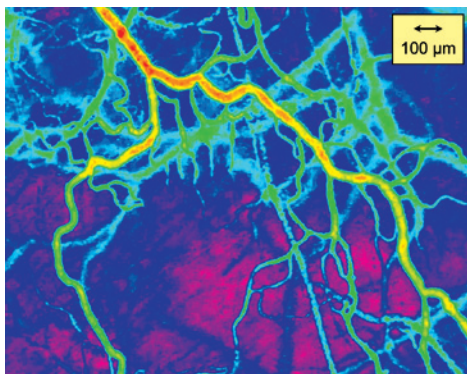


Abb. 5. Änderung des Verteilungszustandes des Plasma-Blutzell-Gemisches in den mikrovaskulären Netzwerken des Targetgewebes bei einem Patienten am 0. Tag (a) und am 10. Tag (b) der Behandlung Verum 2. Vitalmikroskopisches Befundbeispiel (tiefere Subkutis, Wade / Arteriolen, Venolen und kapilläre Netzwerke): Pseudofarbtransformation der PrimärAbb.en (die blutzellperfundierte Mikrogefäßbündel sind grün/gelb/orange markiert).

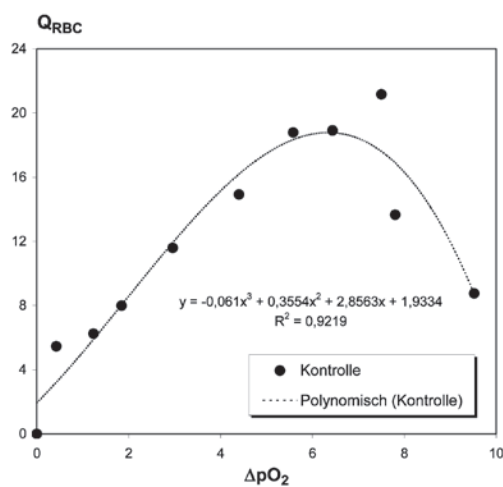


Abb. 6. Nicht-lineare Korrelation der Merkmale „Mittlerer Strömungsfluß der roten Blutzellen QRBC“ und „Venolateralige Sauerstoffausschöpfung DpO₂“ bei Kontrolle Ordinate und Abszisse: jeweilige prozentuale Änderungen.

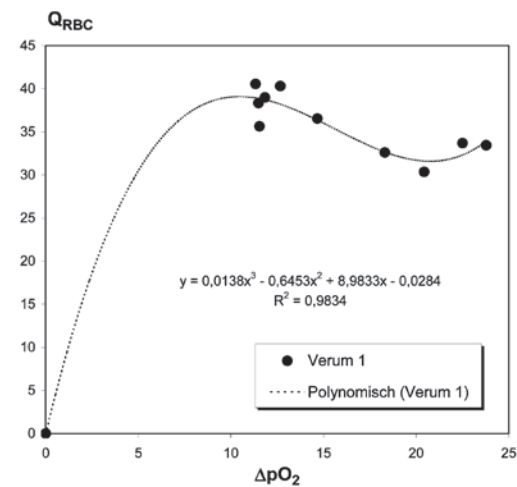


Abb. 7. Nicht-lineare Korrelation der Merkmale „Mittlerer Strömungsfluß der roten Blutzellen QRBC“ und „Venolateralige Sauerstoffausschöpfung DpO₂“ bei Verum 1. Ordinate und Abszisse: jeweilige prozentuale Änderungen.

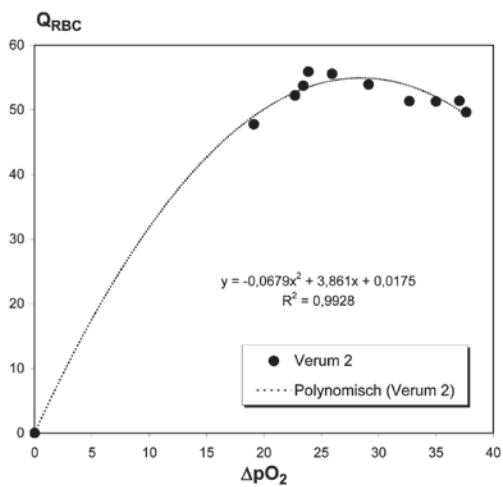


Abb. 8. Nicht-lineare Korrelation der Merkmale „Mittlerer Strömungsfluß der roten Blutzellen QRBC“ und „Venolateralige Sauerstoffausschöpfung ΔpO₂“ bei Verum 2. Ordinate und Abszisse: jeweilige prozentuale Änderungen.

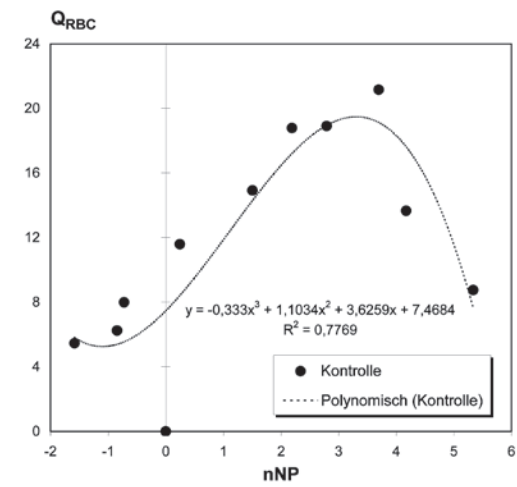


Abb. 9. Nicht-lineare Korrelation der Merkmale „Mittlerer Strömungsfluß der roten Blutzellen QRBC“ und „Anzahl der blutzellperfundierte Knotenpunkte nNP“ bei Kontrolle. Ordinate und Abszisse: jeweilige prozentuale Änderungen.

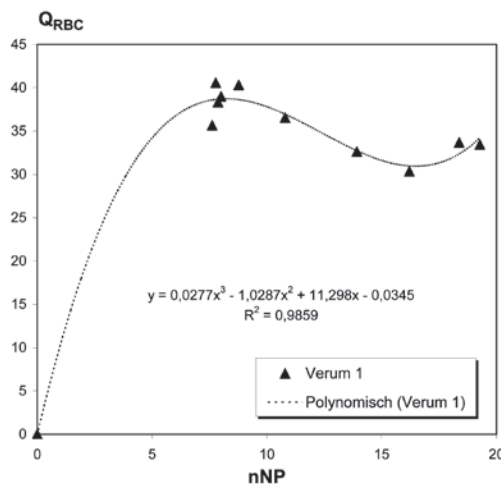


Abb. 10. Nicht-lineare Korrelation der Merkmale „Mittlerer Strömungsfluß der roten Blutzellen QRBC“ und „Anzahl der blutzellperfundierten Knotenpunkte nNP“ bei Verum 1. Ordinate und Abszisse: jeweilige prozentuale Änderungen.

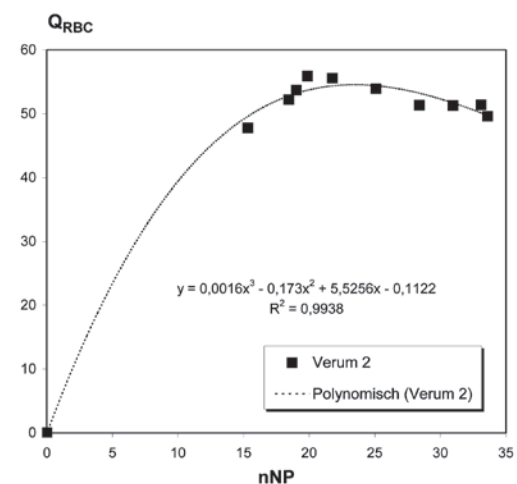


Abb. 11. Nicht-lineare Korrelation der Merkmale „Mittlerer Strömungsfluß der roten Blutzellen QRBC“ und „Anzahl der blutzellperfundierten Knotenpunkte nNP“ bei Verum 2. Ordinate und Abszisse: jeweilige prozentuale Änderungen.

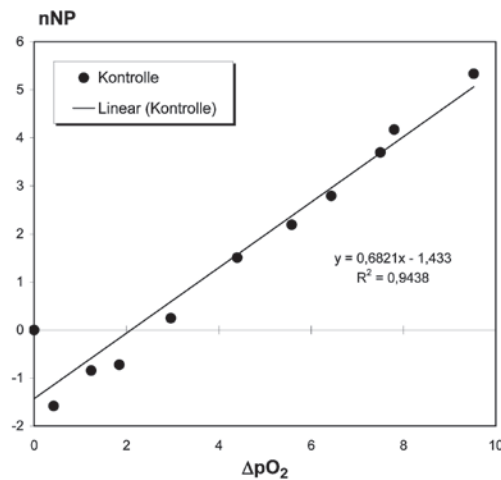


Abb. 12. Lineare Korrelation der Merkmale „Anzahl der blutzellperfundierten Knotenpunkte nNP“ und „Venolenseitige Sauerstoffausschöpfung ΔpO_2 “ bei Kontrolle. Ordinate und Abszisse: jeweilige prozentuale Änderungen.

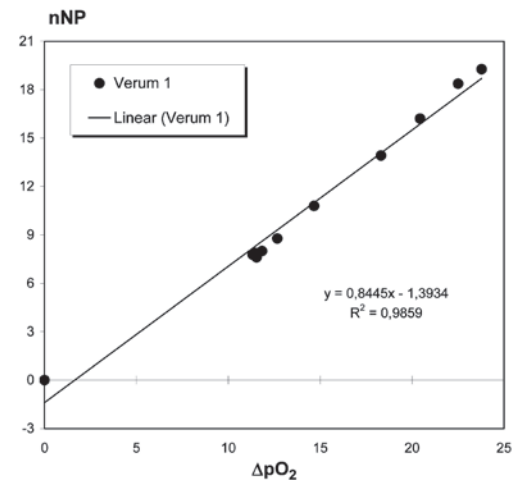
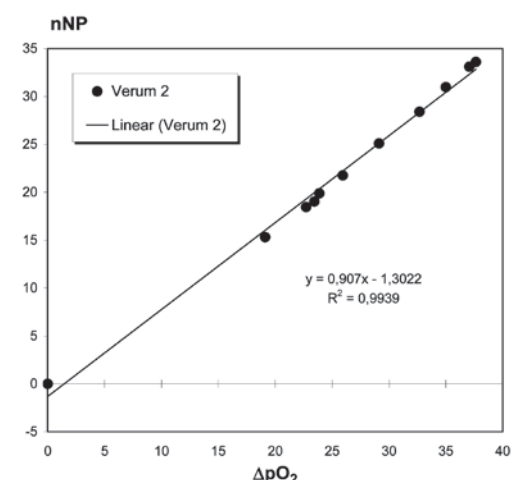


Abb. 13. Lineare Korrelation der Merkmale „Anzahl der blutzellperfundierten Knotenpunkte nNP“ und „Venolenseitige Sauerstoffausschöpfung ΔpO_2 “ bei Verum 1. Ordinate und Abszisse: jeweilige prozentuale Änderungen.

Abb. 14. Lineare Korrelation der Merkmale „Anzahl der blutzellperfundierten Knotenpunkte nNP“ und „Venolenseitige Sauerstoffausschöpfung ΔpO_2 “ bei Verum 2. Ordinate und Abszisse: jeweilige prozentuale Änderungen.



LITERATUR

1. FERGUSON G.A. Statistical Analysis in Psychology and Education. McGraw-Hill, New York (1959)
2. FOURNELL A., T.W. SCHEEREN, L.A. SCHWARTE. Simultaneous, endoscopic measurement of microvascular oxygen saturation and laser-Doppler-flow in gastric mucosa. *Adv Exp Med Biol* (2003) 540, 47–53
3. KLOPP R. Mikrozirkulation im Fokus der Forschung. Mediquant-Verlag AG, Triesen 2008.
4. KLOPP R., J. SCHULZ, W. NIEMER. Effects of the β -receptor blocker nebivolol on the functional state of microcirculation of elderly patients with primary arterial hypertension. *Eur J Ger* (2007) 9, 31–38
5. KLOPP R., W. NIEMER, J. SCHULZ: Effects of physical stimulation of spontaneous arteriolar vasomotion in patients of various ages undergoing rehabilitation. *Complement Integr Med* 10 Suppl (2013) 515–521
6. KLOPP R., W. NIEMER, J. SCHULZ, K.J. RUHNAU: Influence of a specific, biorhythmically defined physical stimulus on deficient vasomotion in small-caliber arterioles in the subcutis in patients with diabetic polyneuropathy. *Complement Integr Med* 10 Suppl (2013) 523–529
7. KLOPP R., W. NIEMER, J. SCHULZ: Complementary-therapeutic stimulation of deficient autorhythmic arteriolar vasomotion by means of a biorhythmically physical stimulus on the microcirculation and the immune system in 50-year-old rehabilitations patients. *Complement Integr Med* 10 Suppl (2013) 531–539
8. KLOPP R., J. SCHULZ, W. NIEMER, K.J. RUHNAU: Wirkungen einer physikalischen Stimulierung der spontanen arteriären Vasomotion auf die Mikrozirkulation und das Immunsystem bei Patienten mit Diabetes Typ II und Wundheilungsstörungen. *Z.f.Gerontologie und Geriatrie/European Journal of Geriatrics* (2014) 47,5 ; 415–423
9. KLOPP R., W. NIEMER, J. SCHULZ: Änderungen des Funktionszustandes der Mikrozirkulation durch eine adjuvante Biokorrektur-Behandlung bei Patienten mit Diabetes mellitus Typ II. *archiv euromedica* (2014), 4, 1; 36–44
10. LAKOWICZ J.R. (ED.). Topics in Fluorescence Spectroscopy. Plenum Press, New York, London, Vol. 1–5, 1991–1997.
11. SCHARTEL M., M. GESSLER, A.V. ECKARDSTEIN. Biochemie und Molekularbiologie des Menschen. Urban & Fischer München 2009.
12. SCHMIDT R.F., F. LANG, G. THEWS (HRSG.). Physiologie des Menschen. Springer Heidelberg 29. Aufl. 2005.
13. SCHULZ J., S. HEYMANN, U. FUCHS, M. STURM, R. KLOPP: Individuelle systemische BioKorrektur – adjuvantes Behandlungsverfahren bei Diabetes mellitus Typ II. *archiv euromedica* (2013) 3,2, 40–44
14. TUMA R.F., W.N. DURÁN, K. LEY (HRSG.). Handbook of Physiology. Microcirculation. Elsevier Amsterdam, Boston, Heidelberg, London, New York, Oxford, Paris, San Francisco, Sydney, Tokyo 2008.
15. WALTER B., R. BAUER, A. KRUG, TH. DERFUSS, D. TRAICHEL, N. SOMMER. Simultaneous measurement of local cortical blood flow and tissue oxygen saturation by near infra-red laser Doppler flowmetry and remission spectroscopy in the pig brain. *Acta Neurochir Suppl.* (2002) 81, 197–199
16. WUNDER C., R.W. BROCK, A. KRUG, N. ROEWER, O. EICHELBRÖNNER. A remission spectroscopy system for in vivo monitoring of hemoglobin oxygen saturation in murine hepatic sinusoids, in early systemic inflammation. *Comp Hepatol* (2005) 4, 1–8

EFFECT OF NICKELIDE TITANIUM IMPLANT ON THE DEHYDRONENASE ACTIVITY OF LYMPHOCYTES OF REGIONAL LYMPHATIC NODE

A.G. Loginov, V.N. Gorchakov

Novosibirsk State University, Institute of Clinic and Experimental Lymphology, Novosibirsk, Russia

ABSTRACT — The dehydrogenase activity of lymphocytes of lymphatic node has been studied under the intraosreal nickelide titanium implantation. Obtained data show nickelide titanium implantation has caused the changes of energetic status of lymphocytes with essential differences in activity of redox ferment systems. The moderate increase of SDG activity and decrease of NAD-dependent dehydrogenases have manifested a disturbance of the main path of energy providing of cells; the activity of shuttle system (α -GPDG) coordinating interaction between processes of respiration and glycolysis is increased; a tendency of anaerobic path of energy production through activation of glycolysis (LDG) is observed. Immune processes have the central place in biocompatibility problem so observed change of energetic metabolism of lymphocytes may be regard as a sign of immune reconstruction of organism.

KEYWORDS — lymphatic node, lymphocyte dehydrogenases, nickelide titanium implantation

The study of mechanisms of interaction between construction materials and biological media is actual. This problem is very import because of dental implantation methods are used in practice. Successes of the last years connecting with the creation of new implantation materials on the base of nickelide titanium [4] demand their verification in the tissue structures. The lymphologic development permits to appreciate the effect of implantation material on organism with a new methodological approach. The interest of biologists and clinicians to the fermentative activity of intracellular metabolism of lymphocyte is explained, from the one side, phylogenetically fastened lymphocyte ability to react to any homeostasis changes, and, from the other side, the fact that the change of lymphocyte ferment activity is appeared earlier than the quantitative changes of leukocyte formula, blood serum proteins etc.

The study of R.P. Narcissov and collaborators (1969–1980) has showed the lymphocyte is an “enzyme mirror” reflecting the state of metabolic processes in internal organs which can't be studied directly. So R.P. Narcissov [5] has named the cytological analysis of lymphocyte ferment status an “indirect biopsy”



Vladimir N. Gorchakov
Dr., professor, head of laboratory
vgorchat@yandex.ru



Aleksandr G. Loginov
Dr., professor of department
of surgical diseases
psz2008@mail.ru

permitting to estimate the state of metabolic processes of organs and systems. Lymphocyte cytoenzymology gives notion about quantitative changes in lymphocyte populations, subpopulation reconstructions, prognosis and character, hardness and affectivity of disease treatment, dynamics of adaptative process [8, 9].

The aim of this work is to study the effect of intraosteal nickelide titanium implantation on the change of dehydrogenase activity of lymphocytes of regional lymphatic node in experiment.

MATERIAL AND METHODS

100 Wistar breed white rat males with body mass 180–200 g grown in the vivarium of Scientific Research Institute of Cytology and Genetics of SB RAMS have been used. Animals have been divided into two groups: the first group of pseudooperated animals is control; the second group with nickelide titanium implant is experimental. Implantation bed has been formed in the alveolar process of low jaw in the molar teeth region with ball-shaped dental drill under ether narcosis. Nickelide titanium alloy (NT-10) has been introduced. Operative wound is stapled.

Pseudooperated animal group has been included animals with formed implantation bed without introduced nickelide titanium. Lymphocytes have been studied on smears-impressions made from incision of surfaced neck lymphatic nodes located on the upper pole of the under low salivary gland on the 7, 14,

30, 60 and 120th days after implantation. The same smears-impressions of pseudooperated animals have been used as controls. Animals have been decapitated under the ether narcosis. Not less than 10 animals in each group have been used.

The cytochemical indexes of activity of important intracellular ferments such as lactate dehydrogenase [L-lactate NAD-oxidoreductase, (*KP* 1.1.1.27), LDG] catalyzing the final stage of glycolysis namely reverse reaction of pyruvate reduction into lactate; succinate dehydrogenase [succinate; (acceptor) – oxidoreductase, (*KP* 1.3.99), SDG] catalyzing the reaction of succinate oxidation into fumarate in the Crebs' cycle: *NADH*-diaforase (*KP* 1.6.99.1), *NADH-R*; mitochondrial glycerophosphate dehydrogenase [L-glycerol-3-phosphate:acceptor]-oxidoreductase, (*KP* 1.1.99.5), α -GPDG(m)], cytoplasmatic glycerophosphate dehydrogenase [L-glycerol-3-phosphate: *NAD*-oxidoreductase, (*KP* 1.1.1.8) α -GPDG(c) have been estimated as key ferments of electron carrier.

The ferment activity has been estimated with quantitative method of R.P. Narcissov [5] in M.V. Robinson's modification [9] based on the counting of visible formasane granules formed in 30–50 lymphocytes after dyeing with n-nitrotetrasole violet. Reliability of results has been estimated with Student's t-criterion.

RESULTS AND DISCUSSION

This study has shown the specific change of energetic metabolism of lymphocytes of regional lymphatic node under endosteal implantation of nickelide titanium in various period of a study.

SDG

Nickelide titanium implantation has lead to the change of ferment activity of SDG lymphocytes of regional lymphatic node (fig.1). At the 7th day of study SDG activity hasn't reliably differed from control value. At the 14th day ferment activity has increased up to $16,68 \pm 1,01$, that is more than control value on 25,03%. At the 30th day SDG activity has increased up to $17,33 \pm 0,58$ and is reliably more than control value on 28,45%. At the 60th day SDG activity has decreased to $15,21 \pm 0,54$, but this value is reliably more than control value of corresponding period of study on 16,92%. Dynamics of decrease of SDG activity has remained at the 120th day of study. Ferment activity is $14,92 \pm 0,55$, that is reliably more than control value on 9,79%. It should be note that SDG activity is increased during the study period reaching the maximal value at the 30th day. SDG is metabolically important because it is supposed that lactate isn't accumulated in the cells rich in this ferment and the complete oxidation of glucose may be expected through the cycle of

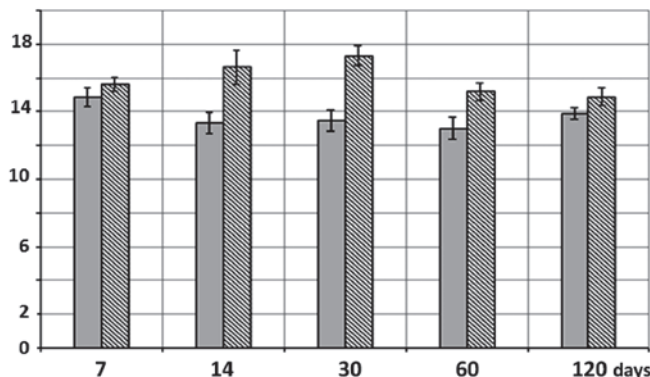


Fig. 1. The change of SDG activity of lymphocytes of regional lymphatic node at experimental implantation with nickelide titanium (the left column is pseudooperated animals; the right column is implantation with nickelide titanium. On the vertical axis shows the value of the ratio of granules at one lymphocyte)

tricarbon acids with big quantity energy release under the main aerobe type of lymphocyte metabolism [9, 10]. And the increase of SDG activity is exactly accounted for this fact. The increase of energetic potential of cell through the SDG activity increase is possible to be a manifestation of adaptive reaction of cell to the nickelide titanium implant and its biologic action. Decreased SDG activity at the 60th and 120th day may be explained with passive action of alloy observed after 30 days [2].

LGD

The change of LDG activity has phase character during the experiment: maximal ferment activities have been observed at 7th and 30th day ($14,88 \pm 0,35$ and $14,5 \pm 0,92$), accordingly, minimal ferment activities have been observed at 60 and 120th day ($10,9 \pm 0,73$ and $9,43 \pm 0,31$). LDG activity in experimental group is higher than in control group during the first 60 days and lower than control value at the 120th day of experiment (fig. 2).

NADH-R activity is different in various periods of study (fig.3). Minimal *NADH-R* activity has been observed at the 7th day is $18,42 \pm 0,63$ (control value is $22,82 \pm 1,48$). At the 14th day activity is increased on 16,42% and is $21,50 \pm 0,84$ (control value is $24,32 \pm 0,76$). At the 30th day ferment activity in the experimental group is increased on $24,32 \pm 0,76$ in comparison with 14th day of experiment. Because of this dynamics the statistically relevant differences of *NADH-R* activity in control and experimental groups haven't been observed at the 30th day of experiment ($26,36 \pm 1,56$ и $25,67 \pm 1,05$), accordingly. At the 60th day ferment activity is increased still more on 3,47% in animal group with nickelide titanium implant and

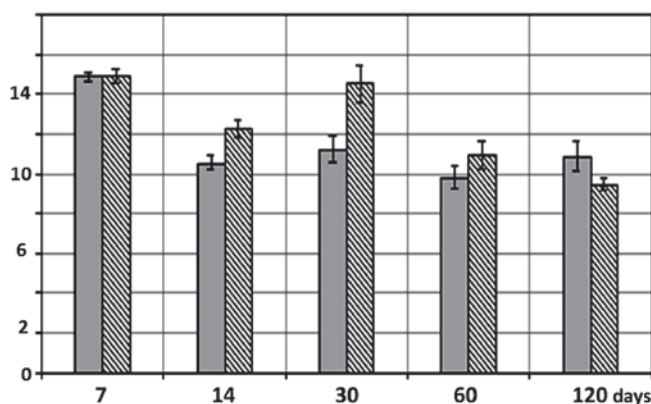


Fig. 2. The change of LDG activity of lymphocytes of regional lymphatic node at experimental implantation with nickelide titanium (the left column is pseudooperated animals; the right column is implantation with nickelide titanium. On the vertical axis shows the value of the ratio of granules at one lymphocyte)

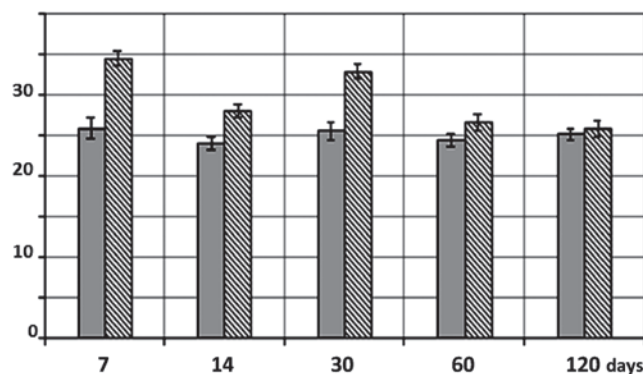


Fig. 3. The change of GPDG (mitochondrial) activity of lymphocytes of regional lymphatic node at experimental implantation with nickelide titanium (the left column is pseudooperated animals; the right column is implantation with nickelide titanium. On the vertical axis shows the value of the ratio of granules at one lymphocyte)

decreased on 3,2% in control group and is $26,64 \pm 0,65$ and $25,54 \pm 1,23$, accordingly. At the 120th day the change of NADH-R activity is observed as a tendency: increase in the group of pseudooperated animals, decrease in the group with nickelide titanium implant. Because of this dynamics at the 120th day of experiment the statistically relevant differences of NADH-R activity in control and experimental groups haven't been observed. NADH-R together with SDG play the most important role among the flavine dependent dehydrogenases. They catalyze the carrier of NAD-H electrons to acceptor, one of protein of respiratory chain containing nongemine iron. Flavoproteids play the role of intermediate carrier of electrons between dehydrogenases and cytochromes. Molecules being the carrier

of electrons are grouped into supramolecular structures so named respiratory ensembles. These ensembles containing strictly defined number of molecules of each carrier of electrons are included in the structure of inner mitochondrial membrane. The dynamics of NADH-R activity change permits to analyze the state of mechanisms providing the dynamic balance of redox reactions in lymphocytes under implantation. Respiratory accept looks like a cascade device bringing free energy portions convenient for cell. Reactions of oxidation phosphorylation preserve about 40% energy releasing in the process of electron carrier.

The study of dynamics of NADH-R activity of lymphocytes of regional lymphatic node under conditions of experimental nickelide titanium implantation permits to note the decrease of ferment activity at the 7th and 14th day of experiment. Statistically relevant differences of NADH-R activity in control and experimental groups haven't been observed at the 30th, 60th and 120th day of experiment. Intramitochondrial ATF and ADF pool is separated from cytoplasmic pool, but exchange between them is possible through the carrier. The very complicate exchange of tricarbon acids cycle products and phosphate takes also place between cytoplasm and intramitochondrial compartment. Reduction equivalents of cytoplasmic NAD-H may indirectly introduce into mitochondria with the help of glycerophosphate shuttle mechanism. Because of existence of this mechanism electrons releasing at the oxidation stage of glycolysis in cytoplasm are included in electron carrier in mitochondria that leads to the form of pyruvate as a final product of anaerobic reactions. There are special shuttle mechanisms carrying the reduction equivalents from mitochondria (where they formed) into cytoplasm. Glycerophosphate shuttle mechanism is the most important.

α -GPDG (mitochondrial)

α -GPDG mitochondrial activity is reliably higher than in control group during the experiment (fig. 4). Maximal ferment activities at the 7th and 30th days are higher than control values on 32,95% and 28,74%, accordingly, at the 14th day – on 16,43%, at the 60th day – on 9,17%, at the 120th day a tendency of increase of α -GPDG mitochondrial activity has been observed. High amplitude change of α -GPDG mitochondrial activity under the nickelide titanium implantation is unfavorable prognostic sign which significantly overtakes the other possible immune and clinic manifestations [6].

α -GPDG (cytoplasmatic)

The most high α -GPDG cytoplasmic activity observed at the 7th day ($30,83 \pm 1,2$) is higher than control value on 24,51%. At the 14th day activity is decreased to $26,48 \pm 0,89$, that is higher than control value on

14,03%. From 14th to 30th days it is observed the following decrease of α -GPDG cytoplasmic activity, and at the 30th and 60th day statistically reliable differences haven't been observed. At the 120th day α -GPDG cytoplasmic activity is increased once more up to $25,91 \pm 0,58$ that reliably is higher than control value on 11,7% (fig.5). Described dynamics shows the intensification of coordinating role of glycerophosphate shunt and intensive cooperation of various ferment systems for energy providing of cell that permits cell to use protein catalysts more economically [1, 7].

CONCLUSION

Experimental nickelide titanium implantation has caused the change of energetic status of lymphocytes of regional lymphatic node. Essential differences in dynamics of oxidative-reductive ferment systems have been observed. The moderate increase of SDG activity and decrease of NAD-dependent dehydrogenases have manifested a disturbance of the main path of energy providing of cells. At those conditions the significance of reserve paths is increased: a tendency of anaerobic path of energy production [activation of glycolysis (LDG)] is observed, and activity of shuttle systems (α -GPDG) coordinating interaction between processes of respiration and glycolysis is also increased.

Immune processes have the central place in biocompatibility problem so observed change of energetic metabolism of lymphocytes may be regard as a sign of immune reconstruction of organism. Obtained data show expediency of correction of energetic metabolism of immune competent cells being in the state of energetic tension under the nickelide titanium implantation.

REFERENCES

- BULYGIN G. V. Metabolic status of peripheral blood lymphocytes in mechanisms of adaptation of man to new ecologic conditions // Thesis of dissertation of DM. – Tomsk, 1992. – 34 p. (In Russia)
- GOZAYA L.D. Allergic diseases in orthopedic stomatology. M., – 1988. (In Russia)
- LENINJER A. The Basises of biochemistry: translation from English. – M., 1985. (In Russia)
- Medical materials and implants with form memory / Gyunter V.E., Dambaev G.C., Sysolyatin P.G. et al. – Tomsk, 1998. (In Russia)
- NARCISSOV R.P. The use of n-nitrotetrasole violet for quantitave cytochemistry of dehydrogenases of lymphocytes of man // Archive of anatomy. – 1969. – № 5. – P. 55–91. (In Russia)
- NARCISSOV R.P. Prognostic abilities of clinic cytochemistry // Soviet pediatrics. Instl. 2. – M., 1984. – P.267–275. (In Russia)
- POLONSKAYA M.G. The study of dynamics of correlative connections between physiologic parameters on the different stages of pathologic process // Thesis of dissertation of Phd. of medicine. – Krasnoyarsk, 1992. – 18 p. (In Russia)
- ROBINSON M.V. Morphology and metabolism of lymphocytes / M.V. Robinson, L.B. Toporkova, V.A. Trufakin. – Novosibirsk, 1986. – 76 p. (In Russia)
- ROBINSON M.V. Morphocytochemical features of lymphocytes in norm under destabilizing influences and autoimmune processes and diseases // Thesis of dissertation of DM. – Novosibirsk, 1994. – 58 p. (In Russia)
- SOKOLOV V.V. Cytochemistry of ferments in prophylactic pathology / V.V. Sokolov, R.P. Narcissov, L.A. Ivanova – M., 1975. – 123 p. (In Russia)

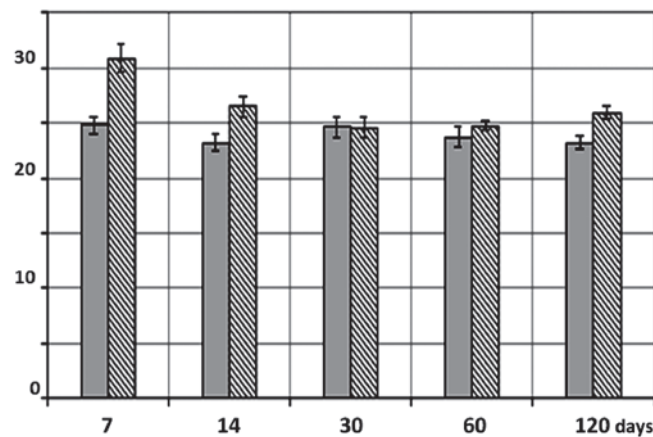


Fig. 4. The change of GPDG (cytoplasmatic) activity of lymphocytes of regional lymphatic node at experimental implantation with nickelide titanium (the left column is pseudooperated animals; the right column is implantation with nickelide titanium. On the vertical axis shows the value of the ratio of granules at one lymphocyte)

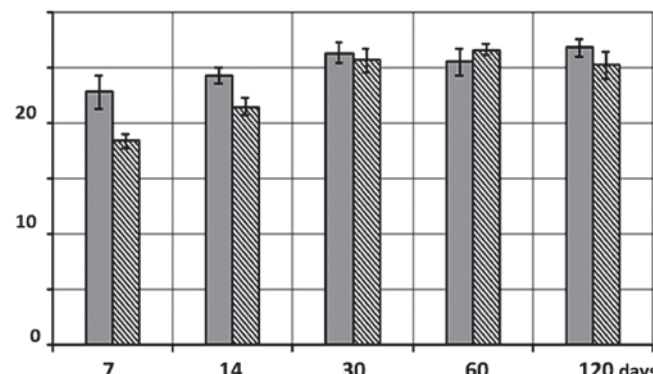


Fig. 5. The change of NAD-reduced form activity of lymphocytes of regional lymphatic node at experimental implantation with nickelide titanium (the left column is pseudooperated animals; the right column is implantation with nickelide titanium. On the vertical axis shows the value of the ratio of granules at one lymphocyte)

MEDICAL NURSE STAFF EMOTIONAL INTELLIGENCE QUOTIENT STUDY

I.M. Lopanova, A.N. Nikolaeva, N.L. Khmarhaya

Vladimir Medical College, Vladimir,
Russia

The work of medical nurse staff is characterized not only by hard physical labor, but also by a big emotional tension. Nurses are exposed to many stressful demands, their constant contact with people pain, fear, anxiety, suffering leads to an emotional burnout syndrome. Medical care efficiency could be significantly improved by paying special attention to the medical staff emotional state which is based on the formed emotional intelligence.

Emotional Quotient (EQ) — is a number of mental abilities that help perceive and understand one's own emotions and surrounding emotions (Ability Pattern). In the context of the emotional intelligence study, we can distinguish the following hierarchically organized abilities: perception and expression of feelings, thinking efficiency improvement with the help of emotions, understanding of one's own emotions and emotions of the others, emotional control [7].

The theoretical and methodological basis of the study were the Emotional Intelligence Model by P. Salovey/ J.Mayer (1990r.) and psychological emotional models (by K. Langhe, A.N. Leontiev, S.L. Rubenshtain and others).

The study looked into the emotional intelligence components in different spheres of activity (*Psychiatry, Hospital Admission, Outpatient Clinic, Paramedics, Oncology, Anesthesiology Critical Care, Surgical Nurses*).

The study was carried out at the premises of the Advanced Training Unit of Vladimir Medical College. 324 medical officers from the city of Vladimir and from Vladimir Region took part in the study.

- The following methods and techniques were used:
- theoretical analysis of published surveys;
 - Emotional Intelligence level detection method (N. Hall);
 - personality emotional burnout diagnostic method (V.V.Boiko);
 - diagnostic method for «troubles» in establishing emotional contact (V.V.Boiko);
 - mathematical statistics method (correlation analysis).

The practical and theoretical importance of the study is that its results and materials can be used in the formation of emotional competence and in the prevention of emotional burnout syndrome in nursing staff.

The scientific novelty of this research is in the study of nursing staff emotional intelligence components, and comparison of EQ level and degree of manifestation of emotional burnout syndrome.

Interpretation of the results:

1. The results of the study show that 37,8 % of the nursing staff have low EQ. It means that the problem is significant, as it affects both patients and wellbeing of the medical staff itself.

2. Regarding the EQ component called ***Emotional self-control*** — the results are below the norm in all activity spheres. Inability to cope with one's internal tension leads to the state of emotional and intelligent dead-end. This is confirmed by the results of the correlation analysis. There exists a significant direct negative correlation with the emotional burnout syndrome called *Being driven into a cage* ($r = -0,34 p \leq 0,01; n \geq 125$)).

3. Regarding the EQ component called ***Self-motivation*** — the results are average in all activity spheres of the nursing staff. If people do not know their emotional capacities they might become aware of stressful factors in their profession and as a rule it will make them either change their job or transfer to another department with less stressful activity. This is confirmed by the results of the correlation analysis. There exists a significant direct negative correlation with the emotional burnout syndrome called «Getting through stressful situations» ($r = -0,32 p \leq 0,01; n \geq 125$)).

4. Regarding the EQ component called ***Empathy*** — the results are below the norm in the spheres of *Hospital Admission, Anesthesiology Critical Care* and *Paramedics*:

— Working conditions in the *Hospital Admission* are characterized by stressors, constant contact with physical and psychological suffering of the patients and big flow of patients during one shift, which leads to reluctance to perceive emotions, necessities and anxieties of other people. And there comes an obstacle to establishing an emotional contact *Reluctance to become emotionally closer to people*. For the sphere *Hospital acceptance*, a developed phase of emotional burnout syndrome called *Exhaustion* is a distinctive feature.

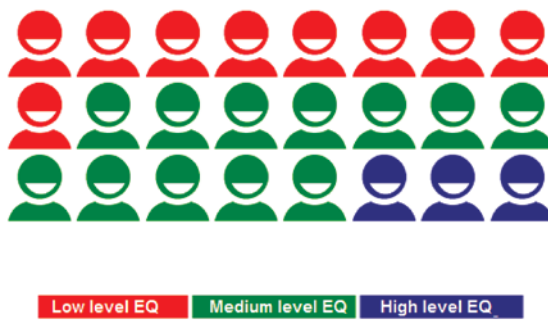


Fig.1. EQ level in average nursing staff

—In the spheres *Anesthesiology Critical Care* and *Paramedical*, it can be explained by brevity of contact duration but at the same time maximum responsibility for a patient life. Obstacles to establish a contact are considered to be *inflexibility and emotional inexpressiveness*. This is confirmed by the results of the correlation analysis. There exists a significant direct negative relation between the component *Recognition of other people emotions* and the above mentioned obstacle in establishing emotional contact ($r = -0,35$, $p \leq 0,01$; $n = >125$).

5. It is also necessary to point out that in the course of the study there has been discovered a significant correlation between the following factors: the obstacle to establish an emotional contact **Inability to control one's emotions** and symptoms *Getting through stressful circumstances* and *Expansion of the sphere of economy of emotion*, which furthermore leads to a formation of Emotional burnout syndrome phases ($r = 0,45$, $r = 0,43$, $r = 0,43$ $p \leq 0,01$; $n \geq 125$). Inability to control one's own emotions leads to the fact that getting through the stressful situations becomes more acute, and this in its turn leads to Emotion burnout syndrome.

The following conclusions have been made to summarize the results of the study:

1. Emotional components have been studied in average nursing staff in different spheres of medical activity.
2. Obstacles to establishing emotional contacts have been defined in average nursing staff (the main of them are *Inability to control one's own emotions*, *Inflexibility and inexpressiveness of emotions*, *Reluctance to get emotionally closer to people*).
3. Correlation between the low level of emotional intelligence and formation of the emotional burnout syndrome has been shown.
4. Recommendations on work arrangement for the nursing staff have been presented:
 - a course of lectures on «*Emotional intelligence components in nursing staff work*» has been developed;

- a training course *Emotional intelligence development in nursing staff* has been created;
- a timely EQ diagnosis in nursing staff is necessary;
- psychological follow-up is necessary for nursing staff at any stage of their work in medical institutions.

If we speak about health care in general, it is necessary to pay attention to the development of the emotional intelligence in nursing staff to increase the quality of the rendered services. In the study, an obvious correlation between the development of the emotional burnout syndrome and a low level of emotional intelligence quotient had been shown, which does affect the life quality of the medical staff. A broader view on usage of psychological knowledge in health care system is necessary as well as its practical application.

REFERENCES

1. I. N. ANDREEVA Emotional intelligence: Usage of the Phenomenon // Psychology questions. 2006. № 3. PP. 78–86.
2. I. N. ANDREEVA Emotional Intelligence as a Phenomenon of the Modern Psychology. — Novopolotsk: Polotsk State University, 2011. — P. 388. — 100 pcs. — ISBN 978-985-531-260-5
3. D. GOLEMAN. Emotional Intelligence: Why It Can Matter More Than IQ — M.: «Mann, Ivanov and Ferber», 2013. — P. 560. — ISBN 978-5-91657-684-9
4. D. GOLEMAN Emotional Intelligence M.: ACT, 2008. ISBN 978-5-17-039134-9
5. D. GOLEMAN. Primal Leadership: Learning to Lead with Emotional Intelligence. — M.: «Alpina Publishers», 2011. — C. 301. — ISBN 978-5-9614-1646-6
6. STEVEN J. STEIN. The EQ Edge — M.: Balance Business Books, 2005. — P. 384. — ISBN 978-966-415-016-0
7. http://www.psychologos.ru/articles/view/emocionalnyy_intellekt

Correspondence address:

IRINA M. LOPANOVA, TEACHER
Vladimir Medical College
lopanova.i@gmail.com

ALLA N. NIKOLAEVA, TEACHER
AND PSYCHOLOGIST
Vladimir Medical College
aguseva@yandex.ru

NADEZHDA L. KHMARNAYA,
CURRICULUM DIRECTOR
Vladimir Medical College
odin790@gmail.com

EVALUATION OF BLOOD FLOW IN THE MEDIAL CEREBRAL ARTERY IN FETUSES WITH HYPOPLASTIC LEFT HEART SYNDROME

O.V. Marzoeva, E.D. Bespalova,
R.M. Gasanova, M.N. Bartagova,
O.A. Pitirimova

Bakoulev Scientific Center for Cardiovascular
Surgery, Russian Academy of Medical
Sciences, Moscow, Russia



Olga W. Marzoeva,
physician



Elena D. Bespalova, MD
Professor, Director



Rena M. Gasanova, MD,
cardiologist

ABSTRACT — In the present study, we have attempted to systematize the possibility of Doppler sonography as a non-invasive diagnostic tool for monitoring the development of the central nervous system in the fetus with congenital heart disease. The detailed analysis of fetal hemodynamic changes in fetuses with hypoplastic left heart syndromes at different gestation stages was performed. The dynamic study of intrafetal hemodynamics was clearly demonstrated to help professionals to organize a more thorough prenatal care the fetuses of which have congenital heart diseases with obstructive lesions of the main arteries, and to predict the initial manifestations of developing the central nervous system pathologies, as well as to choose the optimal method of treatment to reduce complications in the postnatal period. Comprehensive assessment of the intrafetal hemodynamics in fetuses with congenital heart disease allows clearly identifying the stages of a pathological condition in the central nervous system and the degree of their severity.

KEYWORDS — congenital heart disease, dopplerometry, hypoplastic left heart syndrome, fetus, the medial cerebral artery.



Maria N. Bartagova,
physician



Olga A. Pitirimova, MD
Obstetrician, Vice-Director

INTRODUCTION

Hypoplastic left heart syndrome includes a group of cardiac pathologies characterized by underdevelopment (hypoplasia) of the left heart cavities, atresia and/or stenosis of the aortic and/or mitral valves, and aortic hypoplasia.

Reliable diagnostic criteria of hypoplastic left heart syndrome are:

- Deviation from the norm of all linear parameters of the fetal heart at all gestation stages;
- A significant reduction in linear indices of the left heart combined with compensatory increase in similar parameters of the right heart;
- Predominant (atypical) hypertrophy of the left ventricle myocardium over the right ventricle at all gestation stages;

— Diameter of the patent ductus arteriosus is 1.5–2 times more than the norm during pregnancy, especially after the 30th week of gestation.

— Great variability of blood flow nature and its velocity parameters, and a significant difference from the standard values for all studied gestational subgroups in all cases of hypoplastic left heart syndrome.

— In pulsed Doppler blood flow mode in mitral valve stenosis, single-phase flow is recorded, it is high-velocity in the case of a moderate narrowing of the valve ring, and low-velocity in apparent stenosis.

— Retrograde filling of the ascending aorta through a patent ductus arteriosus is recorded in atresia of the mitral valve and aortic valve in color Doppler mapping.

Peculiarities of hemodynamics of the hypoplastic left heart syndrome before birth are such that the right ventricle provides blood flow in the descending aorta through the pulmonary artery and patent ductus arteriosus and retrogradely in the aortic arch, the ascending part and in the coronary vessels.

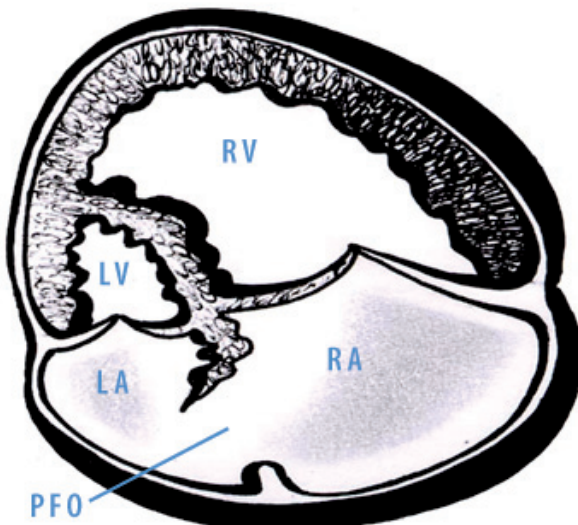


Fig. 1a. Scheme of the 4-chamber heart section: RA — the right atrium, LA — the left atrium, RV — the right ventricle, LV — the left ventricle, PFO — patent foramen ovale. The LV cavity is dramatically reduced compared to the RV cavity, being compensatory dilated, PFO diameter is increased

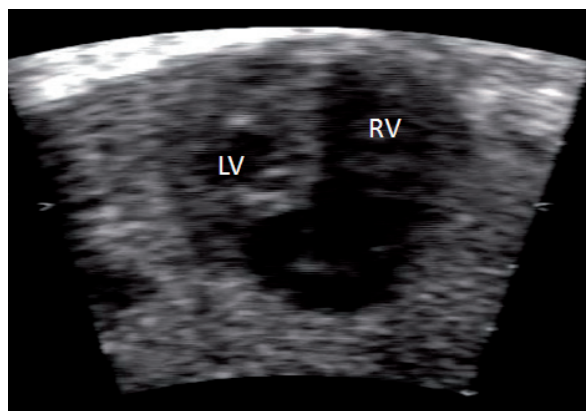


Fig. 1b. 23 gestation weeks. HLHS. Scan is in gray scale mode Projection of four chambers of the heart. Hypoplastic left heart syndrome. The left ventricle (LV) is dramatically hypoplastic, has a characteristic spherical shape (borders are shown in dotted lines). The cardiac apex is formed by the myocardium of the right ventricle (RV) - indicated by the arrow

According to popular opinion, the expressed overload of the right heart, reducing blood flow in the aorta and coronary arteries leads to the development of tissue hypoxia, decreased myocardial contractility, and congestive heart failure only after the child's birth. [1]

However, neonatologists face problems on the part of the central nervous system development from the first week of life of children with congenital heart disease against functioning fetal communications [2–8].

So, according to Mahle WT data, the third of 138 examined school-aged children with various congenital heart diseases and operated in early childhood visits correctional educational institutions, the intake of various drugs was prescribed to 64% of patients to support the central nervous system work, and 18% of children demonstrated mental retardation; all this indicates the high percentage of patients with congenital heart diseases with signs of mental retardation [9]. Pathological phenomena on the part of the central nervous system development are determined in 50% of children with congenital heart disease before the heart defect correction [10–12] and persisted after the 1st and 2nd stages of surgical treatment. But the most dangerous is that patients undergo the great risk even in the preoperative period. This is confirmed by numerous reports of our foreign colleagues studying the influence of congenital heart diseases on the developing brain of fetus and newborn [13–18].

Priority of the nervous tissue in regulating all kinds of the organism vital activity depends directly on the features of its development and blood supply [19]. Several theories about the etiology of intrauterine growth retardation of the central nervous system in fetuses with congenital heart disease were proposed. As a result, scientists have unanimously concluded that the probable factor influencing this is the change in the circulation resulting from certain structural cardiac abnormalities, and which, in turn, may affect fetal growth and its brain development [20, 21, 22, 23–24].

In the pathogenesis of impaired fetal hemodynamics, the leading place belongs to chronic intrauterine hypoxia, which may be caused by malformations [25]. At the same time, the degree of disorder of the central nervous system development has not yet been sufficiently studied.

Nervous tissue is more sensitive to oxygen deficiency, and the change of its blood supply nature primarily affects the development of the brain [25].

Thus, studying the state of the fetal brain in congenital heart diseases should be extended, and the assessment of the functional state of the nervous system in patients with congenital heart diseases should become standard practice.

The objectives of perinatologist should include not only the identification of cardiac abnormality in fetus, but also the determination of patients' risk group for developing the central nervous system pathology.

Under hypoxic conditions, compensatory-adaptive mechanism for protecting the fetal brain (*brain sparing*) the effect of which is aimed at strengthening the blood supply and maintaining the necessary level of brain oxygenation is activated. Decrease in sympathetic innervation of the vascular wall leading to an expansion of the lumen of cerebral vessels is the basis of this mechanism; arteriovenous anastomoses not fully functioning under physiological conditions and capillary network open, redistribution of blood flow aimed at ensuring a vital organ occurs. As a result, a reduction in brain vascular resistance occurs [8, 25]. According to summarized data from the world literature the method of antenatal diagnostics of fetal hemodynamics — Doppler sonography may shed light on the study of this problem [19]. In this regard, the aim of our work was the Doppler sonography study of the blood flow in the medial cerebral artery in fetuses with the presence of one or more complex heart defects — hypoplastic left heart syndrome

MATERIALS AND METHODS

The data of Doppler examination of blood flow in the medial cerebral artery of 24 fetuses with hypoplastic left heart syndrome are in the basis of this work. The control group consisted of 120 healthy fetuses. All patients in the group of congenital heart disease with obstructive lesions of fetal main arteries underwent a comprehensive study including:

- Assessment of the obstetric and gynecological history and extragenital pathology;
- The aimed comprehensive fetal Doppler echocardiography with the use of B-mode scanning and Doppler flow mapping techniques;
- Complete obstetrical ultrasound examination including fetometry as well as aimed examination of fetal anatomy;
- Doppler examination of fetoplacental and intrafetal blood flow.

To clarify the etiological factors of the development of intrafetal hemodynamic disorders, to identify intrafetal hypoxia and exclude fetal genotypic abnormalities, as well as to exclude the presence of maternal burdened gynecological and obstetric history, additional examinations were performed in pregnant women of this group:

- Cardiotocography;
- Immunologic examination
- Genetic testing of the fetus

— Clinical and laboratory examination of pregnant woman (to exclude somatic pathology).

Resulting from the data obtained, cases with gestational age of pregnancy being less than 30 weeks, cases of concomitant cardiac pathology in a fetus with intrauterine growth retardation, echographic signs of intrauterine infection of the fetus, chromosomal abnormalities, cardiographic and echographic signs of intrauterine hypoxia, congenital cerebral brain defects, in addition, the cases with the presence of maternal hypertension, anemia, urogenital infections, cardiovascular, respiratory or endocrine systems diseases were excluded from the study.

The age of pregnant patients did not exceed 35 years, the average one was $27,6 \pm 5,4$ years.

The standard values of Doppler indices of intrafetal circulation at different gestation stages (gestational standards) including the registration of the spectrum profiles of blood flow in the medial cerebral artery proposed by the staff of the Department of ultrasound diagnostics of RMAPO were used for comparative analysis. To assess the state of blood circulation, angular independent indices were used. Resistance index (RI) is calculated by the formula $(SD)/S$, and systolic-diastolic ratio (SDR) with the calculation formula S/D , where S is a maximal systolic velocity, and D is an end-diastolic velocity.

In order to monitor changes of intrafetal hemodynamics, dynamic Doppler examination of intrafetal blood flow on the 30–32, 32–35, 35–39 gestation weeks as well as fetal echocardiography carried out on methodological advanced algorithm developed at the Perinatal Cardiology Center of SCCVS named after AN Bakulev of RAMS was performed in all women to exclude cases of changes in the initially diagnosis of CHD.

All cases of fetal congenital heart diseases that are included in this study were followed throughout the third trimester of pregnancy. The diagnosis was verified postnatally, intraoperatively during autopsy. This series of observations was carried out on the apparatus GE VOLUSON 730 Pro with the use of duplex sensor 3.5–5 MHz. When scanning in Doppler modes of the study, regulation of the Doppler angle «Doppler-angle» was used to obtain the optimal insonation angle, and frequency filter of 50 Hz was applied.

STUDY RESULTS AND DISCUSSION

At the initial stage of the study the analysis of specific measurements of fetal hemodynamics during uncomplicated pregnancy was performed. The study of fetuses without hypoxia, signs of intrauterine growth retardation and without congenital heart diseases was

necessary for further comparative analysis of quantitative parameters characterizing the fetal hemodynamics with various cardiac abnormalities, and identification of more important indicators in the diagnostic and prognostic aspects.

For this purpose, fetal echocardiography and study of intrafetal blood flow velocity curves were carried out in the dynamics in 30 women with physiological pregnancy on the 30–32, 32–35 and 35–39 gestation weeks.

Table 1 shows the total number of observations of Doppler sonography parameters in the medial cerebral artery at each gestational period in norm.

SUMMARY

Table 1. Indices of fetal Dopplerometry in the medial cerebral artery estimated in the group of norms ($N = 120$)

Parameter Age	Values	Medial cerebral artery	
		SDR	RI
30–32 weeks	middle	$4,89 \pm 0,91$	$0,80 \pm 0,04$
	min - max	3,6–6,9	0,73–0,87
33–35 weeks	middle	$5,06 \pm 0,9$	$0,80 \pm 0,03$
	min - max	3,9–7,0	0,74–0,85
36–39 weeks	middle	$5,89 \pm 1,21$	$0,82 \pm 0,04$
	min - max	3,5–7,4	0,71–0,87

Analysis of velocity curves in the middle cerebral artery of the fetus in norm showed:

- The increase in the diastolic component of blood flow in the fetal middle cerebral artery was determined during the third trimester of pregnancy
- The indices of vascular resistance in the fetal medial cerebral artery increased in direct proportion to the gestation age until the middle of the third trimester of pregnancy and remained constant to the end of the third trimester (it should be noted that in the very late stages of pregnancy, 38-39 weeks, we have seen a slight decrease in peripheral resistance indices, but given that the latter group includes a wide range of studied periods, this feature is not so obvious).
- There was no registration of zero and negative values of end-diastolic blood flow in the fetal medial cerebral artery. Our data obtained do not contradict the data obtained by researchers previously [25].

This is explained by decrease in the partial oxygen pressure in the fetal blood leading to a compensatory increase of blood flow in the brain vessels resulting

from increasing volume blood flow and decreasing perfusion capabilities of the placenta during these periods [25].

Given that our data of Doppler indices in the fetal medial cerebral artery fit into the norm, the study of blood flow in the descending aorta and the CM (BPI) did not make sense.

At the second stage, we performed dynamic study of blood flow in the fetal medial cerebral artery in fetuses with hypoplastic left heart syndrome. While analyzing our own data, we found that fetuses with hypoplastic left heart syndrome on the 30–32, 32–35 gestation weeks have no deviations in the numerical values of RI and SDR below standard indicators in the middle cerebral artery, there were no zero and negative values of end-diastolic blood flow, as well as the signs of circulatory centralization.

However, at the age of 35–39 weeks reliable anomaly in peripheral resistance indices was found in the medial cerebral artery, while the blood flow nature in the aorta did not show increase in the numerical values of RI and SDR above the norm, there was no registration of zero and negative values of end-diastolic blood flow, as well. The study of blood flow in the ductus venosus also did not reveal velocity reduction into the late diastole phase below the normative values; zero and negative parameters were not detected respectively. It is possible that abnormalities in the oxygen transport to the fetal brain were caused by oxygen deficiency arising due to the fetus hypoplastic left heart syndrome. We have concluded that in the presence of this heart pathology in the fetus, deviations in brain development can be expected taking into account the changes in hemodynamic parameters in the medial cerebral artery caused by the cerebral [9, 25].

Thus, timely fetal monitoring and carrying out standard maintenance microcirculatory therapy (in particular, the use of drugs improving blood rheology and oxygen transport to the tissues) prior to delivery can improve the child's condition at birth and reduce the risk of functional disorders of the central nervous system.

Today, there are a large number of neuroimaging. The brain assessment is performed using US (neurosonography) and by magnetic resonance tomography. Preoperative neurosonography may reveal abnormalities in 15–59% of patients with congenital heart disease [3]. Magnetic resonance imaging also shows a high level of detection of preoperative brain abnormalities. Using these methods, it is possible to determine whether this deviation is of acquired nature or congenital.

The results of our study show that the evaluation of fetal hemodynamics using Doppler sonography

Table 2. Dopplerometry indices of the fetal medial cerebral artery, the aorta and ductus venosus evaluated in the group of fetuses with hypoplastic left heart syndrome ($N=24$)

Age \ Parameter	30–32 weeks	33–35 weeks	36–39 weeks	P
MCA	SDR	5,04 ± 1,39	5,18 ± 1,78	2,4 ± 0,49 p < 0,05
	RI	0,77 ± 0,04	0,78 ± 0,05	0,59 ± 0,08 p < 0,05
Aorta	SDR	5,72 ± 0,85	5,84 ± 0,57	5,73 ± 0,84 NS
	RI	0,82 ± 0,02	0,83 ± 0,02	0,82 ± 0,04 NS
DV	S/E	1,15 ± 0,04	1,14 ± 0,04	1,13 ± 0,03 NS
	S/A	1,99 ± 0,24	1,93 ± 0,18	1,97 ± 0,15 NS

NS – no reliable statistical differences in parameters values.

should be carried out targeting in the presence of hypoplastic left heart syndrome in fetus. Performing at the age of 35–39 gestation weeks is more appropriate and informative, while the method is not enough reliable in earlier periods.

CONCLUSIONS

- Changes of intrafetal blood flow in the medial cerebral artery are characteristic of fetuses with hypoplastic left heart syndrome, which is a diagnostic criterion in predicting the development of neurological abnormalities after birth in this group of patients.
- In the presence of fetal hypoplastic left heart syndrome, evaluation of intrafetal blood flow should be a standard diagnostics method in predicting the occurrence of neurological abnormalities
- The change of intrafetal hemodynamics according to Dopplerometry is a risk factor for neurologic abnormalities in fetuses with hypoplastic left heart syndrome.

REFERENCES

- SHARYKIN AS Congenital heart diseases. The second edition // M.: BINOM, 2009. p. 284
- AGEEVA MI Classification of fetal hemodynamics abnormalities for determining the perinatal prognosis and choosing the obstetric tactics. Ultrasound and functional diagnostics. 2007, 5: 55–65.
- DONTRIO MT, DUPLESSIS AJ, LIMPEROPOULOS C// Impact of congenital heart disease on fetal brain development and injury. Curr Opin Pediatr 2011 Oct;23(5):502–11
- GUORONG L., SHAOHUI L., PENG J., HUITONG L., BOYI L., WANHONG X. ET AL. Cerebravascular blood flow dynamic changes in fetuses with congenital heart disease// Fetal diagn ther.2009;25(1):167–72.
- MASSARO AN, EL-DIB M, GLASS P, ALY H. Factors associated with adverse neurodevelopmental outcomes in infants with congenital heart disease // Brain Dev. 2008 Aug;30(7):437–46.
- Mc QUILLEN PS., MILLER SP. Congenital heart disease and brain development. Ann NY Acad Sci. 2010 Jan;1184:68–86.
- MILLER SP, MC QUILLEN PS, HAMRICK S, XU D, GLIDDEN DV, CHARLTON N, ET AL. Abnormal brain development in newborns with congenital heart disease. N Engl J Med. 2007 Nov 8;357(19):1928–38.
- WERNOVSKY G, SHILLINGFORD AJ, GAYNOR JW. Central nervous system outcomes in children with complex congenital heart disease// Curr Opin Cardiol. 2005 Mar;20(2):94–9.
- MAHLE WT, CLANCY RR, MOSS EM, ET AL. Neurodevelopmental outcome and lifestyle assessment in school-aged and adolescent children with hypoplastic left heart syndrome. Pediatrics 2000;105:1082–9
- CLANCY RR, MCGAURN SA, WERNOVSKY G, GAYNOR JW, SPRAY TL, NORWOOD WI ET AL. Risk of seizures in survivors of newborn heart surgery using deep hypothermic circulatory arrest. Pediatrics 2003; 111: 592–601
- C. LIMPEROPOULOS, A. MAJNEMER, M. I. SHEVELL, B. ROSENBLATT, C. ROHLICEK, AND C. TCHERVENKOV, Neurodevelopmental status of newborns and infants with congenital heart defects before and after open heart surgery, Journal of Pediatrics, vol. 137, no. 5, pp. 638–645, 2000.
- MAHLE WT, TAVANI F, ZIMMERMAN R, NICOLSON S, GALLI KK, GAYNOR JW ET AL. An MRI study of neurological injury before and after congenital heart surgery. Circulation 2002; 106: 1109–1114.
- BELLINGER DC, WYPIJ D, DUPLESSIS AJ, RAPPAPORT LA, JONAS RA, WERNOVSKY G, NEWBURGER JW. Neurodevelopmental status at eight years in children with dextro-transposition of the great arteries: the Boston Circulatory Arrest Trial. J Thorac Cardiovasc Surg 2003; 126: 1385–1396.
- R. S. BONEVA, L. D. BOTTO, C. A. MOORE, Q. YANG, A. CORREA, AND J. D. ERICKSON, Mortality

- associated with congenital heart defects in the United States: trends and racial disparities, 1979–1997, Circulation, vol. 103, no. 19, pp. 2376–2381, 2001.
15. H DITTRICH, C BÜHRER, I GRIMMER, S DITTRICH, H ABDUL-KHALIQ, AND P E LANGE, Neurodevelopment at 1 year of age in infants with congenital heart disease//Heart. 2003 April; 89(4): 436–441.
 16. H. H. HÖVELS-GÜRICH, M.-C. SEGHAYE, AND M.-C. SEGHAYE, Long-term neurodevelopmental outcomes in school-aged children after neonatal arterial switch operation, Journal of Thoracic and Cardiovascular Surgery, vol. 124, no. 3, pp. 448–458, 2002
 17. C. LIMPEROPOULOS, A. MAJNEMER, M. I. SHEVELL, B. ROSENBLATT, C. ROHLICEK, C. TCHERVENKOV, AND H. Z. DARWISH, Functional limitations in young children with congenital heart defects after cardiac surgery, Pediatrics, vol. 108, no. 6, pp. 1325–1331, 2001.
 18. A. MAJNEMER, C. LIMPEROPOULOS, M. SHEVELL, B. ROSENBLATT, C. ROHLICEK, AND C. TCHERVENKOV, Long-term neuromotor outcome at school entry of infants with congenital heart defects requiring open-heart surgery, Journal of Pediatrics, vol. 148, no. 1, pp. 72–77, 2006.
 19. AGEEVA MI Classification of fetal hemodynamics abnormalities for determining the perinatal prognosis and choosing the obstetric tactics. Ultrasound and functional diagnostics. 2007, 5: 55–65.
 20. BELLINGER DC, WYPIJ D, duPLESSIS AJ, RAPPAPORT LA, JONAS RA, WERNOVSKY G, NEWBURGER JW, Neurodevelopmental status at eight years in children with dextro-transposition of the great arteries: the Boston Circulatory Arrest Trial. J Thorac Cardiovasc Surg 2003; 126: 1385–1396.
 21. M.T. DONOFRIO, F.N. NASSARO, Impact of Congenital Heart Disease on Brain Development and Neurodevelopmental Outcome// International Journal of Pediatrics Volume 2010 (2010), 13 pages.
 22. ITSUKAICHI M, KIKUCHI A, YOSHIHARA K, SERIKAWA T, TAKAKUWA K, TANAKA K, Changes in fetal circulation associated with congenital heart disease and their effects on fetal growth.// Fetal Diagn Ther. 2011;30(3):219–24.
 23. LIMPEROPOULOS C, MAJNEMER A, SHEVELL MI, ROHLICEK C, ROSENBLATT B, TCHERVENKOV C, DARWISH HZ, Predictors of developmental disabilities after open heart surgery in young children with congenital heart defects. J Pediatr 2002; 141: 51–58
 24. MAJNEMER A, LIMPEROPOULOS C, SHEVELL MI, ROHLICEK C, ROSENBLATT B, TCHERVENKOV C. A new look at outcomes of infants with congenital heart disease. Pediatr Neurol 2009; 40: 197–204.
 25. MI AGEVA, IA OZERSKAYA, EV FEDOROVA, VV MITKOV. Doppler examination of fetal hemodynamics // manual for physicians. M.: RMAPO, 2006, p. 31–34

The article is devoted to attempts to systematize the possibility of Doppler sonography as a non-invasive diagnostic tool for monitoring the development of the central nervous system in the fetus with congenital heart disease. The research was conducted in a careful and objective way and can be recommended for publishing in the medical Journal *Archiv Euromedica*.

DR. MED. E.L. BOKERIA,
Bakulev Scientific Center
of Cardiovascular Surgery
Moscow, Russia

ANTITOXIC PROTECTION OF THE BODY USING ANTIDOTES, ANTIOXIDANTS AND OTHER MEMBRANE PROTECTORS

V.A. Myshkin¹, D.A. Enikeev², D.V. Srublin

¹Ufa Institute of Occupational Health and Human Ecology

²Bashkirian State Medical University,
Ufa, Russia

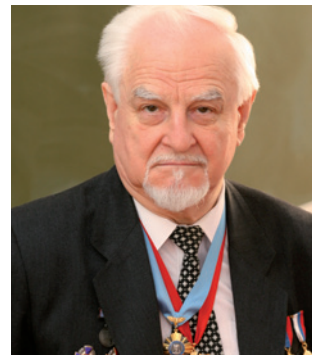
ABSTRACT — Results obtained in the experimental study on further possibilities of the body's palliative protection against chemical exposures (occupational toxicants) using antioxidants — derivatives of pyrimidine, benzimidazol, succinate-pyrimidine complex compounds, α -tocopherol, ionol and other drugs are presented. Marked antioxidant, hepatoprotective actions of 5-hydroxy-6-methyluracil (oxymethyluracil) and its complex combination with succinate and glycyrrhizinic acid have been determined. Cytolytic and membrane protective effects are confirmed by reduced enzymatic activity of urokininase, AlAt, AsAt compared with control indicators. The data obtained also allow us to conclude that a disturbance in the lipid peroxidation processes is a common toxogenesis link in the chain: metabolic disturbance – cytosis and requires adequate correction by an antioxidant regardless its character: primary or secondary. The models of the body damage caused by the action of ethanol, dichlorethan, polychlorbiphenils, nitrates, chlorophenols and phosphororganic antidotes are used.

KEYWORDS — intoxication, pathogenesis, lipid peroxidation, pyrimidine derivatives, antioxidants, membrane protectors, antidotes.

At present, an important trend of research into chemical safety is associated with "therapeutic protection" [20, 21]. Current knowledge linking advances in molecular and cell biology, general pathology, neurochemistry and neuro-endocrinology to integrated efforts of toxicologists and representatives of other medico-biological disciplines has opened possibilities for identification of fundamental mechanisms underlying cellular toxicity, analysis of hypoxic and free radical mechanisms of cellular necrobiosis [1, 5], development of a methodological concept - the theory of general mechanisms of toxicity [1]. While considering this concept, we used the differentiation and integral approaches to assess toxic effects of the substances studied at different levels of structural and functional organization of living systems: at the whole-organism, organism-tissue and molecular-cellular levels. One of general mechanisms of toxic effects of hepatotropic poisons is activation of lipid peroxidation (LPO) and reduced antioxidant activity, particularly in the liver [1]. Ethanol, dichlorethan (DCE), polychlorbiphenils (PCB), chlorophenols, tetrachlormethan (TCM) and



Prof. V.A. Myshkin
MD, Leading Researcher,
Colonel of reserved medical
service



Prof. D.A. Enikeev
MD, Head of Pathophysiology
Department

phosphororganic compounds were experimentally used in our trials.

The purpose of the present study is to review major results of experimental studies on further possibilities of the body's palliative protection against toxic damage caused by occupational toxicants based on patho-physiological significance of lipid peroxidation processes.

Complex studies on LPO processes in alcohol intoxication, efficacy of antioxidant correction performed along with assessment of efficiency of correction of survival, metabolic disturbances and the condition of biological membranes show LPO advantages in its pathogenesis. This is confirmed by a high protective effect of antioxidants – ionol, mexidol and certain pyrimidine derivatives in mice intoxication with ethanol at a dose of 8g/kg, a 1.5-fold increase in LPO activity in the liver and erythrocytes of rats after a single administration of the toxicant at a dose of 6 g/kg as well as daily administration of alcohol for a week. It is noteworthy that LPO activation in the liver is preserved during the post-intoxication period at 2-3, 7-8 and 14-15 days following severe intoxication and is accompanied by marked hyperenzymotemia, disorders in erythrocyte membrane permeability. LPO activation and reduced superoxide dismutase (SOD) activity in erythrocytes can be observed within 2 hours after a single ethanol administration to rats [16, 18].

With two-week alcoholization, another sequence of metabolic changes is seen. These changes accompany LPO activation: the period of LPO intensity and

antioxidant enzymes activity stabilizaton is followed by the period of their enhancement. In alcoholization, LPO activity is accompanied by hepatocyte membrane damage and a decrease in mitochondrial energy formation. This is confirmed by a fall in Na-, K-ATPhase, NAD H-dehydrogenase and succinated hydrogenase (SDG) as well as an increase in the amount of TBK-reacting products. We failed to identify a significant change in the number of dien conjugates in the liver and cerebral cortex exposed to alcoholization [18].

With dichlorethan-induced liver damage, imbalance in the liver pro-oxidant-antioxidant is detected. A hepatoprotective effect of pyrimidine derivatives in acute and sub-acute dichlorethan intoxication was first studied. Positive effects of 1,3,6-trimethyl-5-hydroxyuracil and 5-hydroxy-6-methyluracil (oximethyluracil) on cells, metabolic processes, LPO activity and rats' longevity were shown.

The model of sub-acute intoxication by polychlorbiphenils (PCB) demonstrated that LPO activation process in the liver is due to a reduction in natural antioxidant factors — superoxide dismutase and glutathione peroxidase. A certain advantage of oxymethyluracil over α -tocopherol was revealed. In comparative experiments, a higher hepatoprotective efficiency of oxymethyluracil compared with carsil — a standard hepatoprotector — as well as other referent agents — methyluracil, tykveol, Liv-52, methionin and heptral was shown. In contrast, esseintiale increased PCB hepatodamaging effect [8, 12, 15, 19].

To provide strong evidence that LPO activation is a leading pathogenesis link of chemically-induced liver damage by PCB (except for a significant decrease in LPO activity following administration of great toxicant doses to the body) trials were performed. Antioxidants (α -tocopherol and ionol) were profilactically administered (before intoxication) and simultaneously with the toxicant for 4 weeks. The data obtained have shown that α -tocopherol and ionol unlike carsil (silymarine) not only stabilize LPO but prevent lethality. This fact confirms pathogenetic significance of LPO processes in PCB intoxication. By inhibiting LPO activity, the antioxidants under discussion significantly prevent enzymotemia and necrobiotic changes in hepatocytes [12, 18].

Meanwhile, despite differences at the beginning of the free-radical mechanism of hepatocyte damage, its final stages are similar and interconnected with a breakdown in bioenergetic mechanisms. This is confirmed by a progressing reduction in liver ATP content under conditions of long-term PCB intoxication [17]. That is why we think that for the purposes of restorative correction of toxic hepatopathia, agents

combining antioxidant and antihypoxic properties are more preferable. To implement this research trend, an experimental study on their hepatoprotective activity and related pharmacologic properties of the above agents was launched. Preliminary promising results were obtained [16, 19].

The next few experiments showed that in some forms of intoxication by phosphororganic compounds (POC) there was a dysregulation of free-radical oxidation processes resulting in oxidative stress [19]. Oxidative stress is a poorly studied link in the pathogenesis of FOC severe intoxications. The most significant for POC toxigenesis are cytochrome P-450-dependent monooxygenase reactions, contributing to the generation of reactive oxygen species (ROS), formation of free-radical xenobiotics with subsequent LPO activation. We may suppose that with POC intoxication having a high level of hydrophobicity (carbophos, mercaptophos), oxidative stress mechanisms are involved before their own biotransformation in the liver monooxygenase system and interaction with active acetylcholinesterase (ACE) centres. Meanwhile, armin or phosphacol being more hydrophil and rapidly metabolizing poisons, interact selectively first of all with ACE with subsequent development of hypercholinergic effect and circulatory hypoxia as a leading pathogenesis link. With the current intoxication forms, the possibility of oxidative stress development and disturbance of LPO process activity should be further explored.

Using models of acute carbophos and armin intoxication the antioxidant system (AOS) state, LPO reactions in target organs during toxicogenic and somatogenic intoxication phases, ACE activity and some integral indicators of the experimental animals' organism condition (survival/death) were studied. Acute carbophos intoxication was induced by a single enteral administration to rats of the poison at a dose of 0,9 LD₅₀ (320mg/kg), acute armin intoxication — by a single intramuscular toxicant administration at a dose of 0,75 mg/kg (0,9LD₅₀). LPO products: dien (DC), trien conjugates (TC) and shif bases (SB) were determined in lipid extracts of the cortex and myocardium using the spectrophotometric method. Superoxide dismutase (SOD) activity was determined by the V.N. Chumakov method, acetylcholinesterase — the Elman method. A variety of variation statistics methods were used for the analysis of the data obtained.

It has been shown that in rats with acute carbophos intoxication SOD activity fall in the cerebral cortex, LPO process activation in the brain and heart occur within 2 hours after the poison administration. In the brain, the amount of DK increases after 2-24 hours and by 2-14 days it exceeds control indicators

by 1,5 and 3,3 times. In the myocardium, during the same period DK content increases by 1,4-3,8 times and by 28-30 days it becomes within norm as well as in the brain. However, in this particular case normalization is not veritable since by 42 post-intoxication day DK amount in brain lipids falls reaching negative values and accounts for only 33,3% compared with control. The level of secondary LPO-SO products increases by 1,6-2,5 times, respectively compared with control. Imbalance detected between SOD activity and the number of LPO products occurring between 41 and 43 experimental days [6] precedes the time of rats' mass death [8,18].

The antidote treatment of the intoxicated rats by atropine or atropine and dipiroxyne (dextixymom) does not produce practical effect on intoxication clinical manifestations and biochemical indicators. So, with the first intoxication signs, intramuscular administration of atropine M-cholinomimetic (5 and 10 mg/kg) is not effective similar its long-term use. Co-administration of atropine (10 mg/kg) and dyperoxyne cholinesterase (or dextixim) reactivator at a dose of 25 mg/kg does not impact on the indicators studied, either, including brain and erythrocyte ACE activity. So, after 5 hours, minimal residual ACE activity in erythrocytes of rats intoxicated by carbophos accounts for $32,0 \pm 2\%$ while in antidote treated rats it is $36,7 \pm 6\%$ ($P > 0,1$). Meanwhile, addition of antidotes to antioxidants – tonarol or emoxypin (50 mg/kg) is beneficial for SOD activity, DK and SO content in the brain, intoxication clinical symptoms and significantly prevents lethal outcome by 41-43 post-intoxication day [6]. Free-radical oxidation reaction inhibitor – oxymethyluracil as well as benzimidazole derivatives – bemethyl, etomersol and 2-(3,4-dihydroxifenacylsio) having antiradical and antihypoxic activity produce antioxidant effect under conditions of monotherapy [8,18,19]. Since under conditions of mortal carbophos intoxication the use of antioxidants prevents organ LPO/AOS imbalance and mass death of the animals in the post-intoxication period we may conclude that oxidative stress is an important pathogenetic link in carbophos intoxication and demands appropriate pharmacological correction by agents having an antioxidant effect. With acute carbophos intoxication, one of the most possible causes of atropine low efficiency is associated with structural changes in erythrocytes and related microcirculation impairment.

To identify pathochemical mechanisms of erythron damage and to determine methods of its pharmacological correction, rat experiments were conducted. Morphofunctional specificities of erythrocytes under acute carbophos intoxication were studied. An assessment of erythrocyte membrane state, AOS, LPO

process activity was performed. The number of erythrocytes and reticulocytes, hemoglobin concentration, hematocrit index, blood colour index (CI), hemoglobin in average concentration (HAC), hemoglobin average volume (HAV), hemoglobin average concentration (HAC) in 1 erythrocyte and electric charge of erythrocyte membranes were determined. It has been shown that carbophos at a dose of 0,9 LD₅₀ causes death of 30% of rats during a day and produces a marked toxic effect on the erythron system. In intoxicated rats, an increase in blood reticulocyte content, a decrease in osmotic resistance and electric charge, AOS activity suppression and an increase in concentrations of primary (DC) and secondary LPO products (SO) were identified [13]. Atropin administration prevents death of 30% of rats during the first day, and development of reticulocytosis and limits accumulation of DC in erythrocytes. However, atropinization doesn't influence on the erythron antioxidant system, the amount of TBA-reacting products, osmotic resistance and membrane electric charge.

The use of actoprotectors – benzimidazole derivatives (bemethyl, tiamazol) having antioxidant, membrane stabilizing effects along with atropine and their subsequent administration to rats under conditions of monotherapy produces marked therapeutic effects on the majority of disturbed indicators including reticulocyte content, SOD and catalase activity, the amount of LPO products, osmotic resistance and an electric charge of erythrocyte membranes. The current study indicates that morphofunctional state disturbance including pro-oxidant-antioxidant balance in erythron subjected to acute carbophos intoxication is an important disturbance mechanism of erythrocyte membranes. Bemethyl or tiamazol involvement into the treatment regimen prevents pro-oxidant and membrane toxic action of erythron poison [13].

In acute and chronic intoxication by sodium nitrate, there are certain prerequisites for oxidative stress development. They are oxidant properties of the toxicant itself, its methemoglobin effect supplemented by inhibiting effect on enzymes of mitochondria respiratory chain [9, 18, 19]. Sodium nitrate in toxic doses brings about methemoglobinemia, LPO process enhancement and metabolic process disturbance in erythrocytes. This is confirmed by a significant increase in methemoglobin, DK amounts, a decrease in enzyme activity of AOS-SOD, catalase and glucose-6-phosphate dehydrogenase (G-6-PD). An increase in DK content is also observed in the cerebral cortex and liver of nitrite mice and rats. Maximum DK accumulation is seen after 6 hours following sodium nitrate administration (0,9 LD₅₀). It exceeds control indicators by 75,8% in the cerebral cortex and 67,2%

— in the liver. An elevated DK level is preserved in both organs after 12–24 hours and by 7–14 days during post-intoxication period. The same regularity is revealed in rat experiments during the first 48 hours. A maximum DK increase in the cerebral cortex and liver occurs after 6 hours following toxicant administration. In erythrocytes, this shift in LPO activity is observed in 2 experimental hours: DK amount in intoxicated animals exceeds as much as 2 times control indicators. However, SO amount in the brain and liver is preserved at the control level. This is probably due to the fact that the toxicant under current experiment conditions does not cause stitching in amino-phospholipid membranes underlying the reversible character of their damage [14].

Antioxidants — pyrimidine derivatives (oxymethyluracil) as well as cystamine limit methemoglobin accumulation in blood of intoxicated mice. The above agents as well as bemethyl and mexidol decrease DK level in mice brain and liver during the first 24 hours and by 7, 14 days following sodium nitrate administration.

In rat experiments, oxymethyluracil prevents a decrease in activity of catalase, SOD, G-6-PDG and reduces the elevated number of DK in erythrocytes to the normal limits. Cytoprotective and antioxidant effects of oxymethyluracil are also detected under conditions of long-term nitrite intoxication.

Thus, the results of the present study suggest that in experimental intoxications by hepatotrope poisons – ethanol, dichlorethan, PCB, as well as POS and sodium nitrate – the major consequences of disturbances in pro-oxidant-antioxidant balance are:

- oxidative stress;
- LPO disturbance (activation or activity suppression);
- permeability disturbance and electric charge change in biological membranes;
- enzyme activity disturbance;
- methemoglobinemia and hypoxia;
- bioenergetic process disturbance;
- disruptions in the body state integral indicators (lethal effect).

The use of certain pyrimidine and benzimidazole derivatives with antioxidant, antihypoxic, actoprotective activity as pharmacological correctors in mono-therapy or in combination with antidotes is beneficial for pro-oxidant-antioxidant balance in the toxicologically damaged organs and tissues. It significantly limits or prevents development of hazardous consequences of this damage. Taking into account the complex character of pro-oxidant-antioxidant imbalance during different intoxication stages we may conclude that pharmacological agents with a broad spectrum of

protective-restorative activity influencing on basal cellular processes, determining cell resistance and ability to reparation, increasing the body's general adaptation possibilities are necessary for their correction.

The results of studies on hepatoprotective effects of the agents under conditions of chemically-induced liver pathology demonstrate that agents referring to different pharmacological groups having antioxidant activity are effective (Table). Effects of acetylcysteine, oxymethyluracil and its derivatives as well as α -tocopherol are well marked on liver damage models accompanied by a high level of LPO activity (models 1, 2, 3). Mexidol, the well known antioxidant, produces marked hepatoprotective effect on ethanol-induced hepatosis-hepatitis model (model 2), liver fibrosis induced by a combination of sovtol and alcoholization (model 3) [2, 11, 17] as well as age differentiated models of tetrachlormetan hepatitis (models 4, 5). Synthetic analogues of purine based nucleic acid - benzimidazol derivatives (bemethyl, thyetazol, ethomerzol) as well as cytomak - an agent with an antioxidant action mechanism are effective on chlorphenol and trichlormetaphos-induced hepatitis models (models 6,7) [3, 4, 19]. With the liver injured by high doses of tetrachlormetan, ethanol, polychlorbiphenyls, dichlorethan, POS, the liver damage accompanied by suppression of LPO activity and liver functional-metabolic state develops. Antioxidant monotherapy is less effective. Co-administration of antioxidants and antioxidants with direct energizing activity is beneficial [19].

CONCLUSIONS

1. The data obtained allow us to conclude that a change in the lipid peroxidation processes is a common toxigenesis link in the chain: metabolic disturbance – cytosis and requires adequate pharmacological correction by an antioxidant regardless its character: primary or secondary. Not only the lipid peroxidation activation but its suppression may be of pathogenetic value.
2. With intoxication, the most important condition for the lipid peroxidation activation in the organs (tissues) is the weakening of natural antioxidant factors — an impairment of the antioxidant system enzymatic link activity. Among intoxication pathogenesis factors, hypoxia, energetic deficiency, direct membrane-toxic effect are of great importance.
3. Effective therapy for chemical types of pathology is possible if to take into account the basic (specific) and co-factor (nonspecific) pathogenesis. Examples of practical implementation of this trend include new derivatives of benzimidazol,

Table. The differentiation approach to pharmacological correction of chemically-induced liver pathology due to lipid peroxidation processes disturbance [2–4, 8, 10–12, 15–19]

Experimental model, pathogenesis	Correction methods
Hepatitis induced by dichlorethan with LPO high level activity, reduced amount of restorative glutathione and SH- protein group	Acetylcysteine, oxymethyluracil, 1,3,6-trimethyl-5-hydroxyuracil, α -tocopherol
2. Hepatosis-hepatitis induced by ethanol, with LPO high level activity, elevated volume of fat dystrophy, high level of transaminase activity	Oxymethyluracil, mexidol, silymarin, a combination of oxymethyluracil with mexidol, sodium succinate
3. Hepatitis-fibrosis induced by sovtol and excessive alcohol, with LPO high level activity, antioxidant deficiency, suppression of Krebs cycle enzyme activity	Oxymethyluracil, its combinations with sodium succinate, mexidol, succinate-pyrimidine complexes
4. Hepatitis-cirrhosis in young and elderly rats induced by TCM, with moderate and high LPO activity level, severe cytolysis and cholestasis events, liver dysfunction	Bemethyl, ethomerzol, thyetazol, mexidol, succinate-pyrimidine complexes
5. Hepatitis-cirrhosis in old rats induced by TCM, with LPO phase dynamics, ATP deficiency, the body reduced general resistance to high-altitude hypoxia	Mexidol, sodium succinate-oxymethyluracil, antihypoxicants, phytopreparations
6. Hepatitis induced by chlorphenils, with moderate LPO activation, suppression of bioenergetic and metabolic processes, oxidation separation and phosphorylation	Thyetazol, cytomak + vitamin B, C, E supplementations; oxymethyluracil
7. Hepatitis induced by trichlormetaphos, with moderate LPO activation, suppression of antioxidant defense system, activation of lysosomal hydrolases	Bemethyl, ethomerzol, thyetazol, antihypoxicants
8. Toxic hepatalgia induced by high doses of TCM, ethanol, PCB, DCE, POS occurring with suppressed LPO activity, liver functional-metabolic state	Desintoxified therapy, antidotes, antihypoxicants of direct energizing action

pyrimidine, complex combinations of pyrimidine derivatives with biologically active substances and their combinations with antidotes.

- The differentiated approach to metabolic correction of chemically-induced liver pathologies due to lipid peroxidation process disturbances has been developed. In the mechanism of oxymethyluracil protective-restorative action, antiradical activity, an impact on the antioxidant protection enzymes, bioenergetic processes and the biologic membrane state are of great value.

REFERENCES

- GOLIKOV S.N., SANOTSKIY N.B., TIUNOV I.A. General mechanisms of toxic effect. – M.: Medicine, 1986. – 279 p.
- IBATULLINA R.B., MYSHKIN V.A., BAKIROV A.B. A method of chronic hepatopathy modeling // RF invention patent N 2343556 of 10.01.2009.
- IBATULLINA R.B., MYSHKIN V.A., SERGEEVA S.A., ET AL. Prophylactic efficiency of thyetazol and oxymethyluracil in chlorphenol exposures // Occupational health and industrial ecology. – 2002. – N5. – P.16–19.
- IBATULLINA R.B., MYSHKIN V.A. Antioxidant protective-restorative effects in experimental intoxication by chlorphenols // Occupational health and industrial ecology. – 2002. – N5. – P.28–31.
- KRYZHANOVSKIY G.N. Basics of general pathophysiology. – M.: MIA, 2011. – 252 p.
- MYSHKIN V.A. Antioxidant action and pharmacological properties of pyrimidine derivatives // Perspectives of bioorganic chemistry in the development of new medicines: All-Russia Symposium theses. – Riga, 1982. P. 214.
- MYSHKIN V.A., KHAIBULLINA Z.G., BASHKATOV S.A., ET AL. The impact of methyluracil and oxymethyluracil on free-radical oxidation in model systems // Bulletin of experimental biology and medicine. – 1995. N8. – P.142–145.
- MYSHKIN V.A., BAKIROV A.B. Oxymethyluracil. Essays on experimental pharmacology. – Ufa, 2001. – 218 p.
- MYSHKIN V.A., BAKIROV A.B. Experimental correction of liver chemical damage by pyrimidine derivatives. Its effectiveness and mechanism of action. – Ufa, 2002. – 150 p.
- MYSHKIN V.A., IBATULLINA R.B., SIMONOV A.I., BAKIROV A.B. A method of toxic hepatopathy modeling // Invention patent N 2188457 of 27.08.2002.
- MYSHKIN V.A., IBATULLINA R.B., SAVLUKOV A.I. A method of liver cirrhosis modeling // Invention patent N 2197018 of 20.01.2003.
- MYSHKIN V.A., IBATULLINA R.B., VOLKOVA E.S., ET AL. The use of sylimarine and α -tocopherol for correction of metabolic and morphofunctional disorders in rat liver intoxicated by polychlorobiphenyls // Toxicology Vestnik. – M.: 2004. N3. P. 30–33.
- MYSHKIN V.A., GULYAeva I.A., IBATULLINA R.B., ET AL. The impact of actoprotectors on lipid peroxidation and the state of rat erythrocyte membranes under

- carbophos intoxication // Pathological physiology and experimental therapy. – M., 2004. – N 3. – P.10–12.
14. **MYSHKIN V.A., IGBAYEV R.K., IBATULLINA R.B., ET AL.** Combined pharmacocorrection of hypoxia induced by experimental nitrate intoxication // University science: looking into the future. Proceedings of the KGMU jubilee conference. – Kursk, KGMU. – 2005. – V.2. – P.135–136.
15. **MYSHKIN V.A., VOLKOVA E.S., IBATULLINA R.B., ET AL.** Morphofunctional indicators of rat liver intoxicated by polychlorbiphenyls // Toxicology Vestnik – 2006. – N6. –P. 159–160.
16. **MYSHKIN V.A., IBATULLINA R.B., BAKIROV A.B.** Liver damage by chemicals: functional-metabolic damages, pharmacological correction. – Ufa: Gilem, 2007. – 177 p.
17. **MYSHKIN V.A., BAKIROV A.B.** Polychlorbiphenyls and new models of liver pathology // RAMS Bulletin. – 2009. – N1(65). – P.255–259.
18. **MYSHKIN V.A.** Lipid peroxidation correction in experimental intoxications by a variety of chemicals. – Doctorate thesis. – Chelyabinsk. 1998. – 393 p.
19. **MYSHKIN V.A., BAKIROV A.B.** Oxidative stress and liver pathology under chemical exposures. – Ufa, 2010. – 176 p.
20. **ONTSHCHENKO G.G.** Urgent issues of chemical and biological safety // Up to-date problems of hygienic science and occupational health. Coll. of sci. papers. All-Russia scientific conference with international participation. – Ufa, 2010. – P.17–19.
21. **SANOTSKIY I.V.** The problem of palliative protection measures under chemical exposures // Occupational health and industrial ecology. – 2007. – N2. – P. 10–14.

COMPLEX RADIATION DIAGNOSTICS OF MYOCARDIAL PERFUSION IN CIVIL AVIATION FLIGHT PERSONNEL WITH THE EXPERIENCE ABOVE 20 YEARS

N.S. Qamalyan, G.H. Khachatryan, A.G. Karapetyan,
K.V. Khondkaryan

Department of Radiological Diagnostics, Mkhitar Heratsi Yerevan State Medical University after, Yerevan, Republic of Armenia
Scientific Center of Radiation Medicine and Burns, Ministry of Health, Yerevan, Republic of Armenia

KEY WORDS — perfusion, myocardium, civil aviation pilots, SPECT-tomography

INTRODUCTION

Arsenal of radiological methods is the most informative part of all the diagnostic methods of clinical medicine; they allow the *in vivo* study on both the anatomical and functional parameters of various organs and systems. However, each of the methods (R-CT, NMR-tomography, ultrasound and radionuclide methods of research) has its positive and negative aspects and limits of information value.

The latter is especially important for the study on such multi-functional organs and systems, as the heart is. Therefore, a physician has a very important task: to choose clinically appropriate and methodologically most informative method of investigation for a specific clinical purpose and design of the final diagnosis.

In the available literature no data on SPECT-tomography of the myocardium and its combination with other radiation methods in the selected sub-population (contingent) was identified.

TOPICALITY

Within this study, taking into account the specifics of the work (the presence of positive and negative accelerations/overloads, vibrations, noise) we have chosen the method for heart tomography, which allows the closest approach to the pathophysiological mechanisms of myocardial perfusion disorders.

The state of myocardial perfusion in patients without myocardial infarction, but with severe pains of varying degrees of intensity, is a relevant and challenging clinical problem. It is even more complicated because of the numerous ambiguous factors affecting development of the pathological process occurring

in flight personnel with experience not less than 20 years.

Among the factors that may affect the state of myocardial perfusion are additional loads to which the aircrew is exposed.

GOAL AND TASKS

Based on the above, the purpose of the present study was to evaluate myocardial perfusion in flight personnel via identifying features of this disorder. To achieve these objectives the following tasks were set forth:

1. Detection of myocardial perfusion disorders;
2. Identification of the site of disorder and the total area of myocardial damage;
3. The response of myocardium to pharmacological tests and to determine the features of changes in response to the stress factor;
4. Identification of general and specific patterns of myocardial perfusion disorders of the left ventricle at rest and under pharmacological stress and their comparative characteristics.
5. Features of violations perfusion in flight personnel.

MATERIAL AND METHODS

The survey involved 16 people (pilots with experience of over 20 years) with no clinical or laboratory signs of myocardial infarction.

Among the causes of visits to a doctor there were: unstable angina, arrhythmias and blood pressure disorders.

Method of research: perfusion scintigraphy with radioactive technetium and MIBI kit (technetrol). Investigations were carried out on «SPECT» tomograph («Mediso», Hungary). The tomography step was 5.6°, angle of detector circulation around the heart — from 60° to 240°. The number of frames: 32. The image made 5 mm in all three tomography axes. Investigations were carried out in 2 stages: the first stage was performed an hour after intravenous administration of Tc-MIBI with activity 22–24 mCi, the second stage occurred immediately after the first scan /tomography taking with the intake of 2 pills of nitroglycerin. Final evaluation of the information received was done in the form of a qualitative and quantitative assessment of

myocardial perfusion disorders in all three axes, all the slices based on a «map of the heart» and the total percentage of left ventricular myocardial damage [1, 2, 4].

Then a comparative characterization of tomoscintigrams was conducted before and after the loading test.

In order to optimize the interpretation of tomographic data we selected the following standards: IAEA software package and IAEA recommendations for evaluation of perfusion disorders.

Normal capture was estimated at diffusely uniform redistribution of the indicator from 100% to 70% of the administered activity, slight reduction of blood flow — 70–50%, average — 50–30%, significant — 30–10%, the absence of perfusion — 0–10%.

Another point of reference for assessing the extent of damage in the left ventricular myocardium is the number of damaged segments in a 9-segment model.

Upon the damage of 1–2 segments there was a minor perfusion disorder, at involvement of 3–4 segments — moderate, at more than 5 segments — significant impairment of perfusion.

RESULTS AND DISCUSSION

The following results were obtained:

1. Varying degrees of perfusion disorders were found in all subjects.
2. The most vulnerable areas were localized along the apex-septal and antero-lateral wall of the left ventricle. The largest areas of damage were on the back wall, in the direction from septum o lateral parts. Accordingly, the degree of reduction was 50%, the number of segments made 3–4.
3. The 90% of patients showed signs of concentric left ventricular hypertrophy, 10% — the signs of eccentric hypertrophy; the degree of reduction in the latter reached 70%, the number of segments was 4–5.
4. Upon the comparative evaluation of the two-stage study (rest and stress) mainly the signs of activity redistribution (91%) were identified; signs of latent defects made 57%, signs of steal syndrome — 36%, improvement in overall perfusion was recorded only in two cases improving local zones — in 36–38%. The latter fact (improvement of local zones) is the most important clinical and pathophysiological feature of the possible recovery of myocardial perfusion.

The analysis of tomoscintigraphy results suggests that state of myocardium perfusion in the left ventricle in flight personnel might serve a model of hibernating myocardium described by Rahimtoola S.H. (1980) and Narahara R.A. (1990).

The main issue of this communication was defining areas of reversible ischemia and unviable myocardium areas, whereas disorders of the perfusion, as presented by Narahara RA (1990) can be also identified in the areas of viable but «hibernating» or stunned myocardium.

Perfusion single-photon imaging at rest and myocardial scintigraphy in combination with nitroglycerine test enabled using the quantitative analysis method to specify the zones of increased accumulation of the indicator. Myocardial viability (in different portions of the left ventricle myocardium) was detected almost in one third of patients.

The authors, Rahimtoola S.H. and Narahara R.A. [6, 7], have identified the principal / fundamental point of hibernation essence: «inhibition of myocardial contractile function occurs in parallel» with the ischemia degree. At the same time, reducing inotropic function of hibernating myocardium appears as regulatory defensive reaction in response to an energy deficit in cardiomyocytes. If at worsening of myocardial perfusion the total ejection fraction remains high, it is considered a good prognostic sign and vice versa: if upon the worsened perfusion of myocardium there is a simultaneous decrease of both the total ejection fraction and the local one, then it is a bad predictive sign.

All clinical states that can lead to hibernating myocardium are met in the surveyed contingent due not only professional, but also, and especially, noxious continuing professional factors of work.

From a practical point of view, the presence of hibernating myocardium is a significant predictor of recovery in the impaired perfusion.

CONCLUSION

With a decrease in coronary blood flow to a critical level or at the relative deficiency of myocardial oxygen supply the hypoxia occurs at the level of «respiratory chain». As a consequence of aerobic catabolism termination, the glycogenolysis and anaerobic glycolysis are increased; the volume of energy production is a direct function of myocardial perfusion.

This latter emphasizes the importance to study myocardial perfusion for determination of ischemia degree of the heart muscle.

The effective perfusion helps to restore contractile function of reversibly damaged cardiomyocytes only after normalization of energy production and reduction of the intracellular calcium concentration. Sometimes the recovery of contractile function of the heart after the restoration of coronary blood flow occurs with some delay («stunned myocardium») [3, 8].

In the absence of adequate reoxygenation cardiac ischemic changes of intracellular metabolism lead to

structural and morphological changes in cardiomyocytes until their death with post-infarction scar formation. The consequence of such disorder (damage) is irreversible disturbance of myocardial contractile function [3].

REFERENCES

1. KRAMER A.A. Radionuclide methods of investigation of the myocardium. Moscow. 1982. 78p. (published in Russian).
2. CHERNOV V.I., SALPAGAROV S.M. ET AL. Methodological aspects of using SPECT with Tc-99m- technetil for prognosis of coronary heart disease course. Medical Radiology and Radiation Safety. 2002, №1, p. 39–40 (published in Russian).
3. LISHMANOV YU.B., CHERNOV V.I., BABOKIN V.E. ET AL. Scintigraphic, ultrasonic evaluation of myocardial viability of hibernating myocardium upon dopamine / Medical Radiology and Radiation Safety. 2002, №1, p. 46–53 (published in Russian)..
4. KUZIN A.I., GABBASOVA L.A., VAZHENIN A.V. Clinical and radiological analysis of myocardial scintigraphy with Tc-99m - technetil / Vestnik rentgenologii I radiologii (Bulletin of Roentgenology and Radiology). 1999, №1, p. 9–11 (published in Russian).
5. NARAHARA R.A., VILLANUEVA-MAYER J., THOMPSON C.J./ American Journal of Cardiology, 1990, 66(20), p.1438–1444.
6. RAHIMTOOLA S.H. Importance of diagnosing hibernating myocardium: how and in whom./American Journal of Cardiology, 1997, 30, p.1701–1706.
7. RAHIMTOOLA S.H. The hibernating myocardium. American Journal Hearth, 1989, 117, p.211–221.
8. MAKAROVA E.V., CHERNOV, V.I. ET AL. Radionuclide diagnostics of the metabolic processes of the myocardium in ischemic heart disease / Medical Radiology and Radiation Safety, 2005, №3, -p.53–60.

EPIDEMIOLOGICAL ASPECTS OF THE PUBLIC HEALTH IN THE ZONE OF ECOLOGICAL DISASTER OF THE ARAL SEA REGION

G.A. Tussupbekova¹, S.T. Tuleukhanov¹, N.T. Ablaikhanova¹,
E.N. Kuandykov²

¹al-Farabi Kazakh National University, Almaty, Kazakhstan

²Nauchno-Prakticheskij Centr Sanitarno-Epidemiologicheskoy Ekspertizy i Monitoringa, Almaty, Kazakhstan

RELEVANCE

In the past few years, the Aral Sea region has received much attention in Kazakhstan. The complex environmental situation in the area related to agro-chemical pollution significantly worsened the physical and chemical properties of the water of the river Syr Darya. That has been led to a change in climatic conditions of the whole region and had a very negative impact on the public health, physical sexual development of the younger generation [1].

Currently, there are a great deal of research on the negative effects of aridity of the region on the public health. There are unresolved legal, social, medical and organizational aspects of these problems [2]. One of the ways to stabilize the health situation in these conditions is to improve the governance and organizational structure of the state sanitary and epidemiological service in the field of active influence on the habitat and the public health. A very important factor is the adaptation of the activity of the sanitary and epidemiological service to the rapidly changing economic conditions which suggests the most efficient use of available resources [3, 4]. In this regard, special priority is improving the management and evaluation of the services of the sanitary and epidemiological supervision. The basis of evaluation of Sanitary-Epidemiological Service should be indicators of efficiency and effectiveness. It is necessary to develop estimates of the efficiency indicators of Sanitary-Epidemiological Service activity based on available resources and opportunities for their rational use. In ecologically adverse regions, as is the lower of the river Syr Darya, the development of such approach is the actual scientific problem, so the search for the new methodological approaches, the development of innovative management systems is an extremely urgent task of the hygienic science.

Our study included the follow objectives: giving a qualitative and quantitative description of the dy-



Gulmira Tussupbekova,
MD, Senior Lecturer
gulmira.274@mail.ru

namics of multicomponent hygienic water pollution, drinking water in the Aral Sea region in the contemporary social and economic conditions of the region; establishing a quantitative relationship between the degree of contamination of drinking water and levels of intestinal infections and noninfectious diseases in order to draw up medium term hygiene forecasts.

MATERIALS AND METHODS

Natural ecological hygienic, sanitary and epidemiological, medical and sanitary, sanitary and toxicological studies. During the natural studies of sanitary and hygiene water research of water bodies and tap water were used standard methods of the laboratory determinations. The total mineralization, acidity, the presence of the heavy metals, oil products were determined by the in the water samples.

The real data of the materials of population treatment for out-patient clinics from the "Development history" (f.112 u) and "The individual card of outpatient" (f.25u) were recorded on a specially designed "study map of the morbidity level of the population treatment for out-patient clinics".

RESULTS AND DISCUSSION

Studying the dynamics of mineralization of the Aral Sea region water sources has shown that the level in the water dug wells for the period from 2007 to 2012 rose to 1701.4 1902.1 mg/l. Moreover, there is high content of calcium cations, magnesium and sodium. Content of chloride anion also exceeded the threshold limit concentration in 1 times. In this, population of 10 settlements are supplied with water from wells. And 18 settlements in the region use

imported method of drinking water. In the content of the imported water the level of sodium reached $48,4 \pm 5,2$ mg/l and magnesium $42,1 \pm 3,9$ mg/l. The mineral content is at around $997,4 \pm 92,3$ mg/l, that comes close to its threshold limit concentration.

In accordance with the results of the sanitary water quality assessment the Aral Sea region population were divided into 2 groups: the first group use higher mineralization water, the second group (control) use optimal water salt composition water corresponding Sanitary norms and rules 3.01.067-97 The Republic of Kazakhstan.

Comparative evaluation of overall morbidity indicators suggests that the highest level it had in the first group of the population. In this group the level of disease was in 1.9 times higher than in the second. One of the most reasons for the treatment of the population of the first group was hypertension ($18,2 \pm 1,6$ per 1000 population) that is almost in 2 times higher than the morbidity incidence rate of the second group ($9,5 \pm 0,9$ %). In the first group compared to the second is also high incidence of ischemic ($7,3 \pm 0,7$ vs. $3,8 \pm 0,08$ %), cholelithiasis ($6,1 \pm 0,6$ vs. $1,6 \pm 0,1$ %), urolithiasis ($3,3 \pm 0,3$ vs. $0,9 \pm 0,009$ %) disease. The difference in the levels of indicators for the above diseases among population the first and the second groups was credibly ($P < 0,001$) and morbidity of the population of the first group higher to 1.9 times than in the second group.

We found a high level of functional dependence of general morbidity of the population with the chloride content ($r=0,8$), sulfate ($r=0,7$), the quantity of dry residue ($r=0,9$). Hypertension, diseases of blood and blood-forming organs, diseases of the digestive organs have an average relationship with the level of mineralization, total hardness and chloride. The given values of the correlation coefficients are statistically credibly as they exceed their mistake more than in three times that is considered to be accepted in such calculations. Unfortunately, such dependence is still assessed without quantitative parameters, which did not give specific ideas about the regularities of changes in the public health status from the intensity of exposure to the water factor in the studied conditions. Meanwhile, the parameters of the quantitative dependence of changes in the health public indicators of the impact of environmental factors allow selecting the priority circle of the significant available on the factors of the evaluation indicators. That can greatly simplify the monitoring public health system. In the hot climate of the arid zone, in contrast to other climatic zones, with increasing hardness of the water increases the risk of urolithiasis disease with more severe clinical course.

We have studied the effect of higher water min-

eralization and water on the optimal content on the specific functions of the female body and gynecological morbidity. According to the age studied women of both groups was as follows: up to 20 years - from 2 to 5%, 21-30 years - from 25-30%, 31-40 years - from 36.9 to 44%, 41-50 years - 25.3 to 27%.

Most patients (95%) living in the area permanently. Menstrual function of women was studied based on inspections (conducted over 3 years), for this questionnaires were designed. The cellular composition of the vaginal contents of 150 women with menstrual disorders was investigated. The reproductive function was studied by statistical data development of the maternity hospital, antenatal clinic. Neonates status were evaluated on a hangar scale taking into account body weight, growth of neonates, length of hospital stay and recovery time of initial mass loss.

Comparative analysis of the menstrual function among women indicates that the most disorders had women among the first group who for a long time used the higher mineralization water. These women often have either a short menstrual cycle (less than 21 days; $p < 0,01$) or longer (more than 31 days; $p < 0,01$), or irregular menstruation. Noteworthy in this group is more frequent ovarian failure function in the form of heavy and prolonged menstrual periods ($p < 0,01$). Menstrual disorders function had women in both groups, most often in the first group ($68,13 \pm 2,94\%$; $p < 0,001$). Individuals in this group had predominant disorder type hyper menstrual syndrome ($32,64 \pm 2,83\%$), while in the control group ($11,02 \pm 3,18\%$; $p < 0,001$); As for other types of menstrual pathology, they also detected in women in the highly mineralized water.

When studying cytogram at women suffering menstrual disorders it was detected a higher and prolonged maintenance of estrogens, which were determined also in the second phase of the menstrual cycle. This indicates the formation of anovulatory cycles as it seems cause menstrual disorders.

Data analysis of the reproductive function showed that women who drank high mineralization water has reduced number of pregnancies ($p < 0,05$), increased specific gravity of spontaneous abortion ($p < 0,001$), increased frequency of pregnancy pathology – toxicosis of the first and second half of pregnancy ($p < 0,001$).

During child-bearing among women who drank higher mineralization water complicated untimely amniorrhea, coordination labor, abnormal bleeding in the third stage of labor. This pathology was observed in 2-3 times less among the women of the second group.

Particular interest is the data on the evaluation of neonates in the early neonatal period. Dur-

ing the analysis of the collected material was found that women who drank higher mineralization water gave birth to children in a satisfactory state (with an estimate of 7–10 points), that is in 1.5 times less than women using water on the optimal salt composition ($p<0.001$). However, children with asphyxia mild and moderate limits (5–6 points) were born almost in 4 times more often among women of the first group than the control group.

High water mineralization has an adverse effect on fetal development, as evidenced by a decrease in body weight of neonates in women of the first group compared with the control group. The significant differences between the treatment groups is $p<0.001$. The body length of neonates of women in both groups were relatively equal. Thus, underweight at normal growth of neonates among the second group can be explained by a certain delay of fetal development which is seems cause by the disturbed metabolism and uteroplacental circulation due to morphological changes in the placenta.

Among the children whose mothers drank high mineralization water significantly reduced the adaptive indicators: the dynamic weight of neonates, the maximum loss of their initial body weight of more than 10% were significantly higher in the first group ($28,41 \pm 4,11\%$), than in the control group. ($13,19 \pm 3,59\%$). Analysis of gynecological morbidity showed that $68,7 \pm 2,91\%$ of women who drank higher mineralization water had a variety of gynecological diseases, the structure of which was dominated by inflammation of the uterus and appendages. In the control group of female gynecological disease was in 2 times lower. Thus, higher mineralization water is a factor of high intensity, have adverse effects on the specific functions of the female body (menstrual and fertility), as well as during pregnancy and child-bearing, the fetus and neonate. In addition, higher mineralization water increases gynecological morbidity which is in direct proportion to the duration of such water consumption ($r = 0,8$).

Increased mineralization water significantly disorders the specific functions of the female body. It is revealed more frequent violation of ovarian function by type hyper menstrual syndrome (in 3 times), significantly decreased the number of pregnancies, in 2 times increased spontaneous abortions and other disorders of pregnancy (toxicosis, nephropathy). Significantly reduced the number of children with various degrees of pathology (in 4 times), reduced birth weight.

CONCLUSION

Thus, the results of the assessment of the public health status in the Aral Sea region in such nosologi-

cal forms of diseases like hypertension, cholelithiasis, gastric ulcer show the importance of the salt composition of the water in the etiopathogenesis of these diseases. Drinking water with high mineralization and hardness, increased content of some components of the salt composition leads to various physiological changes, especially in hot and dry climate of the Aral Sea region.

Analysis of the many years results of the medical and hygiene studies in the Aral Sea region have allowed us to improve the methodology for forecasting the hygienic conditions of water use and the level of morbidity associated with the water factor. Parts of this prediction were: hygienic forecasting of water quality of the river Syr Darya; hygienic drinking water quality forecasting and levels of morbidity associated with the water factor.

REFERENCES:

1. A.M. BOLSHAKOV. About the complex hygienic evaluation of the environmental sustainability and its impact on the public health of the region /A.M.Bolshakov, E.M.Cherepov, E.I.Akimova // Hygiene and sanitary. – 2011. – №2. 47–49p.
2. A.A. BELONOG. Development of criteria for monitoring effects of environmental factors on the public health of the Republic of Kazakhstan /A.A. Belonog //Public health and the environment. – 2004. № 1 (130). – 1–4 p.
3. The impact of drinking water quality on public health of Yaroslavl /G.F. Veselova, T.M.Glazkova, L.K.Merkulova, G.P.Fedorova // Hygiene and sanitary. 2009. – №4. – 11–13p.
4. YE.N. KUANDYKOV. Methods of analysis and assessment of the public health condition, activity of the sanitary and epidemiological service //Bulletin of the South Kazakhstan Medical Academy. 2010. - №7–8. – 88–90 p.

EXPRESSION OF GLYCERALDEHYDE-3-PHOSPHATE DEHYDROGENASE IN THE TUMOR TISSUE OF BREAST CANCERS

E.A. Shliakhtunou

Vitebsk State Medical University,
Vitebsk, Belarus

ABSTRACT — Tumor proliferation of cancer cells requires a high intake of oxygen by angiogenesis. Deep cancer cells suffer from asphyxia and meet their energy needs through the enzymes of glycolysis. The antiangiogenesis approach has been recognized for therapeutic purposes, but the deep cancers, difficult to reach by this therapy, could be targeted by inhibiting an enzyme of the glycolytic cycle. Our work focused on the study of the expression of GAPDH, a key enzyme of glycolysis, in breast tumor, for two approaches: Fundamental and targeted therapeutics. 63 samples, taken at the Anatomopathology laboratory of the Vitebsk State Medical University, were examined histologically and immunohistochemically, demonstrating the expression and cellular localization of GAPDH. Breast organ have shown an overexpression of GAPDH in tumor tissues. At the cellular level, the localization of GAPDH in cancer tissue is diffuse but mostly nuclear whereas it remains focused at the membrane and/or the cytoplasm in benign tumor tissues. From these results we could assume that GAPDH is involved in the cancer process and draws attention to a possible new nuclear role that could be either specific to one form or different isoforms of GAPDH enzyme.

KEYWORDS — Cancer; GAPDH; Immunohistochemistry; Expression; Isoforms

INTRODUCTION

According to WHO, cancer is a disease that affects over 10 million people worldwide. Due to its potential severity, the disease affects the quality of the patient's life. It seems to affect people at random and the treatment remains heavy expensive. Usually, Cancer is presented as a tumor mass which is the culmination of a series of transformations that can occur over a period of several years. The understanding of cancer natural history remains unclear/uneasy because of its frequency, complexity, malignity and diversity of signaling pathways and therefore, more difficult to develop new therapeutic strategies.

Oxygen plays a key role in the functioning of healthy and cancer cells. Some studies estimate that the tumor proliferation of cancer cells requires a high intake of oxygen via angiogenesis. In the case of less advanced cancers, some antiangiogenic therapies seek to



Euheni A. Shliakhtunou
MD, Associate Professor,
Department of Oncology
evgenij-shlyakhtunov@yandex.ru

cause cell degeneration by preventing the proliferation of blood vessels that feed oxygen. However, deep cancer cells escape this therapy, because they suffer from asphyxia and instead rely on the conversion of glucose to energy needs through the enzymes of glycolysis [1]. This is in accordance with the Warburg studies; which demonstrated that tumor cells have an increased rate of glycolysis [2].

The glyceraldehyde-3-phosphate dehydrogenase (GAPDH), is described as a key enzyme of glycolysis. It is considered one of the best characterized glycolytic enzymes at the biochemical and structural level [3, 4].

It catalyzes the oxidative phosphorylation of D-glyceraldehyde-3-phosphate (G3P) to 1,3 diphosphoglyceric acid (1,3 DPG).

In addition to glycolysis, this enzyme is also implicated in the Krebs cycle and pentose phosphate pathway, being in this way involved in all three lanes of central carbon metabolism [5]. GAPDH is a ubiquitous enzyme known among all living beings including the three major evolutionary lineages; Archaeabacteria, Eubacteria and Eukaryotes. It is considered among the best conserved proteins [5, 6].

The native protein is a tetramer with a molecular mass of 140 kDa and 220 kDa depending on the type of GAPDH. Each monomer consists of approximately 330–498 amino acids and has a molecular weight between 35 and 50 kDa. [7].

Human GAPDH gene organization was examined using the selective loss of human chromosomes in human-rodent somatic cell hybrids [8]. The GAPDH gene was localized to chromosome 12 based on its concordant expression with lactate dehydrogenase B (LDH-B), with triosephosphateisomerase (TPI) as well as the lack of such associations with 28 other human enzymes [9].

Apart from its glycolytic function, phosphorylating GAPDH presents a variety of activities depending on its membrane, cytoplasmic or nuclear localization [10]. Having in addition to its catalytic function other roles in physiological processes, a series of studies has shown the involvement of GAPDH in initiating the cascade of hepatocyte apoptosis [11].

Further investigations have shown that cancers have a metabolism based on glycolysis, comprising the conversion of glucose into pyruvate and in the case of oxidative stress; the accumulation of errors in the post-translational structure of GAPDH increases the aging process [12].

Recently different teams have examined the expression analysis of GAPDH in tumors and human cancer cell lines. Thereby in Ovarian cancer, GAPDH expression increases mRNA stability of CSF, an important cytokine in tumor progression [13]. In Thyroid cancer, GAPDH undergoes S-nitrosylation to facilitate its trans- location to the nucleus in order to activate the TRAIL (Tumor Necrosis Factor Related Apoptosis Inducing Ligand) [14].

What about the expression of GAPDH in breast cancers, representing an estimated 25% of the cancer deaths in women [15].

MATERIALS AND METHODS

Patients

63 samples including breast were recruited at the Anatomopathology laboratory of the Vitebsk State Order of Peoples Friendship Medical University from patients for diagnosing, were studied histologically and immunohistochemically. We studied the expression of GAPDH in both malignant (34) and benign (29) lesions.

Methods. Histological Study

The Histological study was performed on surgical specimens, collected by the specialist, fixed in formalin, and then routed to the Laboratory of Anatomopathology where they are listed. The samples were then subjected to a macroscopic study and were described by the pathologist. Then they were passed through a series of intermediate liquids in a circulation automaton before being embedded in paraffin to obtain blocks ready to be cut by microtome in

order to obtain transparent ultrathin sections with a thickness of about 4 to 5 micrometers. The biofilms were delicately placed on slides previously treated with distilled water and a drop of glycerine albumin that allows the bonding of biofilm on the slide to be stained with hematoxylin eosin (HE).

Methods. Immunohistochemical Study

Sections of 5 µm were made from paraffin blocks used for diagnosis. These sections were collected on silanized slides and were dried overnight in a stove at 37° C. They were then deparaffinized in three toluene baths: 5 min (x3), Rehydrated in decreasing degree alcohol baths: Absolute ethanol: 5 min, Absolute ethanol: 5 min, 96° Ethanol: 5 min, 80° Ethanol: 5 min, 70° Ethanol: 5 min. Washed with distilled water: 10 min. Placed in 10% citrate buffer in a water bath preheated to 75° C for 20 minutes to unmask specific antigenic sites. The sections were then left to cool for 15 minutes in the same buffer at room temperature and washed with PBS (Phosphate Buffer Salin) for 5 minutes. The outline of each cut was dried with filter paper and circled with Pap Pen. The endogenous peroxidase activity was inhibited by incubating the sections for 5 minutes in 3% hydrogen peroxide followed by rinsing with two PBS baths for 5 min (x2). Tissue sections were incubated in the presence of skim milk for 5 min then for 45 minutes at room temperature with primary antibody polyclonal anti human GAPDH [17] diluted to 1:50, 1:80, 1:100, 1:500, 1:800, 1:1000 and 1:1500 in PBS buffer. After rinsing with PBS, sections were incubated for 30 minutes at room temperature in a humid chamber with secondary antibody linked to peroxidase diluted to 1:1000 in PBS and then rinsed with PBS. Before adding the substrate/chromogenic solution, the slides were rinsed with distilled water and stained with hematoxylin of Mayer. Negative controls were obtained by replacing the primary antibody with buffer. The immunostaining was performed through slides observation at optical microscope in white light using the objectives (x10) and (x40).

RESULTS AND DISCUSSION

The immunohistochemical results were used to estimate the expression level of GAPDH and its immunolocalization in different lesions of breast.

We found that the expression level of GAPDH became more intense and diffuse in tumor tissues compared with benign tissue. This applies to the breast tissue (Figures 1–2). These results complement and are consistent with those of Aparecida Corrêa et al. for breast cancer [16]. This result seems to prove the involvement of GAPDH in the tumor process. It is also clear that the localization of GAPDH in the three

organs vary with the degree of tumor differentiation (Table 1). Thus, in breast cancer, it was demonstrated that the expression of GAPDH was dependent on the stage of the disease so that it increased significantly in the most advanced stages. It should be noted that it has cytoplasmic or membrane localization in breast, cervix and prostate benign lesions. Whereas the membrane localization is probably related to its role as a carrier and its ability to bind to the membrane, as described by Sirover [9], the cytoplasmic localization can be related to its pivotal role as glycolytic enzyme [10, 11]. Or it may be related to its role as kinase capable of phosphorylating cytoplasmic proteins [9].

Table 1. Identification of the immunolocalization of GAPDH in breast lesions by immunohistochemical study
(- Absent; + Scarce; ++ Abundant; +++ Excessive)

Lesions	Localization		
	Membrane	Cytoplasmic	Nuclear
Solitary cyst with sore	+	+	-
Adenosis	+	+	-
Fibroadenoma	++	++	-
Carcinoma	+++	+++	+++

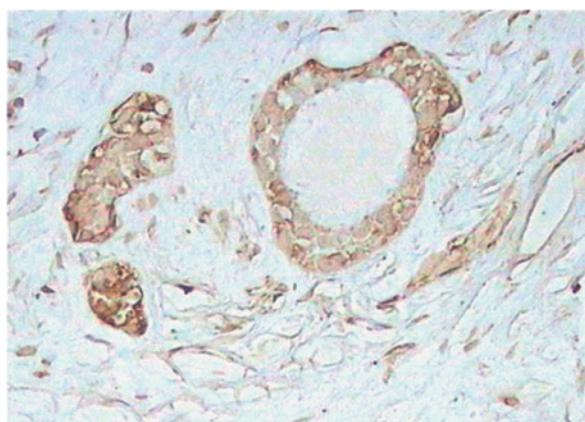


Figure 1. Detection of GAPDH expression in benign breast lesion by immunohistochemical analysis with the polyclonal anti human GAPDH ($\times 40$)

In breast cancer cases, we have found a membrane, cytoplasmic and particularly a nuclear overexpression. This overexpression suggests either its involvement in the cancer process, and therefore, draws attention to a new possible role of GAPDH in carcinogenesis which can be added to those already described or it suggests that GAPDH undergoes regulation in tumor tissue, in relation to carcinogenesis, being involved in other roles independently of its classical glycolytic role

[17]. Although GAPDH seems involved in malignant tumor process, until now, there is no certainty about this likely role.

This could help to develop a gene therapy with antisense oligodeoxynucleotides directed against the mRNA isoform (s) in cancer cases involving overexpression of GAPDH.

CONCLUSIONS

Our study has shown that in organ Breast GAPDH showed an overexpression in malignant tumor tissues. It has been shown that labeling was essentially nuclear in malignant lesions.

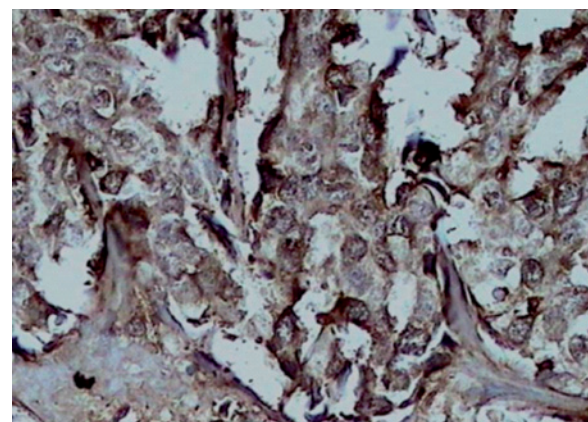


Figure 2. Detection of GAPDH expression in malignant breast lesion by immunohistochemical analysis with the polyclonal anti human GAPDH ($\times 40$)

These results suggest GAPDH involvement in cancer process and draw attention to a probable new nuclear role. In addition to other functions already described such as its implication in glycolysis, apoptosis or oxidative stress, GAPDH may be implicated in DNA replication or repair.

Although GAPDH seems to be involved in malignant tumor process, there is no certainty about its specific role in the studied pathologies. Therefore it

would be very interesting to evaluate the expression of the gene encoding this enzyme.

Moreover, it seems important to demonstrate whether the new role of GAPDH remains specific to a single form, or it is related to different isoforms of the enzyme, which can help to develop a gene therapy with antisense oligodeoxynucleotides directed against isoform(s) mRNA(s) in cases of cancer involving overexpression of GAPDH. Oligodeoxynucleotides directed against isoform(s) mRNA(s) in cases of cancer involving overexpression of GAPDH.

REFERENCES

1. SYGUSCH, J., AZEMA, L. AND DAX, C. (2006) A first weapon against cancer metastases. *Univolar Journal*, 1, 1–2.
2. WARBURG, O.H. (1956) On the origin of cancer cells. *Science*, 123, 309–314.
3. SOUKRI, A., VALVERDE, F., HAFID, N., ELKEBBAJ, M.S. AND SERRANO, A. (1996) Occurrence of a differential expression of the glyceraldehyde-3-phosphate dehydrogenase gene in muscle and liver from eutherian and induced hibernating jerboa (*Jaculus orientalis*). *Gene Journal*, 181, 139–145.
4. IDDAR, A., VALVERDE, F., SERRANO, A. AND SOUKRI, A. (2002) Expression, purification and characterization of recombinant non-phosphorylating NADP-dependent glyceraldehyde-3-phosphate dehydrogenase from *Clostridium acetobutylicum*. *Journal of Protein Expression and Purification*, 25, 519–526.
5. FOTHERGILL-GILMORE, L.A. AND PAM, M. (1993) Evolution of Glycolysis. *Journal of Progress in Biophysics and Molecular Biology*, 95, 105–135.
6. FIGGE, R.M., SCHUBERT, M., BRINKMAN, H. AND CERFF, R. (1999) Glyceraldehyde phosphate dehydrogenase gene diversity in eubacteria and eukaryotes: Evidence for intra- and interkingdom gene transfer. *Journal of Molecular Biology and Evolution*, 16, 429–440.
7. HABENICHT, A. (1997) The non-phosphorylating glycerol-dehyde-3-phosphate dehydrogenase: Biochemistry, structure, occurrence and evolution. *Journal of Biological Chemistry*, 378, 1413–1419.
8. BRUNS, G.A.P. AND GERALD, P.S. (1976) Human glycerol-dehyde-3-phosphate dehydrogenase in man-rodent somatic cell hybrids. *Science*, 192, 54–56.
9. SIROVER, M.A. (1999) New insights into an old protein: The functional diversity of mammalian glyceraldehyde-3-phosphate dehydrogenase. *Journal of Biochimica and Biophysica Acta*, 1432, 159–184.
10. BARBINI, L., RODRÍGUEZ, J., DOMINGUEZ, F. AND VEGA, F. (2007) Glyceraldehyde-3-phosphate dehydrogenase exerts different biologic activities in apoptotic and proliferating hepatocytes according to its subcellular localization. *Journal of Molecular and Cellular Biochemistry*, 300, 19–28.
11. SIROVER, M.A. (2005) New nuclear functions of the glycolytic protein, glyceraldehyde-3-phosphate dehydrogenase, in mammalian cells. *Journal of Cellular Biochemistry*, 95, 45–52.
12. PITOT, H.C. (1986) The biochemistry of neoplasia in vivo. *Fundamentals of Oncology*, Marcel Dekker, New York, 323–346.
13. ZHOU, Y.Y.X., STOFFER, B.J., BONAFE, N., GILMORE-HEBERT, M., MCALPINE, M. AND CHAMBERS, S.K. (2008) The multifunctional protein glyceraldehyde-3-phosphate dehydrogenase is both regulated and controls colonystimulating factor-1 messenger RNA Stability in Ovarian Cancer. *Journal of Molecular Cancer Research*, 6, 1375–1384.
14. DU, Z.-X., WANG, H.Q., ZHANG, H.Y. AND GAO, D.X. (2007) Involvement of glyceraldehyde-3-phosphate dehydrogenase in tumor necrosis factor-related apoptosis-inducing ligand-mediated death of thyroid cancer cells. *Journal of endocrinology*, 148, 4352.
15. LAFFARGUE, F., DARGENT, D. AND PIANA, L. (2002) Contribution des Sociétés françaises de chirurgie d'organe. *Bulletin du Cancer*, 89, 52–54.
16. CORREA, C.R., BERTOLLO, C.M., ZOUAIN, C.S. AND GOES A.M. (2010) Glyceraldehyde-3-phosphate dehydrogenase as an associated antigen on human breast cancer cell lines MACL-1 and MGSO-3. *Journal of Oncology Reports*, 24, 677–685.
17. SIROVER, M.A. (1990) Cell cycle regulation of DNA repair enzymes and pathways. In: Milo, G.E. and Casto, B.C., Eds., *Transformation of Human Diploid Fibroblasts*, CRC Press, Boca Raton, 29–55.

The article is devoted to the subjects of basic oncology, and highlights the study of the metabolism of the tumor tissue of breast cancer and identifies new and promising therapeutic approaches for the treatment of this disease. The research was conducted in a *careful* and *objective* way and can be recommended for publishing in the medical Journal *Archiv Euromedica*.

PROF. V.M. SEMENOV,
Vitebsk State Medical University
Vitebsk, Belarus

DIAGNOSIS OF SENSORY-PREDOMINANT CHRONIC INFLAMMATORY DEMYELINATING POLYNEUROPATHY: THE EXPERIENCE OF OUR CLINIC

N. Shnayder¹, T. Popova¹, M. Petrova¹, T. Nikolaeva², E. Chesheiko¹,
 S. Dyuzhakov¹, A. Semenov², E. Kantimirova¹, A. Dyuzhakova¹,
 K. Gazeckampf¹, Yu. Panina¹

¹V.F. Voino-Yasenetsky Krasnoyarsk State Medical University,

University Clinic, Krasnoyarsk, Russia

²M.K. Ammosov North-Eastern State University, Yakutsk, Russia

ABSTRACT — We present our experience in diagnosis of sensory-predominant chronic inflammatory demyelinating polyneuropathy (SP-CIDP), which utilizes unique approach, including computerized pallesthesiometry and thermosensometry, transcutaneous oxymetry and stabilometry. We strongly emphasize the connection between Herpes viridae infection and SP-CIDP. Attention to chief complaint of patient and multimodal testing of superficial and deep sensation is accentuated. We suggest our approach to diagnosis for wider utilization considering high prevalence of SP-CIDP in general population. We believe, that implementation of our diagnostic approach in clinical medicine will clarify epidemiology of SP-CIDP. Our system helps practitioner in differential diagnosis and further management of patient with SP-CIDP.

KEYWORDS — sensory-predominant chronic inflammatory demyelinating polyneuropathy (SP-CIDP), diagnosis, human.

INTRODUCTION

Chronic inflammatory demyelinating polyneuropathy (CIDP) belongs to a group of dysimmune neuropathies. The prevalence of CIDP varies between 0.5 in children [1] and 9.0 per 100000 of population in adults [2, 3, 4]. In Krasnoyarsk krai the prevalence of CIDP is significantly higher – 25.5 per 100000 of population [5], which is thought to be due to climate and higher prevalence of immunodeficiency among the population of Siberia. Risk factors of CIDP are immunodeficiency, diabetes and neurotrophic viruses [6]. Antigens which trigger autoimmune response are currently not known [4]. Interestingly, *Herpes viridae* infection is found in 80% of CIDP cases [5]. Cellular and humoral immune response play major role in pathogenesis of CIDP, where demyelination transforms into axonal degeneration of peripheral nerves [4, 7]. CIDP has diverse clinical presentation. Classic CIDP is characterized by sensorimotor symptoms, including hyporeflexia, sensory disturbances in distal segments of extremities with muscle weakness appearing in later stages of disease [1]. Usually, the

diagnosis of CIDP is not difficult. However, sensory-predominant CIDP (SP-CIDP) is frequently underdiagnosed in outpatient clinic. The reason for this is that patient usually doesn't have any complaints during early stage of disease. Underdiagnosis of SP-CIDP and lack of adequate therapy results in further progression of symptoms and worsening of patient's condition. Approximately 50% of polyneuropathies of unknown cause may be attributed to SP-CIDP [8]. Diagnosis suggested to be established by electromyography (EMG), nerve biopsy, nerve ultrasound and cerebrospinal fluid (CSF) testing [1, 9]. Diagnostic criteria for CIDP are not strictly specific in these methods, but they verify the presence of demyelination. Unfortunately, demyelination is universal process of damage to nervous system, including peripheral nerves. Because of this, these methods have low specificity for CIDP. Similar presentation may occur in diabetic polyneuropathy, Charcot-Marie-Tooth disease type 1, paraneoplastic and other forms of polyneuropathies. Furthermore, nerve biopsy and CSF testing are highly invasive methods which are only done in the setting of inpatient departments. Thus, development of new diagnostic approach to SP-CIDP in outpatient clinic, which utilizes modern non-invasive neurophysiological testing, is needed. Furthermore, implementation of new diagnostic battery will improve epidemiologic data on CIDP.

There are two stages in the diagnosis of SP-CIDP in our clinic.

STAGE 1: PHYSICAL EXAMINATION

New approach to diagnosis of SP-CIDP was developed in the Neurological Center of Epileptology, Neurogenetics and Brain Research of the University Clinic of the Krasnoyarsk State Medical University (UC KSMU) in 2013. It is suitable for initial diagnosis of SP-CIDP with utilization of new algorithm. The registry of patient with SP-CIDP has data collected for 5 years. As of now, there are 176 patients in the database. We expect significant increase in patients after implementation of new neurophysiological algorithm of SP-CIDP diagnosis in other clinics.

Analysis of subjective symptoms is done during first visit of patient to UC KSMU. The presence of



Natalya A. Shnayder
MD, Prof., head of the
Neurological Center
naschnaider@yandex.ru



Tatyana E. Popova
MD, Assos. Prof.
tata2504@yandex.ru



Marina M. Petrova
MD, Prof., head of
Department
stk99@yandex.ru



Tatyana Y. Nikolaeva
MD, Prof., head of
Department
tyanic@mail.ru



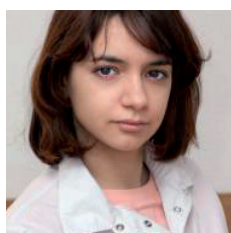
Elena Yu. Chesheiko
MD, physician general
of the University Clinic



Sergei K. Dyuzhakov
Medical Student
callgono@yandex.ru



Elena A. Kantimirova
MD, Assist. Prof.,
kantilea@mail.ru



Anna V. Dyuzhakova
Medical Student
humsterzoa@gmail.com



Kirill A. Gazenkampf
Post-graduate Student
hassenkampf@mail.ru



Yulia S. Panina
Researcher of the Inter-
departmental Laboratory
mrs.yuliapanina@mail.ru

distal paresthesia, numbness in hands and feet, pain in gastrocnemius muscle is noted. These symptoms may be suggestive of other demyelinating polyneuropathies. Chronic *Herpes virus* infection (e.g. orofacial and genital herpes) must be noted as well, including family history of such infections; 28% of patients from our study have had familial cases of *Herpes virus* infection. In our clinic the multimodal evaluation of superficial and deep sensation is available. Interestingly, there is a hyperesthesia in form of "gloves and stockings" during testing of pinprick sensation with Wartenberg pinwheel. Distal hypesthesia is less common. Thermosensation is evaluated with thermoesthesiometer (Tip-Term). Electrothermometer allows measuring of local temperature on the surface of skin. Distal hypothermia is commonly found in polyneuropathies. Touch sensation is tested with monofilaments. In most cases of SP-CIDP the symptoms are initially confined to distal segments of extremities. Sensitive ataxia of varying degree may be present during testing of balance.

STAGE 2: NEW NEUROPHYSIOLOGICAL ALGORITHM OF SP-CIDP DIAGNOSIS

Computerized pallesthesiometry (CPa) is developed for evaluation of thick A β myelinated fibers of distal peripheral nerves, which are responsible for conduction of vibrosense [10, 11]. The vibration is provided in following frequencies – 8, 16, 32, 64, 125, 250 and 500 Hz. Reduced vibrosense may be revealed in preclinical stage of SP-CIDP, when tuning fork test is negative. CPa is a screening method of diagnosis. If SP-CIDP is suspected, computerized thermosensometry (CTh), stabilometry, transcutaneous oxymetry (TCOx) and nerve conduction studies (NCS) follows (fig. 1).

Thinly myelinated fibers of peripheral nerves are responsible for conduction of thermosense. CTh is designed for evaluation of thermosense in distal parts of upper and lower extremities (hands, forearms, feet and calves). Thermodynamic test is carried out in order to evaluate sensation of cold and warmth, as well as pain thresholds for these stimuli. Cold dyesthesia is revealed in 70% of patients with SP-CIDP. Furthermore, slight reduction in sensation of cold and warmth is also characteristic for SP-CIDP. It must be noted, that similar findings may also be present in diabetic polyneuropathy [5].

Sensitive ataxia is evaluated during stabilometry. Rhomberg test on stabilometer is helpful in determination of type of ataxia; it may differentiate between sensitive, cerebellar, cortical and vestibular ataxias.

Our algorithm features TCOx, which measures the amount of transdermal oxygen in lower extremities. TCOx was previously used for evaluation of patients with diabetic foot [12]. Reduction of transdermal oxygen in the presence of SP-CIDP may suggest impairment of peripheral nervi vasorum of lower extremities and may hint on the involvement of autonomic nerve fibers.

Beside aforementioned tests we also do NCS for patients with suspected SP-CIDP. NCS usually reveals axonal demyelina-

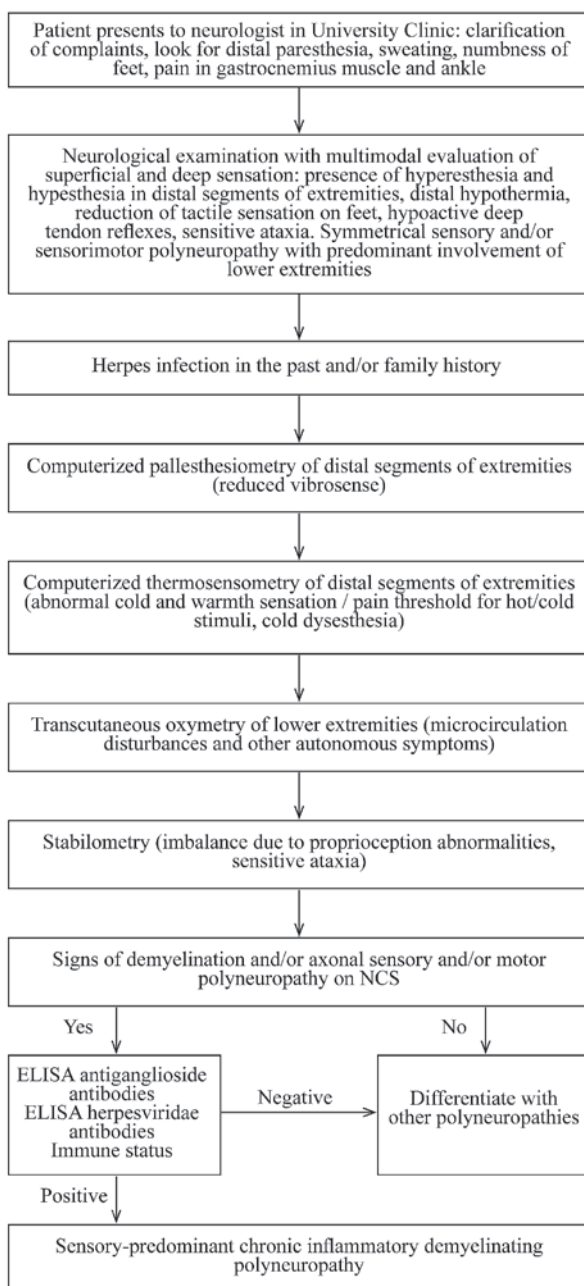


Fig. 1. Diagnostic algorithm of sensory-predominant in our university

tion of motor (in the absence of motor weakness) and sensory fibers. Similar results provided in Chin et al. article [8].

Enzyme-linked immunosorbent assay (ELISA) for IgG and IgM to herpesviridae viruses is done for every patient, as well as immunological status tests [5]. For some patients, antiganglioside antibodies testing is indicated.

If the diagnosis of SP-CIDP is confirmed, immunoglobulin treatment and antiviral therapy is initiated.

Case report

31-year-old female patient complains of headache, feeling of weightlessness and earfullness with bouts of blurred vision for several seconds, weight gain since last year and irregular periods, elevation of blood pressure up to 130/... mmHg, which is accompanied by vertigo and gait disturbance, slight elevation of body temperature up to 37° C. Headache is dull and monotonous, located in frontotemporal region, which is present every day starting two months ago.

Medical history is noted for frequent nasal and labial herpes since childhood.

Patient also complained of auditory hallucinations presenting as if someone is calling her name, which started in 2004 and were accompanied with inadequate behavior and ambulatory automatism. Patient's colleagues called ambulance and she was hospitalized. Patient does not remember this occasion. In autumn of 2013 patient started to hear conversation of a man and woman upon waking up. These hallucinations were regularly experienced for up to two times a month.

Patient's mother occasionally experienced visual hallucinations and was evaluated for epilepsy with negative results. She also had orofacial herpes. Her father had relatives with epilepsy.

Patient links worsening of her condition with recent change of residence – patient lived in Norilsk for 2 years before moving back to Krasnoyarsk in May 2013. After that, patient had irregular periods and rapid weight gain, as well as appearance of bilateral xanthomas on lower eyelids.

Patient has artistic job, which is sedentary (working on PC) and accompanied with stress.

Also, patient's history is notable for car accident in 2010, in which patient sustained head trauma which manifested as retrograde amnesia and spatial disorientation for 2 months. Concussion was diagnosed and patient was treated.

Patient was listed for annual anti-influenza vaccination but because of slightly elevated body temperature she was unlisted and undergone an evaluation for tuberculosis, which was negative.

On physical examination in the outpatient clinic, the patient is oriented, in no acute distress, well developed and overweight. Her skin is moderately moisturized, with xanthomas on lower eyelids bilaterally. There are no edemas. Her eyes are reddish with scant serous discharge. Submandibular lymph nodes are enlarged, no tenderness. Tonsils are enlarged. Nasal breathing is mildly obstructed. Her blood pressure is 90/60 mmHg. Diffuse enlargement of thyroid gland of 2–3 degree is noted.

On neurological examination in UC KSMU revealed facial asymmetry presenting as uneven eye

slits and nasolabial folds on the left side. Mild constitutional exophthalmos was noted. Mild myopia. Eye movements were slightly restricted in extreme horizontal deviations bilaterally. Horizontal nystagmus with moderate oscillations was present, which slightly exacerbated upon left gaze. Reduced pinprick sensation was present on left side of face. Mild tongue deviation to the left. Palmonental reflex was present bilaterally. Muscle tone was reduced in all extremities. Deep tendon reflexes were normoactive and symmetrical. Finger-to-nose test and heel-to-shin test were performed with mild ataxia. Rhomberg's test is negative. Hypesthesia was present in distal segment of arms and hyperesthesia was revealed in distal segment of feet. Gait is normal. Arches of foot were high bilaterally. Sweating was observed in hands and feet. No meningeal signs were found.

Complete blood count test revealed lymphopenia and monocytosis. Immunogram revealed elevation of cytotoxic cells and reduction of CD16. ELISA found IgG antibodies against herpes simplex viruses (HSV) 1 and 2, as well as cytomegaloviruses (CMV) and Epstein-Barr viruses (EBV).

Visual evoked potentials (VEP) demonstrated signs of axonal demyelination of optic nerves on pre- and postchiasmal region, more prominent on the ride side.

Brain magnetic resonance imaging (MRI) with utilization of "epilepsy" program revealed shrinking and deformation of right hippocampus (mesial temporal sclerosis). Video-EEG-monitoring demonstrated prolonged interictal focal epileptiform activity in right temporal lobe.

Patient underwent evaluation using our new algorithm of neurophysiological diagnosing of SP-CIDP, which included CPa, CTh, stabilometry, TCOx and NCS. All tests were done on upper and lower extremities.

NCS ("Neurosoft", Ivanovo, Russia) revealed significant slowing of conduction in both sensory and motor fibers of medial nerve bilaterally, as well as in sensory fibers of tibial and peroneal nerves bilaterally.

Stabilometry showed disturbance of general posture with involvement of visual proprioceptive system (Fig. 2).

CTh (thermodynamic test with identification of pain threshold to cold and warm stimuli) (MBN, Moscow, Russia) did not reveal any harsh abnormality in temperature sensation on upper extremities. However, moderate elevation in pain threshold for cold stimuli was noted, which was progressively getting more pronounced in proximal segments of extremities. Temperature sensation, both for cold and warm stimuli, was slightly reduced on readings from lower extremities. Pain threshold for cold stimuli was markedly elevated

in lower extremities. These data is suggestive of cold dysesthesia, signifying mild damage to non-myelinated and thinly myelinated fibers of distal segments of lower extremities.

CPa (MBN, Moscow, Russia), read from styloid processes of ulnar bone, revealed reduction of vibrosense at frequencies 16, 32, 125, 250 Hz on the left side and at 125 and 500 Hz on the right side. This data can be interpreted as mild damage to thickly myelinated A β fibers of distal segments of upper extremities (Fig. 3).

CPa (MBN, Moscow, Russia), registered from ankles, showed slight reduction of vibrosense in wide range of frequencies on both sides with a more pronounced reduction at frequencies 250, 500 Hz on both sides and at 64, 125 Hz on the right side. This can be interpreted as moderate to severe damage to thickly myelinated A β fibers of distal segments of lower extremities (Fig. 4).

TCOx ("Radiometer TCM4", Copenhagen, Denmark) revealed slight reduction at all points of interest on the right side and at the level of foot on the left side.

Finally, the following diagnosis was made: "Chronic persisting mixt-herpes (HSV-1, 2, CMV, EBV) infection presenting as labial, nasal herpes with frequent exacerbations, currently in remission (last relapse on December 2013). Mild autonomous, sensory type of CIDP, newly diagnosed. Mild sensitive ataxia. Mild chronic bilateral inflammatory axonal demyelinating mononeuropathy multiplex of optic nerve, newly diagnosed. Chronic parainfectious (herpes mix-infection: HSV-1, 2, CMV, EBV) limbic encephalitis presenting as mesial sclerosis. Symptomatic temporal epilepsy of moderate frequency with simple sensory seizures (in form of auditory and olfactory hallucinations) and ambulatory automatisms, newly diagnosed. Moderate lateral ventricular asymmetry. Diencephalic syndrome with abnormalities in lipid and carbohydrate metabolism. Hypertension. Phobic anxiety disorder. Secondary immunodeficiency with constant hyperthermia and disruption of T-cell mediated immunity."

CONCLUSION

This diagnostic program was used in 147 patients with SP-CIDP. They were all revealed starting since 2012 until September 2014. Chronic *Herpes viridae* infection and secondary immunodeficiency was revealed in the majority of patients, which confirms connection between SP-CIDP and *Herpes viridae* infection. Distal paresthesia and numbness, accompanied with distal hypothermia are the main symptoms of SP-CIDP. CPa, CTh, stabilometry, TCOx and NCS are strongly

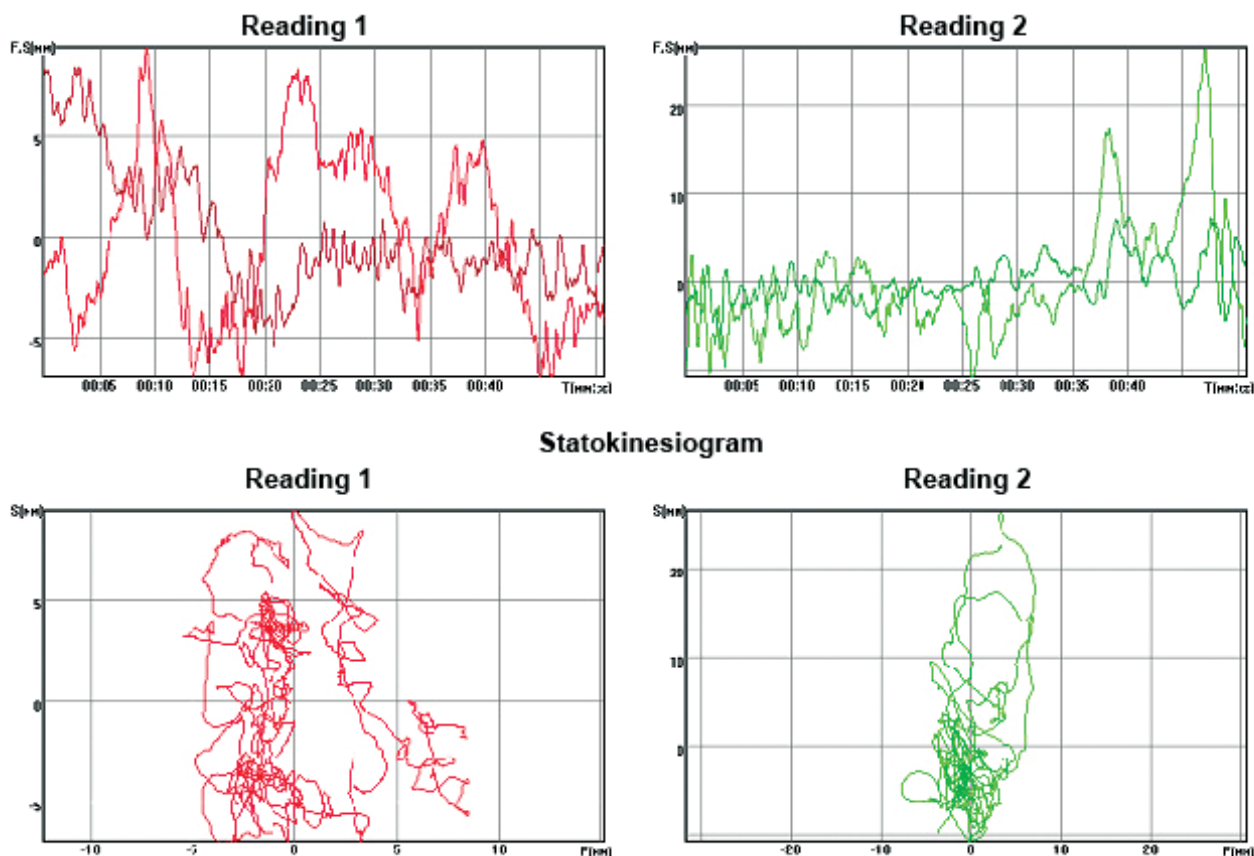


Fig. 2. Stabilometry (case report) – in Rhomberg's position (EU standard) with eyes open (A) and eyes closed (B)

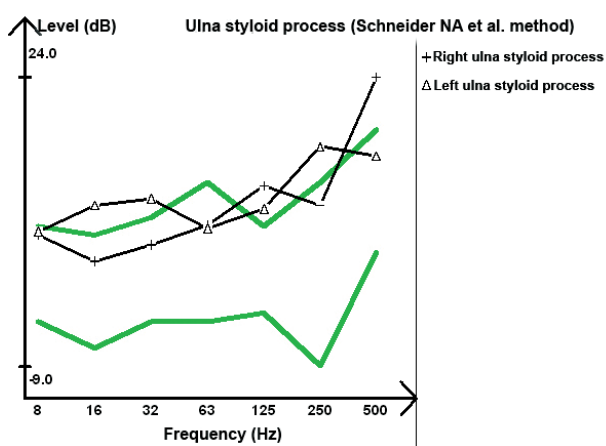


Fig. 3. Computerized pallesthesiometry (CPa), readings from styloid process of elbow bone – reduction of vibrosense on the left at following frequencies: 16, 32, 125, 250 Hz and on the right – 125, 500 Hz (Green line – reference range, black line – actual readings)

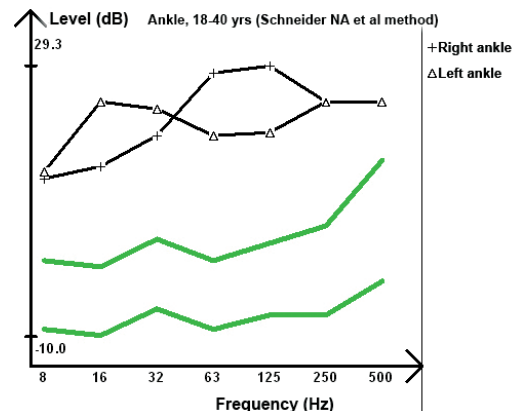


Fig. 4. Computerized pallesthesiometry, readings from ankles – slight reduction of vibrosense in wide range, with more pronounced reduction at 250, 500 Hz bilaterally and 64, 125 Hz on the right side (Green line – reference range, black line – actual readings)

indicated in evaluation of SP-CIDP. In our experience, these tests were very helpful in confirming SP-CIDP. Furthermore, wide utilization of these tests may alter the epidemiological data available.

REFERENCES

1. KERASNOUDIS A. The Role of neuromuscular ultrasound when diagnosing chronic inflammatory demyelinating polyneuropathy. *Europ Neurol Rev* 2013;8(1):52–54.
2. IJIMA M, KOIKE H, HATTORI N, ET AL. Prevalence and incidence rates of chronic inflammatory demyelinating polyneuropathy in the Japanese population. *J Neurol Neurosurg Psychiatry* 2008;79:1040.
3. RAJABALLY YA, NICOLAS G, PIÉRET F, ET AL. Validity of diagnostic criteria for chronic inflammatory demyelinating polyneuropathy: a multicentre European study. *J Neurol Neurosurg Psychiatry* 2009;80:1364.
4. STÜBGEN JP. Biological agents for chronic inflammatory demyelinating polyradiculoneuropathy. *Eur Neurol rev* 2013;8(1):57–61.
5. SHNAYDER NA, KANTIMIROVA EA. Epidemiological and clinical characteristics of several forms of polyneuropathies (ZATO Zhelezogorsk of Krasnoyarsk krai taken as example) [Article in Russian]. *Nervno-myscheschiyi bolezni* 2011;1:34–40.
6. FATEHI F, NAFISSI S, BASIRI K, ET AL. Chronic inflammatory demyelinating polyneuropathy associated with diabetes mellitus. *J Res Med Sci* 2013;18(5):438–441.
7. HUGES RA, ALLEN D, MAKOWSKA A, GREGSON NA. Pathogenesis of chronic inflammatory demyelinating polyradiculoneuropathy. *J Peripher Nerv Syst* 2006;11:30–46.
8. CHIN RL, LATOV N, SANDER HW, ET AL. Sensory CIDP presenting as cryptogenic sensory polyneuropathy. *J Peripher Nerv Syst* 2004;9(3):132–137.
9. SAPERSTEIN DS. Chronic acquired demyelinating polyneuropathies. *Semin Neurol* 2008;28:168–184.
10. KURUMCHINA OB, SHNAYDER NA, PETROVA MM, ET AL. Relation of computer esthesiometry and symptom scores in diagnostics of diabetic polyneuropathy. *Med Health Sci J* 2010;4:101–112.
11. SHNAYDER N A, GLUSHENKO EV, KANTIMIROVA EA, ET AL. Sensitivity of computer esthesiometry on distal parts of the upper extremities at patients with hereditary neuropathy Charcot-Marie-Tooth. *Med Health Sci J* 2011;9:25–30.
12. TERSKOV DV, SHNAYDER NA. Transcutaneous oxymetry as method of evaluation of critical ischemia in patients with diabetic foot syndrome and occluding lesions of lower extremities arteries [Article in Russian]. *Vestnik klinicheskoi bolnitsy №51* 2010;3(8):56–61.

MIKTIONSSTÖRUNGEN BEI M. PARKINSON

W.N. Vance

Funktionsabteilung Neuro-Urologie,
Neurologisches Fachkrankenhaus für
Bewegungsstörungen/Parkinson,
Beelitz-Heilstätten



W.N. Vance

*Facharzt für Urologie,
Funktionsabteilung Neurourologie
Kliniken Beelitz GmbH, Paracelsusring 6a,
14547 Beelitz-Heilstätten
vance@rehaklinik-beelitz.de*

ABSTRACT

Bladder dysfunction in Parkinson's patients are described in the literature with an incidence 37-93 per cent. Nocturia and urinary urgency usually are perceived as particularly disturbing. A classification of bladder dysfunction based on anamnesis is usually not sufficient because the symptoms can be caused by the neurological disease, age-related changes in the urinary bladder, concomitant diseases, medications, and urologic and urogynecologic pathological changes. There is a need in treatment-resistant cases, especially prior to the implementation of urologic and urogynecologic surgery a differentiated diagnostic investigation of complaints.

KEYWORDS — Parkinson's disease, bladder dysfunction.

EINFÜHRUNG

Die in vielen Publikationen beschriebene Diagnose einer zerebral enthemmten Harnblase bei Parkinson-Patienten mit den Symptomen Polakisurie, Nykturie, imperativem Harndrang und Dranginkontinenz, bedarf einer Basisdiagnostik. Die Basisdiagnostik, im optimalen Falle bestehend aus Miktionsprotokoll, Restharnprüfung und Harnstrahlmessung (Uroflow), lässt eine erste Differenzierung zwischen einer Harnblasenentleerungsstörung (z.B. Restharnbildung) und einer Harnspeicherstörung (z.B. Dranginkontinenz) in nahezu allen Fällen zu. Die Therapie einer Harnblasenentleerungsstörung unterscheidet sich von der einer Dranginkontinenz, die empirische Gabe einer anticholinergen Medikation führt hier zu einer Verschlechterung der Harnblasenentleerung, bei der Dranginkontinenz eventuell zu einer Verlängerung der Miktionsintervalle.

In einem zweiten Schritt bedarf es der Ursachen-suche. Eine Harnblasenfunktionsstörung kann neurologische, urologische, urogynäkologische, medikamentöse und organisatorische Ursachen haben.

Das Gebiet der Neuro-Urologie bedarf einer engen Zusammenarbeit mit der Neurologie, anderseits können neurologische Primärziele, wie z. B. Verbesserung der Lebensqualität durch Verbesserung der Motorik und Reduktion von Schlafstörungen, nur dann erreicht werden, wenn urologische Beschwerden reduziert werden können. Bei einer Nykturie von 4–6 mal wird das Schlafdefizit ohne urologische Zusatzbehandlung nicht zu beheben sein, nicht zu vergessen ist die hohe nächtliche Sturzgefahr. Eine stündliche Polakisurie zwingt die Betroffenen und deren Angehörige nicht selten zum Verzicht auf soziale Teilhabe.

Der Schwerpunkt dieses Artikels liegt nicht in der Darstellung der therapeutischen Möglichkeiten, sondern in der diagnostischen Differenzierung, da die Therapie meistens in urologischen Praxen und Kliniken erfolgt. In nicht wenigen Fällen bedarf die differenzierte Abklärung der Miktionsbeschwerden einer erweiterten Ausstattung, welche nicht immer in urologischen Praxen vorrätig sein dürfte.

Dem/r neurologischen Facharzt/-ärztin soll jedoch die Komplexität der urologischen Beschwerden und der Diagnostik vorgestellt werden. Im optimalen Falle arbeiten niedergelassene neurologische Ärzte/Ärztinnen, oder neurologische Kliniken eng mit neuro-urologisch kompetenten, urologischen Ärzten/-innen oder Kliniken zusammen. Meistens lässt sich hierdurch eine urologische Unter- oder Überversorgung der Parkinson-Patienten vermeiden.

DIE NORMALE HARNBLASENFUNKTION:

Sofern keine urologische, neurogene oder altersbedingte Störung der Harnblasenfunktion vorliegt gilt eine Frequenz von bis zu acht Miktionsen in 24 Stunden als normal. Die anatomische und die funktionelle Blasenkapazität betragen ca. 400 bis 500 ml. Eine Nykturie zwischen 0 und 2 mal pro Nacht kann als regelrecht bezeichnet werden. Die Harnblasenentleerung erfolgt nahezu restharnfrei und mit einem einphasigen Harnstrahl. Ein Nachpressen nach Beendigung der Miktions hat keinen Krankheitswert.

Das nachfolgende Miktionssprotokoll über 24 Stunden (50-jähriger Patient) verdeutlicht eine normale Harnblasenfunktion.

Das Miktionssprotokoll (Abb.1) zeigt, dass eine regelrechte Miktionsfrequenz, regelrechte Miktionsvolumina, keine Nykturie und regelrechte Trinkmengen vorliegen. Das Miktionssprotokoll (z.B. über 2 Tage durchgeführt) stellt eines der wichtigsten, kostengünstigsten, zeitsparenden und beliebig oft reproduzierbaren diagnostischen Screeningverfahren dar. Auch kann z.B. eine Nykturie aufgrund einer deutlich überhöhten nächtlichen Urinproduktion Hinweise auf eine internistisch zu behandelnde Herzinsuffizienz geben.

Miktionsmengen und Uhrzeit		Trinkmengen und Uhrzeit	
Uhrzeit	Volumen	Uhrzeit	Volumen
6.00	450 ml	6.10	200 ml
11.10	360 ml	9.00	200 ml
15.05	350 ml	12.00	300 ml
18.10	390 ml	14.30	250 ml
22.05	300 ml	18.00	350 ml
		20.20	250 ml
6.05	500 ml	6.30	200 ml
Gesamtmenge	2350 ml	Gesamtmenge	1750 ml

Abb. 1.

ALTERSBEDINGTE VERÄNDERUNGEN DER HARNBLASENFUNKTION:

Mit zunehmendem Alter (oft ab dem 60. Lebensjahr) kommt es altersbedingt zu anatomischen und funktionellen Veränderungen der Harnblase und ihrer Funktion. Die Kontraktilität des Harnblasenmuskels nimmt ab, eine gewisse Restharnbildung ist tolerabel und der Harnstrahl wird etwas schwächer. Die Blasenkapazität kann sich auf 300 bis 400 ml reduzieren. Durch hormonelle Veränderungen (z.B. veränderte Ausschüttung des Antidiuretischen Hormons) kommt es zu vermehrter nächtlicher Urinproduktion, so daß eine Nykturie von zweimal als normwertig angesehen werden kann. Zusätzliche Erkrankungen wie z. B. Herzinsuffizienz, venöse Erkrankungen und Diabetes mellitus verändern ebenfalls Verhältnis von Diurie und Nykturie.

UROLOGISCHE UND UROGYNÄKOLOGISCHE URSACHEN VON BESCHWERDEN:

Ab dem fünfzigsten bis sechzigsten Lebensjahr ist bei nahezu 50 Prozent aller Männer eine mehr oder weniger deutliche Prostatavergrößerung nachweisbar.

Eine symptomatische benigne Prostatavergrößerung geht häufig, aber nicht immer mit deutlicher Restharnbildung oder einem schwachen Harnstrahl einher. Es können auch ausschließlich Symptome wie Pollakisurie, Nykturie und imperativer Harndrang vorliegen. Eine Restharnbildung kann auch medikamentöse oder neurologische Ursachen haben. Die Basisdiagnostik reicht für eine Differenzierung nicht aus. Die erweiterte diagnostische Abklärung erfordert eine urodynamische (Blasendruckmessung), radiologische (Miktionssysthrethrogramm, bzw. Videourodynamik) und im Einzelfalle endoskopische (Urethrozystoskopie) Abklärung. Eine der schwierigsten Aufgaben des Urologischen Facharztes ist die Abklärung einer subvesikalen Obstruktion bei einem männlichen Parkinson-Patienten. Es gilt eine Differenzierung zu treffen zwischen einer symptomatischen Prostatavergrößerung, einer so genannten Detrusor-Sphinkter-Dyssynergie (unkoordinierte Harnblasenmuskel- und Schließmuskelfunktion, z.B. bei einer Multisystematrophie) und einer passageren, medikamentös ausgelösten Harnblasenmuskelschwäche (Detrusorhypokontraktilität).

Bei jeder zweiten Frau finden sich im fortgeschrittenen Alter mehr oder weniger Symptome einer Belastungskontinenz mit Urinverlust beim Husten, Niesen und Lachen, insbesondere nach einer Hysterktomie. Eine weitere Gruppe von Patientinnen leidet an einer kombinierten Drang- und Belastungskontinenz. Hierbei tritt der imperative Harndrang beim Lagewechsel vom Liegen zum Stehen, bzw. Sitzen auf, nachts bestehen kaum Beschwerden. Auch hier bedarf es einer umfangreichen Diagnostik. Eine der am schwierigsten zu stellenden Diagnose stellt hier eine Harnblasenhals-insuffizienz dar. Mittels Anamnese und Basisdiagnostik kann selten eine Unterscheidung zur zerebral enthemmten Harnblase getroffen werden. Wurde eine neurogene Harnblasenfunktionsstörung ausgeschlossen und eine urogynäkologische Ursache dokumentiert, bedarf es einer weiteren urogynäkologischen Differenzierung um das geeignete konservative oder operative Vorgehen festzulegen.

PATHOPHYSIOLOGIE DER ZEREBRAL ENTHEMMTEN HARNBLASE BEI PARKINSON-SYNDROMEN

Die in der Literatur am häufigsten angeführte neurogene Harnblasenfunktionsstörung ist die zerebral enthemmte Harnblase. Die Symptome sind imperativer Harndrang, Pollakisurie und Nykturie, gegebenenfalls mit einer Dranginkontinenz. Die Harnblasenkontrolle erfolgt durch die Zusammenarbeit des pontinen und des sacralen Miktionszentrums. Das pontine Miktionszentrum befindet sich im Bereich des Nu-

cleus coeruleus des Tegmentums im Mesencephalon. Neben den vesicolumbalen Reflexbögen und der Steuerungsfunktion der mesopontinen Strukturen ist auch das Großhirn an der Koordination der Miktion beteiligt. Mit Befall der diencephalen Kerne und dem Auftreten von Störungen des limbischen Systems entfällt die zentrale Hemmung der mesopontinen Regulationszentren. Das Auftreten urologischer Beschwerden ist beim M. Parkinson u. a. auf die Degeneration nigrostriataler Neurone zurückzuführen, der entsprechende Schweregrad der urologischen Beschwerden wird durch die Degeneration des Nucleus caudatus bestimmt. Die Basalganglien haben einen koordinierenden und hemmenden Einfluss auf das pontine Miktionszentrum und somit auf die Funktion des Harnblasenmuskels. Entfällt dieser hemmende Einfluss können sich die Symptome einer zerebral enthemmten Harnblase mit plötzlichem, imperativem Harndrang, Pollakisurie und Nykturie entwickeln, die Betroffenen können die Harnblase allerdings noch restharnfrei entleeren. Als Folge tritt eine Detrusorhyperreflexie ohne Detrusor-Sphincter-Dyssynergie auf. Zusätzlich kann eine Hypersensibilität der Harnblase bei geringen Blasenfüllungsvolumina auftreten. Werden im fortgeschrittenen Erkrankungsstadium zusätzlich die Neurone der Zona intermedia des sacralen Rückenmarks, bzw. der sacrale Nucleus intermediolateralis befallen und tritt somit eine verminderte Innervation der sympathischen Efferenzen der Nn. Pelvici auf, kann eine zusätzliche Blasenboden- und Sphincterschwäche (innerer Sphincter/Blasenausgang) auftreten.

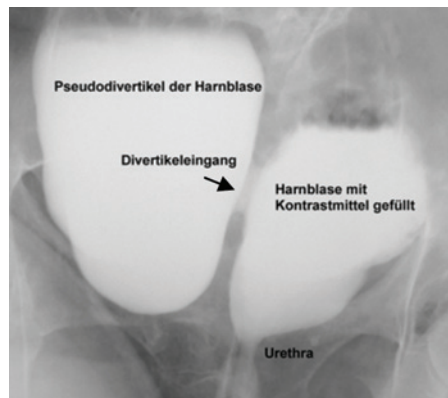


Abb. 2. Miktionszysturethrogramm mit großem Pseudodivertikel der Harnblase eines 70jährigen Mannes mit therapieresistenter Pollakisurie und ohne sonographisch nachweisbarer Prostatavergrößerung. Trotz regelrechten Miktionsvolumina (400 ml) waren jeweils Restharnwerte von bis zu 600 ml nachweisbar, welche auch mittels Einmalkatheterismus nicht entleert werden konnten. Therapie: Prostataresektion und Divertikelabtragung.

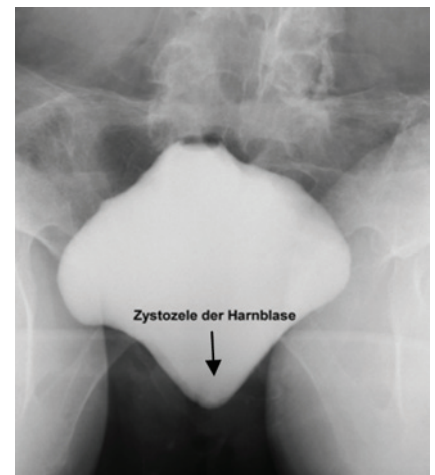


Abb. 3. Miktionszysturethrogramm einer Parkinson-Patientin mit deutlicher Senkung (Zystozele) der Harnblase. Neben einer Belastungssinkkontinenz traten die Symptome einer Pollakisurie, Nykturie und eines nicht unterdrückbaren Harndranges beim Laufen.

Miktionsmengen und Uhrzeit		Trinkmengen und Uhrzeit	
Uhrzeit	Volumen	Uhrzeit	Volumen
7.00	200 ml	7.10	200 ml
8.15	110 ml	9.00	200 ml
10.05	90 ml	12.00	300 ml
12.20	120 ml		
14.05	90 ml	14.30	250 ml
16.10	95 ml		
18.20	70 ml	18.00	150 ml
19.30	100 ml	19.30	200 ml
22.00	140 ml	21.00	150 ml
1.00	50 ml		
2.40	120 ml		
3.30	100 ml		
6.05	280 ml		
Gesamtmenge	1555 ml	Gesamtmenge	1450 ml

Abb. 4.

Das Miktionsschema (Abb. 4) zeigt, dass eine deutliche Pollakisurie und eine Nykturie mit kleinen Harnmengen vorliegen, die Trinkmenge und die Gesamtausscheidung liegen im Normbereich. Weiterhin ist erkennbar, dass keine übermäßige nächtliche Harnproduktion vorliegt, welche z. B. auf eine andere Erkrankung wie z. B. Herzinsuffizienz, oder die nächtliche Ausscheidung von tagsüber auftretenden Beinödemen auftritt. Im Mittel liegen die Harnmengen bei ca. 130 ml (normal: 300–500 ml), die sogenannte maximale (funktionale) Blasenkapazität beträgt im Beispiel 280 ml (normal: 400–500 ml). Das Beispiel weist auf eine überaktive Harnblase hin. Sofern der Patient

zusätzlich ein oder mehrere Inkontinenzepisoden notierte, bestünde der Verdacht auf eine Dranginkontinenz.

HARNBLASENFUNKTIONSTÖRUNGEN BEI EINER MULTISYSTEMATROPHIE

Urologische Beschwerden treten bei einer Multisystematrophie (MSA) noch weitaus häufiger als bei der idiopathischen Parkinson-Erkrankung und mit besonderen Charakteristika auf. Im Vordergrund stehen die dauerhafte, nicht situative Harninkontinenz und die unvollständige Blasenentleerung. Ein weiteres Symptom kann der Verlust des Blasenfüllungs- und entleerungsgefühls sein. Das Auftreten von Blutdruckschwankungen während einer Blasenentleerung ist ein weiteres, mögliches Symptom. Die Evaluation der Beckenbodenmuskulatur zeigt häufig eine Schwäche derselben und gelegentlich eine Schwäche des Analosphinkters an. Häufiger als beim IPS und bei der progressiven supranukleären Parese (PSP) kann eine Detrusor-Sphinkter-Dyssynergie, eine fehlende Koordination von Harnblasenmuskels (Detrusor vesicae) und des Harnblasenschließmuskels (Sphinkter vesicae) nachgewiesen werden. Urodynamisch ergibt sich häufig der Befund einer Hypo- oder Akontraktilität des Harnblasenmuskels (schlaffe Harnblasenlähmung). Entsprechend können bei den Betroffenen hohe Restharnwerte bis zur chronischen Überlaufblase auftreten. Bei anderen Betroffenen kann keine Restharnbildung nachgewiesen werden, hier kann es jedoch zu unkontrollierbarem, kontinuierlichem Harnverlust ohne vorherigen Harndrang kommen. Im weiteren Verlauf einer MSA muss von einer Häufigkeit urologischer Symptome in nahezu 100 Prozent der Fälle ausgegangen werden.

PARKINSON-MEDIKATION UND HARNBLASENFUNKTIONSTÖRUNGEN

Die Interaktionen von urologischen Medikamenten und den häufig verordneten Medikamenten zur Behandlung von Parkinson-Patienten sind bisher nicht umfassend untersucht. Die häufige Kombination mehrerer Parkinsonmedikamente erschwert die Eruierung deren Einzelwirkungen auf die Harnblase. Einerseits kann eine vom Urologen verordnete anticholinerge Medikation die medikamentöse Parkinson-Therapie beeinflussen, im Gegenzug kann die vom Neurologen eingesetzte Parkinson-Medikation, z.B. Anticholinergika die urologische Behandlung beeinflussen. Wenn Patienten über einen zeitlichen Zusammenhang zwischen dem Auftreten ihrer urologischen Beschwerden und einer Veränderung ihrer Parkinson-Medikation berichten, sollte die Mögli-

chkeit einer Anpassung der Parkinsonmedikation geprüft werden.

TIEFE HIRNSTIMULATION UND HARNBLASENFUNKTION

Nach Implantation eines Stimulators zur Hirnstimulation (THS) kann eine Änderung der Blasenspeicher- oder –entleerungssituation eintreten. Auch hier gilt, daß eine abschließende Bewertung aller Wirkungen noch nicht umfassend möglich ist. Wichtig zu wissen ist jedoch, daß nach der Implantation alle urologischen Anwendungen kontraindiziert sind, bei denen elektrische Energie auf den Stimulator übertragen werden kann. Dazu zählen Mikro- und Kurzwelle, therapeutischer Ultraschall, Rotlicht und Elektrostimulation. Bei Nicht-Beachtung ist mit schweren Nebenwirkungen, eventuell mit zerebralen Schäden zu rechnen. Da auch zu den elektrisch gestützten Resektionsverfahren und Laserablationen bei BPH keine generellen Angaben der Hersteller vorliegen, wird vom Hersteller der Stimulatoren im Einzelfall eine Kontaktaufnahme mit diesem und eine gemeinsame Einzelfallentscheidung empfohlen.

KOMPLEXITÄT DER URSAECHEN

In der neuro-urologischen Betreuung von Parkinson-Patienten finden sich überwiegend Patienten, welche keine isolierte neurogene Harnblasenfunktionsstörung haben. Im männlichen Klientel findet sich häufig eine Kombination von zerebral enthemmter Harnblase und einer Prostatahyperplasie. Im weiblichen Klientel eine Kombination von Drang- und Belastungssinkontinenz. Ein besonders Problem stellt die intermittierend auftretende Restharnbildung. Insbesondere ältere Patienten reagieren bei Auftreten einer Harnwegsinfektion nicht mit typischen zystitischen Beschwerden, sondern mit einer vorübergehenden Harnblasenentleerungsstörung. Häufig kann auf die Einlage einer dauerhaften Harnableitung weitgehend verzichtet werden, da die Kombination von intermittierendem Selbst- oder Fremdkatheterismus über mehrere Tage mit einer antibiotischen Therapie zu deutlich rückläufigen und tolerablen Restharnwerten führen kann. Auch eine im Rahmen einer medikamentösen Neueinstellung auftretende Harnverhaltung sollte zunächst durch intermittierenden Katheterismus behandelt werden. Nicht selten ist auch von einer situativ aufgetretenen myogenen Überdehnung der Harnblase auszugehen, welche sich unter dieser Therapie binnen kurzer Zeit bessern kann. Die frühzeitige Einlage einer dauerhaften, transurethralen Harnableitung sollte die Ausnahme sein, bei einem Infektionsrisiko von 3–10 % pro Tag wird die weitere Diagnostik sowie die Behandlung nur erschwert. Die Komplexität der Ursachen steigt mit der

Anzahl der Nebendiagnosen (z.B. Diabetes mellitus, Herzinsuffizienz) und der Art der Medikation.

WEITERFÜHRENDE DIAGNOSTIK BEIM FACHARZT FÜR UROLOGIE:

Einem neuro-urologischen Zentrum oder einer Ambulanz stehen der Uroflow (Harnstrahlmessung), die Urodynamik (Harnblasenfunktionsmessung), die Videourodynamik (kombinierte Röntgen- und Harnblasenfunktionsprüfung), die Urethrozystoskopie (Blasenspiegelung) und die isolierte Röntgenuntersuchung der Harnblase (Miktionszysturethrogramm) zur Verfügung. Insbesondere bei Vorliegen oder bei Verdacht auf eine Multisystematrophie mit oder ohne Restharnbildung sollte auf eine urodynamische Untersuchung nicht verzichtet werden. Eine Röntgenuntersuchung der Harnblase kann bei MSA-Patienten einen offenen, oder sich nicht öffnenden Blasenhals/Sphinkter nachweisen, in der Regel aber nicht beim idiopathischen Parkinsonsyndrom. Aufgrund des relativ hohen Risikos einer postoperativen Inkontinenz wird allgemein eine urodynamische Untersuchung vor urologischen Wahleingriffen (z.B. benigne Prostatahyperplasie) empfohlen. Bei einfachen Symptomen einer überaktiven Harnblase ohne wesentliche Restharnbildung, oder einer Dranginkontinenz, sind unkomplizierte Therapieversuche (s. u.) durch den Facharzt für Neurologie durchführbar.

THERAPEUTISCHE MÖGLICHKEITEN:

Die therapeutischen Möglichkeiten müssen sich immer an den motorischen und kognitiven Voraussetzungen des Patienten und seinem sozialen Umfeld sowie der häuslichen Betreuungsmöglichkeiten orientieren. Liegt der Schwerpunkt auf einer urologischen oder urogynäkologischen Diagnose, so muß individuell und interdisziplinär geklärt werden, ob eine Operation möglich und sinnvoll ist.

ORALE ANTICHOLOLINERGE MEDIKATION

Hierdurch können der imperativen Harndrang, die Nykturie und die Pollakisurie deutlich reduziert werden. Als Beispiele können Trospiumchlorid, Tolterodin, Oxybutinin und Propiverin genannt werden. Bei Einschränkung der kognitiven Leistungen, oder bei Halluzinationen sollten selektiv an peripheren M3-Acetylcholin-Rezeptoren ansetzende Wirkstoffe wie Darifenacin und Solifenacin bevorzugt werden. Bei diesen Medikamenten besteht empirisch ein reduziertes Risiko einer symptomatischen Interaktion mit der bestehenden Parkinson-medikation. Auf typische Nebenwirkungen wie Mundtrockenheit, Obstipation und Sehstörungen sollte hingewiesen werden. In nicht

wenigen Fällen lassen sich durch eine Kombination von Prostatamedikamenten und anticholinergen Substanzen gute Erfolge erzielen.

Liegt eine medikamentös nicht zu beherrschende Blasenentleerungsstörung vor, so sollte dem intermittierenden Einmalkatheterismus (Fremd- oder Selbstkatheterismus) so oft es geht der Vorzug gegeben werden. Über einen Einmalkatheter oder eine Dauerableitung kann Oxybutinin (als Fertigspritze) lokal in die zuvor entleerte Harnblase appliziert werden.

INTRAVESIKALE BOTULINUMTOXIN-INJEKTION

Bei Kontraindikation oder Unwirksamkeit einer oralen anticholinergen Medikation kann endoskopisch Botulinumtoxin in den Detrusor vesicae injiziert werden. In Abhängigkeit von der Dosierung kann hierdurch eine Reduktion der Detrusorkontraktilität, oder eine Detrusorakontraktilität bewirkt werden. Die Fähigkeit zum Selbstkatheterismus, bzw. die Gewährleistung des Fremdkatheterismus sollte zuvor geprüft werden. Die Injektion erfolgt transurethral-endoskopisch in Allgemeinanästhesie, kann bei manchen Patienten auch in Lokalanästhesie erfolgen. Die Wirkung hält im Mittel 6 bis 9 Monate an. Derzeit liegt nur eine Zulassung zum Einsatz von Botulinumtoxin bei Querschnittslähmung und Multipler Sklerose vor, die Anwendung erfolgt bei Parkinson-Patienten im off label use. Als nachteilig wird von manchen Patienten die Häufigkeit der erforderlichen Eingriffe insbesondere in Allgemeinanästhesie empfunden.

E.M.D.A (ELECTRO MOTIVE DRUG ADMINISTRATION)

Hierbei wird eine Kombination von Medikamenten über einen besonderen Katheter in die Harnblase eingebracht und durch Gleichstrom die Struktur der Medikamente derart verändert, daß diese in ionisiertem Zustand nicht nur in die Harnblasenschleimhaut, sondern auch in die Harnblasen-Muskulatur gelangen. So kann zum Beispiel auch Oxybutinin mit dieser Methode eingesetzt werden. Das Verfahren dauert jeweils ca. 30 Minuten und wird an drei aufeinander folgenden Terminen in der Regel stationär durchgeführt. Der Effekt kann mehrere Monate anhalten und eine zusätzliche Medikamenteneinnahme überflüssig machen. Das Verfahren ist nicht ohne Risiken und ist nicht für alle Patienten geeignet.

INTERMITTIERENDER FREMD- ODER SELBSTKATHETERISMUS

Hierdurch können mittel- und langfristig rezidivierende Harnwegsinfekte und morphologische Schäden der Harnblase vermieden werden. Bei



Abb. 5. Normales Miktionszysturethrogramm: keine Druckbelastungszeichen (Divertikel, Trabekulierung), regelrechte Öffnung der Harnblase bei der Miktionsversuch, keine Obstruktion im Bereich der Urethra

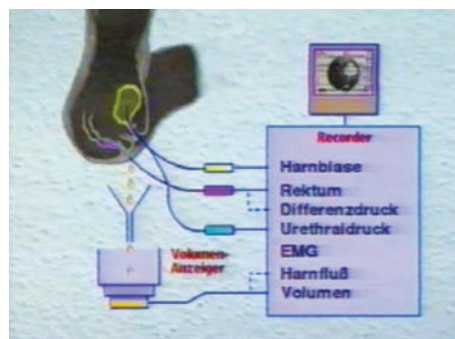


Abb. 6. Schema einer urodynamischen Untersuchung: durch Messung des intravesikalen und abdominellen Druckes und eines Beckenboden-EMG wird der Detrusordruck errechnet und der Verlauf der Harnblasenfüllung und –entleerung graphisch dargestellt.

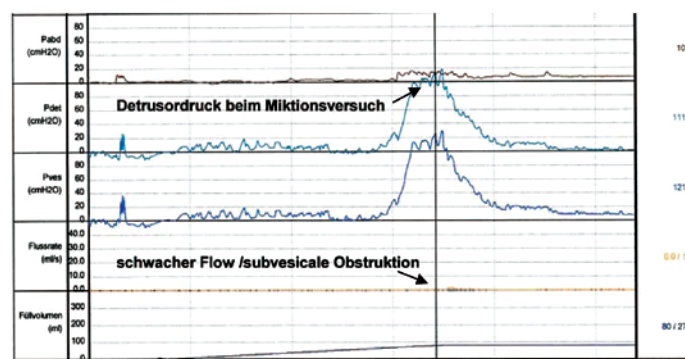


Abb. 7. Urodynamik-Kurve eines Patienten mit den Symptomen einer überaktiven Harnblase, Pollakisurie und Nykturie. Ergebnis der weiterführenden Diagnostik: subvesikale Obstruktion durch eine Prostatavergrößerung mit Restharnbildung. OP-Indikation zur Prostatektomie.

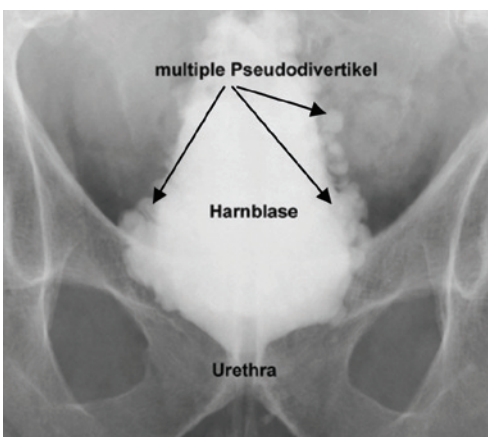


Abb. 9. Miktionszysturethrogramm mit massiver Pseudodivertikelbildung bei zerebral enthemmter Harnblase, ohne nachweisbare Prostatahyperplasie und ohne Restharnbildung.

erhaltener, aber relativ ineffektiver Harnblasenentleerung (hoher Restharn) kann der Einmalkatheterismus zur Restharnentfernung nach vorheriger Spontanmiktion (ohne Bauchpresse) und somit zur Reduktion der Pollakisurie und Nykturie eingesetzt werden. Bei Unfähigkeit zur Spontanmiktion und eingeschränktem Blasenfüllungsgefühl (z. B. bei MSA) erfolgt der Einmalkatheterismus ohne vorherige Blasenentleerung in regelmäßigen

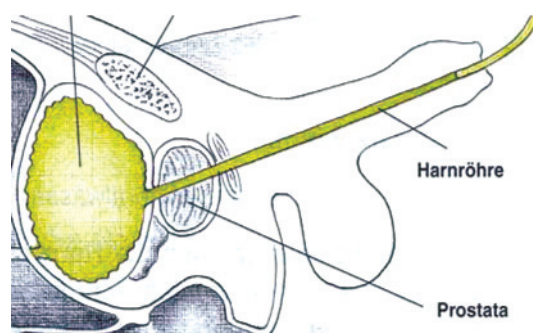


Abb. 8. Zystogramm /Miktionszysturethrogramm: die Harnblase wird retrograd mittels Kontrastmittel gefüllt. Anatomische und funktionelle Störungen der Harnblase und der Urethra können während der sich anschließenden Miktion radiologisch dargestellt und dokumentiert werden. Bei der Videourodynamik wird die radiologische und urodynamische Untersuchung simultan durchgeführt.

zeitlichen Abständen (ca. alle 4 Stunden) insgesamt vier bis fünf mal pro Tag. Bei erhaltenem Blasenfüllungsgefühl erfolgt der Katheterismus bei Auftreten von Harndrang.

MIKTIONS- UND HARNBLASENTRAINING

Als Miktionstraining wird die Anpassung des Lebensrhythmus an den Blasenrhythmus auf der Grundlage eines

Miktionsprotokolls („Blasenentleerung nach der Uhr“) bezeichnet. Aufgrund des Wissens um die eigene Blasenkapazität (z. B. 200 ml) versucht der Betroffene unweigerlich auftretenden Inkontinenz- und Drangepisoden zu entgehen, in dem er vorzeitig, noch vor Auftreten von Harndrang die Harnblase entleert. Unter einem Harnblasentraining versteht man die stufenweise Vermeidung von Miktions-, bzw. die verzögerte Durchführung einer Blasenentleerung. Bei kurzen Miktionsintervallen wird der Patient angeleitet den ersten Harndrang zu unterdrücken.

VERÄNDERUNG DES TRINKVERHALTENS

Wurde mittels Miktionsprotokoll eine deutliche Einschränkung der funktionellen Harnblasenkapazität nachgewiesen (z. B. 150 bis 200 ml), so führt die Anordnung zu hohen Trinkmengen (z. B. 3 Liter/die) zu einer verstärkten Pollakisurie mit bis zu zwanzig Miktionspro Tag. Andererseits reagieren manche Patienten mit einer erheblichen, bewußten Einschränkung ihrer Trinkmenge mit weniger als 1 Liter/ Tag um eine Pollakisurie oder Inkontinenzepisoden zu vermeiden.

Es empfiehlt sich die Vorgabe einer Trinkmenge von 1,5 bis 2,0 Litern pro Tag. Nur in Einzelfällen sollten höhere Trinkmengen bei Vorliegen einer Pollakisurie empfohlen werden. Um eine übermäßige Nykturie zu vermeiden kann die abendliche Trinkmenge reduziert werden.

DOUBLE VOIDING BEI HOHEM RESTHARN

Es handelt sich um ein Verhaltenstraining für Patienten mit Blasenentleerungsstörungen zur Restharnreduktion ohne den Einsatz von Medikamenten. Hierbei entleeren die Patienten ca. 15 bis 30 Minuten nach der letzten Miktionserneut (ohne vorliegenden Harndrang) die Harnblase.

BECKENBODENTRAINING

Die Durchführung und Anlernung von individuell zu gestaltendem Beckenbodentraining zur Muskelkräftigung oder Muskelentspannung nach vorheriger, professioneller Beckenboden-evaluation unterstützt in Kombination mit anderen Therapiemaßnahmen die Möglichkeiten der Betroffenen zur Kontrolle der Blasenentleerung und zur Reduktion von Harninkontinenz.

TRANSCUTANE ELEKTROSTIMULATION DER HARNBLASE (NICHT-INVASIVE NEUROMODULATION)

Die transkutane, intermittierende Elektrostimulation wird zur Behandlung von Harndrang-, Harnbelas-

tungs- und Stuhlinkontinenz eingesetzt. Unter Berücksichtigung möglicher Kontra-indikationen ist die täglich (20 Minuten), von manchen Patienten auch selbstständig und zu Hause durchführbare Therapie frei von Nebenwirkungen. In Einzelfällen kann sie zur Reduktion oder zum Verzicht von Medikamenten eingesetzt werden.

WEITERE UND OPERATIVE THERAPIEN

Bei therapieresistenter Nykturie oder nächtlicher Polyurie (Nachweis: Miktionsprotokoll) kann der Einsatz von Desmopressin (z. B. Nasenspray) indiziert sein. Hierdurch wird die nächtliche Urinproduktion reduziert. Die Anwendung bedarf engmaschiger ärztlicher Kontrollen des Elektrolythaushaltes und dem strikten Ausschluß von Kontraindikationen.

Als invasive, neuromodulatorisch wirksame OP-Methode kann die chronische Stimulation der Sakralwurzel S2/S3 genannt werden. Durch einen gering invasiven vorherigen, peripheren Nervenevaluations-Test (PNE-Test) kann die Effektivität der Methode überprüft werden. Andere operative Maßnahmen werden selten eingesetzt, die Indikationsstellung und Durchführung sollte in neuro-urologisch versierten Zentren erfolgen.

FAZIT FÜR DIE PRAXIS

Die neuro-urologische Diagnostik von urologischen Beschwerden von Parkinson-Patienten erfordert aufgrund der komplexen Ursachen eine entsprechende instrumentelle Ausstattung und eine gewisse Erfahrung in der Behandlung, insbesondere wenn sich die Indikation für einen operativen Eingriff ergibt. Neurologische Kliniken und Praxen sollten die Zusammenarbeit mit entsprechenden neuro-urologischen Zentren und Praxen suchen, da ca. jeder dritte Parkinson-Erkrankte unter urologischen Beschwerden, z.T. mit erheblichem Leidensdruck leidet. Soll nicht nur die Motorik, sondern die Lebensqualität und die soziale Teilhabe verbessert werden und Risiken, wie zum Beispiel die nächtliche Sturzgefahr durch eine erhöhte Nykturie, reduziert werden, so ergibt sich die Erfordernis einer engen Zusammenarbeit zwischen Neurologie und Urologie, bzw. Neuro-Urologie.

ENDOSCOPIC CORRECTION OF THE MOUTH OF THE URETER WHEN VESICOURETERAL-REFLUX IN CHILDREN

A.A. Zhidovinov, P.E. Permjakov,
A.V. Pirogov

*Astrakhan State Academy of Medicine,
Astrakhan, Russia*



*Alexei A. Zhidovinov, Professor,
Head of the Department of
Pediatric Surgery*



*Pavel E. Permyakov, PhD
(Medicine), Department of
Pediatric Surgery*



*Alexandr V. Pirogov, Surgeon,
Department of Pediatric
Surgery*

ABSTRACT — Changes that occur in the renal parenchyma on the background of vesicoureteral reflux (VUR), occupies one of the first places among the various forms of pathology of the urinary tract in children, leading to the obstructive uropathy. To reduce the risk of reflux nephropathy may need to start surgical treatment of VUR in the early stages. At present methods of endoscopic correction of the mouth of the ureter in VUR are a priority at the expense of minimizing trauma, reduction of terms of deposits in hospital and decrease the number of complications.

KEYWORDS — children, vesicoureteral reflux, endoscopic correction of the mouth of the ureter, Vantris

Vesicoureteral reflux in children is one of the topical problems of pediatric urology. Detectability him, efficiency, conservative effective and operative treatment still remain an important task for pediatricians, nephrology, urology, pediatric surgeons. VUR is one of the most frequent forms of disorders of urodynamics and causes of chronic pyelonephritis in children. To date the wrong interpretation of these diagnostic or treatment led to late surgical intervention (1).

VUR is one of the most severe diseases of the urinary system. VUR very often progresses latent, which can cause arose breath of pyelonephritis, resistant to antibiotic therapy and often receiving chronic. However, the VUR may have a latent period without clinical and laboratory signs of urinary tract infection. In its initial stage of development of reflux-nephropathy in VUR has the character of clinical picture, appear-

ing only symptoms of urinary tract infection. Early detection of changes in the renal parenchyma may define further tactics of treatment of patients with this disease and prevent further development of secondary wrinkling kidneys.

Children with this pathological condition after liquidation reflux by surgical correction, i.e. after elimination of pathological effect on the kidney parenchyma, in the next 6–8 months notice significant improvement of its functions (2, 3). Selection of optimal method of treatment of VUR in children acquires a special urgency due to the high prevalence of this disease, rapid progression of complications leading to severe and irreversible morphofunctional changes of the upper urinary tract.

Remain disputable questions of a choice of methods of treatment of VUR in children depending on the degree of functional disorders in combination with other pathological processes.

OBJECTIVE

Optimization of surgical treatment of VUR in children with the use of endoscopic correction methods.

METHODS

the Main indications for carrying out endoscopic correction in VUR can be considered primary VUR 3–5 degrees, flowing with impaired kidney function, the presence of reflux-nephropathy, acute RAS disorders of urodynamics with exacerbations of

secondary pyelonephritis in history. Also indications for endoscopic intervention is VUR 1–2 degrees in the absence of effects from the conservative therapy for 1 year with occasional outbreaks of secondary chronic pyelonephritis. To reduce the efficacy of endoscopic correction pour ureters may complete a doubling of the upper urinary tract, as well as the recurrence of the VUR after re the mouth of the ureter. Methods of endoscopic correction have different technical features, so the results vary considerably. Efficiency of different methods, according to various authors, is common from 30% to 90%.

Currently, the most popular and proven methods are STING, HIT, characterized by the insertion of the needle relative to the mouth of the urine-source. In our clinic is successfully used the method STING (Suburethral transurethral injection). For endoscopic correction of the mouth of the ureter at the VUR used cystourethroscopy company Storz barrel No. of 9,5–10 ch. Now the surgeons used a huge range of products for the correction of reflux. Himself drugs must meet the following requirements: to be biologically compatible with tissues of the organism and not to migrate to succeeding in other tissues or organs, and to be safe. Used implants are divided into two groups — unstable (absorbable) and stable (non-absorbable). As implant we use the hydrogel synthetic origin, Vantris. Once introduced 0,2–0,3 ml of the preparation to closing the mouth of the ureter and create a bolus (Fig. 1, 2).

RESULTS

In the surgical Department of the Regional child's clinical hospital of Astrakhan for the period from 2010 to 2013 was on treatment 72 children with VUR 2–5 degrees, of which the boys were 30, girls — 42 patients. Age received surgical treatment of children ranged from 1 to 17 years old. The distribution of VUR by degrees was as follows: grade 2 — 20 (28%) children, grade 3–4 — 40 (55%) children, 5 degree — 12 (17%) patients. In 25 patients VUR was bilateral, 47 — sided. The duration of the observation of the children ranged from 6 months to 1 year. Control urological examination in these terms include obligatory holding of ultrasound with Doppler and miccion cystography. Analysis of the results of endoscopic correction of the VUR showed that 68 (95,7%) cases with a positive result endoscopic correction — reflux was not determined (Fig. 3, 4), in 2 (2,8%) cases decreased reflux to 1–2 degree, that was regarded as an improvement. A relapse was detected in 1 observation (1,4%), which required repeated endoscopic manipulation. Complications are not registered. Exacerbations secondary chronic pyelonephritis not been identified. Assessment of renal hemodynamics with the definition of the

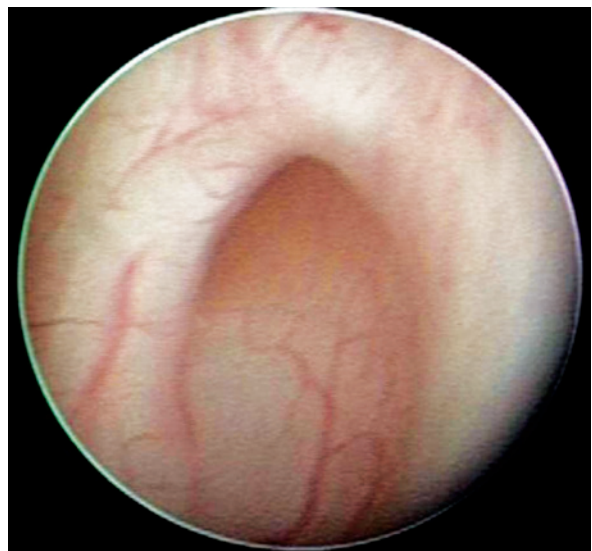


Fig. 1. The mouth of the ureter prior to the introduction of the gel VANTRIS



Fig. 2. The mouth of the ureter after the introduction of the gel VANTRIS

industry of water indexes pulsational (Pi) and resistance (Ri) showed numbers not exceeding the norm: Pi $1,11 \pm 0,26$, Ri $0,68 \pm 0,13$. Depletion of intrarenal vascular figure as one of the signs of the secondary wrinkling of the renal parenchyma was not observed.

CONCLUSIONS

Thus, the good results of endoscopic correction of the mouth of the ureter at the VUR in children can be obtained in case of strict observance of technology of procedure of this method STING. The efficacy of



Fig. 3. Miction cistogramma patient m., 2 years 11 months. Is an active 2-way VUR III-V



Fig. 4. Miction cistogramma the same patient after 6 months after surgery. VUR is not defined

endoscopic correction depends on the degree of reflux and primary treatment. The application of endoscopic correction methods allows to achieve a positive result of treatment of VUR in 95,7% of the cases, that allows to consider them to be the method of choice for carrying primary surgical treatment of this pathology.

REFERENCES

- COOPER, C.S. Diagnosis and treatment of vesicoureteral reflux in children / Nat.Rev.Urol. – 2009. – Vol.6 – P.481–489.
- HODSON, E.M., WHEELER, D.M., SMITH, GH Interventions for primary vesicoureteric reflux/Cochrane Database of Systematic Reviews 2007, issue 3. Art.No. CD0001532.doi/14651858.pub.3.
- LAKGREN, G. Endoscopic treatment of vesicoureteral reflux: Current status / Indian.J.Urol. – 2009. – Vol. 25. – P.34–39.

The article is devoted to endoscopic correction of the mouth of the ureter when vesicoureteral-reflux in children. At present methods of endoscopic correction of the mouth of the ureter in VUR are a priority at the expense of minimizing trauma, reduction of terms of deposits in hospital and decrease the number of complications. The research was conducted in a *careful* and *objective* way and can be recommended for publishing in the medical Journal *Archiv Euromedica*.

PROF. VADIM GELDT

*Moscow Scientific Research Institute
of Pediatrics and Pediatric Surgery,
Moscow, Russia*



Moderne Krebsbehandlung

Schlüsselloch-chirurgie

Bei der Schlüssellochchirurgie, auch „minimal invasive Chirurgie“ genannt, wird mit sehr kleinen Schnitten schonend im Bauchraum operiert. Die minimal invasive Chirurgie stellt einen besonderen Schwerpunkt unserer Klinik dar. Die Vorteile dieser Technik sind vielfältig. Patienten brauchen deutlich weniger Schmerzmittel und erholen sich schneller.

Bei folgenden Erkrankungen wird diese Technik angewendet:

- Leisten- und Narbenbrüche
- Gallensteine
- Blinddarmentzündung
- Divertikelerkrankung des Dickdarms
- Bösartige Erkrankungen des Darms
- Chronisch entzündliche Darmerkrankungen
- Refluxerkrankung
- Kleine Magentumoren
- Speiseröhrenkrebs
- Leberkrebs

Unser Team

Durch die intensive Zusammenarbeit mit angrenzenden Fachgebieten und durch die große Erfahrung unserer Operateure besitzt unsere Abteilung eine besonders hohe Kompetenz im Bereich komplizierter und schwerer Operationen (Speiseröhre, Magen, Leber, Bauchspeicheldrüse, Enddarm) auf.



Prof. Dr. Guido
Schumacher,
Chefarzt

Städtisches Klinikum Braunschweig gGmbH
Klinik für Allgemein- und Viszeralchirurgie
(Bauchchirurgie)
Freisestr. 9/10 38118 Braunschweig

Tel.: 0531/595-0
Fax: 0531/595-1322

info@klinikum-braunschweig.de
www.klinikum-braunschweig.de

DEVIATIONS OF THE SEASONAL PREVALENCE OF BIRTHS IN THE GENERAL POPULATION AND AT CHILDREN WITH AUTISM

**A.P. Chuprikov, A.M. Vayserman, L.V. Mekhova,
E.S. Galchin**

*Shupyk National medical academy of postgraduate education,
Institute of gerontology of National academy of medical sciences
of Ukraine*

Negative dynamics of births of Ukrainians is well-known in the last decades. In comparison with the 60th the quantity of births in 2000s decreased more than by 3 times. In the scientific and popular press there are statements of experts specifying the population, namely about the tendency to the *extinction* of Ukrainians, impossibility of the return to 52 million population which the country had on the independence threshold. The factors, capable to brake the birth rate, first of all are social and psychological instability in the country, the population impoverishment with a significant amount of the educated people understandably seeking to limit themselves to the birth of 1 or 2 children. And the last thing is not enough for the simple reproduction of the population.

The seasonal prevalence of births in 60–70s the Soviet Union as a whole and in Ukraine was rather monotonous: a sharp increase in January and a gradual essential decrease till December were noted. Always it was explained by spring shifts of the hormonal background of the population and the related success of conceptions in April and the next months i.e. these

phenomena relating to one of the signs of the natural selection are possible to refer to a certain confidence to the indicators of the population biological stability.

In this work the mathematical approaches were used in the laboratory of epigenetics (under the direction of A. M. Vayserman) of Institute of gerontology (Kiev). The distribution on the months of births of 32027318 people who were born in Ukraine for 1960–2009 was studied. The birth rate frequencies in each of ten-year cohorts were counted by means of a standard method of pseudo-cohorts designing. For every month of the birth the ratio of the observed frequencies of the birth rate to the expected ones was calculated. In the last two decades some shift was found in the optimum of births (according to the optimum of conceptions) for 6 months. In particular, the birth rate increase was displaced towards the summer-autumnal months i.e. one more sign of a dangerous tendency in the development of this population was found.

The obtained data were used when studying the birth rate of 658 mentally ill children. In particular, within a year the monthly analysis of the birth rate of children with the deviations in the mentality development (children's autism) also showed an existence of the *optimum* and *passimum* (the lowest level) of the births which are authentically different on the terms of manifestations from the seasonal fluctuations in the general population. However, it was not confirmed in relation to the children with the organic affection of the brain and cognitive disorders.

LABORATORY ESSENCE OF ADAPTIVE CHANGES ERYSIPelas ON THE FACE



E.G. Fokina

*Central Scientific Research Institute of Epidemiology,
Moscow, Russia*

KEYWORDS — biochemical passport, erysipelas, total protein, albumin, urea, creatinine, glucose, cholesterol, β -hemolytic streptococcus, thermogenesis, gluconeogenesis, dynamic enzymes performance, erythrocyte aggregation, protamine sulfate, lanthanum chloride, ADP, Willebrand factor, biochemical point of recovery, laboratory paradox erysipelas.

OBJECTIVE

Establish the nature of the metabolic (biochemical and hemocoagulation) changes in primary ery-

sipelas on the face from the standpoint of adaptation mechanisms.

METHODS

The study included 23 patients (15 women and 8 men) aged 31 to 78 years with a diagnosis of "erysipelas, with localization on the face, 2 severity. In 91% of cases of new-onset erysipelas. Patients were treated at the Infectious Diseases Hospital № 2 in Moscow. Average hospital stay was 4 ± 1.6 days. The study of biochemical substrates and enzymes in the blood, electrophoresis of serum proteins, the study of aggregation activity of erythrocytes and platelets, the study state plasma hemostasis (coagulation, fibrinogen level, antithrombin III, D-dimer) and von Willebrand factor were performed on admission at the beginning of the disease (1–3), the dynamics (4–6, 7–9) and in the recovery period (10–12) days of illness.

CONCLUSION

Hemorrhagic disorders in erysipelas faces correspond to the vasculitis-purple type of bleeding with laboratory evidence of DIC: disorders in erythrocyte link of hemostasis and damaging of the endothelium of blood vessels.

Pathogenicity factors β -hemolytic streptococcus group A (neuraminidase) can destroy the red blood cell membrane and start the process of disseminated intravascular coagulation (DIC). Laboratory paradox erysipelas — the discrepancy between high infectious fever and weak thermogenesis. Inhibition of mechanisms of thermogenesis (low AST in early disease) — a phenomenon erysipelas. Special factor of pathogenicity β -hemolytic streptococcus — the enzyme NAD-aza — causes total inhibition of bioenergy processes. On the background of high temperature is observed the low activity transaminases (AST, ALT) and enzymes of the cell membrane (alkaline phosphatase, CPK). Biochemical blood detoxicating barrier depressed. This is offset by increasing the load on the other detoxication mechanisms — red blood cells and albumin. We studied more than 50 different indicators of erysipelas. The simplest and most sensitive indicator of inflammation control was and remains the C-reactive protein.

When compared erysipelas on the face and the legs, we made sure that changes in the hemostasis system and in the biochemical indices in erysipelas on the face expressed less than on the legs. Laboratory starting point of the recovery (growth of ALT 3 times, growth of the transferrin 5 times) is the seventh day of illness.

EXTRAKTIONSUNTERSUCHUNG VON EINIGEN ANTISSYCHOTISCHEN ARZNAISTOFFEN UND SCHLAFMITTELN

**V.A. Kartashov, L.G. Sidelnikova, G.P. Chepurnaya,
L.V. Chernova**

Staatliche Technologische Universität Maikop, Medizinische Hochschule, Abteilung für Pharmazie, Maikop, Russland

Atypische Neuroleptika (Risperidon, Ziprasidon) werden häufig für die Behandlung von psychischen Erkrankungen verwendet, und sie sind die modernen Schlafmittel von dritten Generation (Zolpidem, Zaleplon), die für Schlaftlosigkeit verwendet werden aber haben Toxizität. Es gibt schon geschriebene Fälle einschließlich Todesfälle von Vergiftung durch die genannten Arzneimittel. Die Ergebnisse der chemisch-toxikologischen Analysen sind von großer Bedeutung für den Nachweis einer Vergiftung. Aber die Verfahren zur Bestimmung dieser toxischen Substanzen in biologischen Medien sind nicht ganz genügend untersucht.

Wir haben Versuche zur Extraktion von Risperidon, Ziprasidon, Zolpidem und Zaleplon aus wässrigen

Lösungen durchgeführt. Diese Ergebnisse sind für die Extraktion und Reinigung dieser Substanzen bei der Untersuchung von biologischen Objekten genutzt werden.

Unter den organischen Lösungsmitteln, die üblicherweise in chemisch-toxikologischen Praxis verwendet werden, um toxische Hauptsubstanzen zu extrahieren, untersuchen wir Chloroform, Diethylether und n-Hexan. Um den pH-Wert der Lösung auszuwählen, in der Testsubstanzen in den maximalen und minimalen Mengen extrahiert sind, berechneten wir den Anteil von ionisierten (molekularen) und ionisierter (protonierter) Form der Substanzen bei verschiedenen pH-Werten unter Verwendung der Formel:

$$\alpha = 1 / 10^{pK_a - pH} + 1,$$

wobei α — der Anteil der nicht-ionisierten Form von Stoffen ist, pK_a — Ionisationskonstanten von Risperidon, Ziprasidon, Zolpidem und Zaleplon sind.

Die obengenannten Berechnungen zeigen, daß die Substanzen bei pH 9,0–10,0 hauptsächlich in

molekularer Form durchgeführt sind und sie können auf die maximale Menge extrahiert werden. Als Ergebnis der Berechnung der ionisierten Form ($1 - \alpha$) wird festgestellt, dass bei pH 2,0 Testsubstanzen fast vollständig ionisiert sind, und der Grad der Extraktion muss minimal sein. Deshalb für unsere Experimente wählten wir den pH-Wert von 2,0 und 9,0.

Extraktionsuntersuchungen von Risperidon, Ziprasidon, Zolpidem und Zaleplon aus wässrigen Lösungen bei diesen pH-Werten werden unter Verwendung von Chloroform, Diethylether und n-Hexan durchgeführt. Isolierten Substanzen nach der Entfernung von Extraktionslösungen werden in Ethanol gelöst und die resultierenden Lösungen werden im Bereich von 200–400 nm spektrophotometriert. Es wurden die optische Dichte bei dem Absorptionsmaximum bei Lichtwellenlängen von 272, 315, 243 und 231 nm bei der Untersuchung von Risperidon, Ziprasidon, Zolpidem und Zaleplon entsprechend vermessen. Die Standarten der Testverbindungen

wurden für die Berechnung des Gewichtsanteils der extrahierten Substanzen verwendet. Als ein Ergebnis von Experimenten wurde bestätigt, dass aus den sauren Lösungen (pH 2,0) der Stoff nicht unter Verwendung Diethylether und n-Hexan extrahiert wird. Wobei die neutralen und sauren Verunreinigungen könnten unter Verwendung erwähnten Lösungsmittel extrahiert und entfernt werden. Diese Chloroform-Extraktion aus dem alkalischen Medium (pH 9,0) wurde die höchste Ausbeute der Substanzen beobachtet und die Daten für Risperidon, Ziprasidon, Zolpidem und Zaleplon wurden $85,0 \pm 2,46\%$, $97,45 \pm 2,33\%$, $73,60 \pm 1,45\%$ und $95,93 \pm 0,28\%$ entsprechend festgestellt.

Wir können somit behaupten, dass die erhaltenen Angaben können in der chemisch-toxikologischen Analyse zur Reinigungsextraktion von biologischen und anderen Flüssigkeiten durch Diethylether oder n-Hexan bei pH 2,0 und Gewinnung von Risperidon, Ziprasidon, Zopiclon und Zolpidem durch Chloroform bei pH 9,0 verwendet werden.

BEWEGUNGSREGULATION BEI GESUNDEN UND IHRE STÖRUNGEN BEIM PARKINSON

Priv. Doz. Dr. med. Alexei Korchounov

OA Neurologische Klinik Kevelaer Ltd, Kevelaer

Drei Teile des Gehirns sind für die Entstehung einer Bewegung wichtig.

Eine willkürliche Bewegung ist immer zielgerichtet. Das Erreichen eines Ziels ist immer die Motivation zu einer Bewegung. Die Motivation entsteht in der vorderen Großhirnrinde. Die Motivation bedeutet die Identifikation des Ziels und Planung der notwendigen Bewegungen um das Ziel zu erreichen. Z.B. hier steht ein Glas mit Wasser. Ich habe Durst und möchte etwas trinken. Die vordere Großhirnrinde identifiziert den Glas Wasser als ein Objekt mit welchem ich mein Durst stillen kann und entwickelt dann ein Plan wie ich nach dem Glas greife.

Der zweite Teil ist das Striatum oder Hirnbasiskern. Hirnbasiskern besteht aus Gruppen von Nervenzellen. In den einzelnen Zellengruppen sind einzelne Bewegungen des menschlichen Körpers genetisch abgespeichert: In einer Zellengruppe die Handbewegungen, in der anderen Zellengruppe die Kaubewegungen, in der dritten Zellengruppe die Beinbewegungen und

so weiter. Wenn eine Zellengruppe aktiviert wird, entsendet sie ein Befehl zu den zuständigen Muskeln und die Muskeln führen dann eine entsprechende Bewegung aus: eine Handbewegung, Kaubewegung oder Beinbewegung. Somit ist die Aufgabe des Hirnbasiskerns, die Bewegungen abzuspeichern und bei Aktivierung der Bewegungsbefehl an den Muskel weiterzuleiten.

Der dritte Teil verbindet die vordere Hirnrinde mit dem Hirnbasiskern. Dieser Teil heißt die Schwarze Substanz. Die Schwarze Substanz steuert den Hirnbasiskern für die optimale Ausführung der Bewegung. Diese Steuerung erfolgt mit einem Botenstoff Namens Dopamin. Das Dopamin wird von der Schwarzen Substanz freigesetzt und erreicht die Hirnbasiskerne, wo er steuern soll. Das Dopamin hat zwei Spielarten für die Steuerung der Hirnbasiskerne. Der Spielart der Steuerung ist davon abhängig, wie viel Dopamin von der Schwarzen Substanz freigesetzt wird: viel (mikromolare Menge) oder wenig (nanomolare Menge). Die erste Spielart ist die Steuerung mit wenig Dopamin. Diese Art der Steuerung erfolgt in Ruhe, also dann, wenn kein Bewegungsbefehl existiert. Wenn die Schwarze Substanz nur wenig Dopamin freisetzt, setzt es sich an den Andockstellen Namens D1 ab.

Die Interaktion mit der Andockstellen D1 führt zur Senkung des Muskeltonus – also zur Entspannung der Muskulatur. Der niedrige Tonus hat zwei wichtigen Funktionen: er spart Energie und bereitet den Muskel für das Erreichen einer optimalen Kontraktion.

Die zweite Spielart ist die Steuerung mit viel Dopamin. Die Steuerung mit viel Dopamin erfolgt dann wenn aus der vorderen Hirnrinde ein Bewegungsbefehl kommt. Dabei wird aus der Schwarzen Substanz viel Dopamin freigesetzt. Wenn Dopamin in großen Mengen freigesetzt wird, setzt es sich an den Andockstellen Namens D2 ab. Durch die Interaktion mit den Andockstellen D2 werden die Hirnbasiskerne angeregt. Sie leiten den Bewegungsbefehl an die entsprechenden Muskeln weiter. Die Muskeln spannen an und führen die gewünschte Bewegung aus.

So funktioniert die normale Bewegung. Das Parkinson-Syndrom ist eine Bewegungsstörung. Wie verändert sich dieses Schema beim Parkinson-Syndrom? Beim Parkinson-Syndrom stirbt die Schwarze Substanz langsam ab. Folgend steht weniger Dopamin zur Verfügung. Wenn in Ruhe wenig Dopamin zur Verfügung steht, dann kann der Muskeltonus nicht effektiv gesenkt werden. Es kommt zu Muskelverspannung. Darüber klagen die Parkinson Patienten auch häufig. Medizinisch heißt diese Muskelverspannung „Rigor“.

Eine Folge der Muskelverspannung ist das Zittern. Jeder kann das bei sich prüfen: die Muskeln lange anspannen und merken, dass die Muskeln irgendwann zu zittern beginnen. Wenn ein gesunder Mensch sich dann entspannt, hört das Zittern sofort auf. Ein Parkinson Patient kann seine Muskeln aber nicht komplett entspannen, deswegen zittert er im-

mer weiter. Wie kommt es zum Zittern: Die Muskeln werden nicht nur aus dem Gehirn, sondern auch aus dem Rückenmark gesteuert. Bei einer langen Muskelspannung schaltet die Entspannung über den Rückenmark ein um die Überforderung des Muskels vorzubeugen. Dies bewirkt eine kurzfristige Entspannung des Muskels. Aber das Entspannungssignal aus dem Gehirn fehlt. Deswegen spannt sich der Muskel wieder an. Und so geht der Kreislauf wieder von vorne los. Die ständige Spannung und Entspannung sieht von außen wie das Zittern aus. Das Zittern nennt sich medizinisch „Tremor“. Das ist das zweite typische Zeichen des Parkinson-Syndroms.

Und was passiert, wenn bei einem Bewegungsbefehl auch weniger Dopamin zur Verfügung steht? Dann ist die Übertragung von der Schwarzen Substanz an die Hirnbasiskerne schwach. Entsprechend ist die Weiterleitung des Bewegungsbefehls an die Muskeln auch schwach. Die Muskeln spannen nur langsam an. Deswegen kommt zu einer verzögerten Freisetzung der Bewegungen. Daher kommen die typischen Erscheinungen des Parkinson Syndroms wie monotone, leise Sprache oder schlurfender Gang oder Schwierigkeit bei der Feinmotorik, z.B. beim Essen mit Messer und Gabel und Öffnen und Schließen der Knöpfe. Alle Anzeichen der verlangsamten Bewegungen werden „Bradykinese“ genannt. Das ist das dritte typische Symptom des Parkinson-Syndroms.

Wie wird das Parkinson Syndrom diagnostiziert?

1. Untersuchung
2. DAT-Scan. Dabei wird die verminderte Dopaminversorgung der Hirnbasiskerne festgestellt.
3. Medikamenten-Test

THE NANOSTRUCTURED MEDICINES IN THE FORM OF GEL AND CREAM INCLUDING THE PEROXIDASE OF THE BLACK RADISH

A.N. Serkova, N.V. Glazova

Saint-Petersburg State Chemical Pharmaceutical Academy,
St. Petersburg, Russia
Anastasia.Serkova@pharminnotech.com, nvglazova13@mail.ru

THE WORK PURPOSE – creation of ready forms (gel, cream) on the basis of the nanostructures including the purified concentrate of peroxidase, an antibiotic gentamycin and nanocarriers.

For carrying out experiments used peroxidase of the black radish, gentamycin, nanocarriers (cyclo-dextrins of production Xian Hong Chang Pharmaceuticals Co., Ltd., in particular β -cyclodextrins), excipients for creation of a ready form (sodium alginate, methylisothiasolinone, acrylates copolymer, olive oil).

In work applied a method of Lowry protein assay, a method of determination of enzyme activity of the peroxidase on pyrogallol, quantitative definition of gentamycin sulfate on a ninhydrin method, the gel

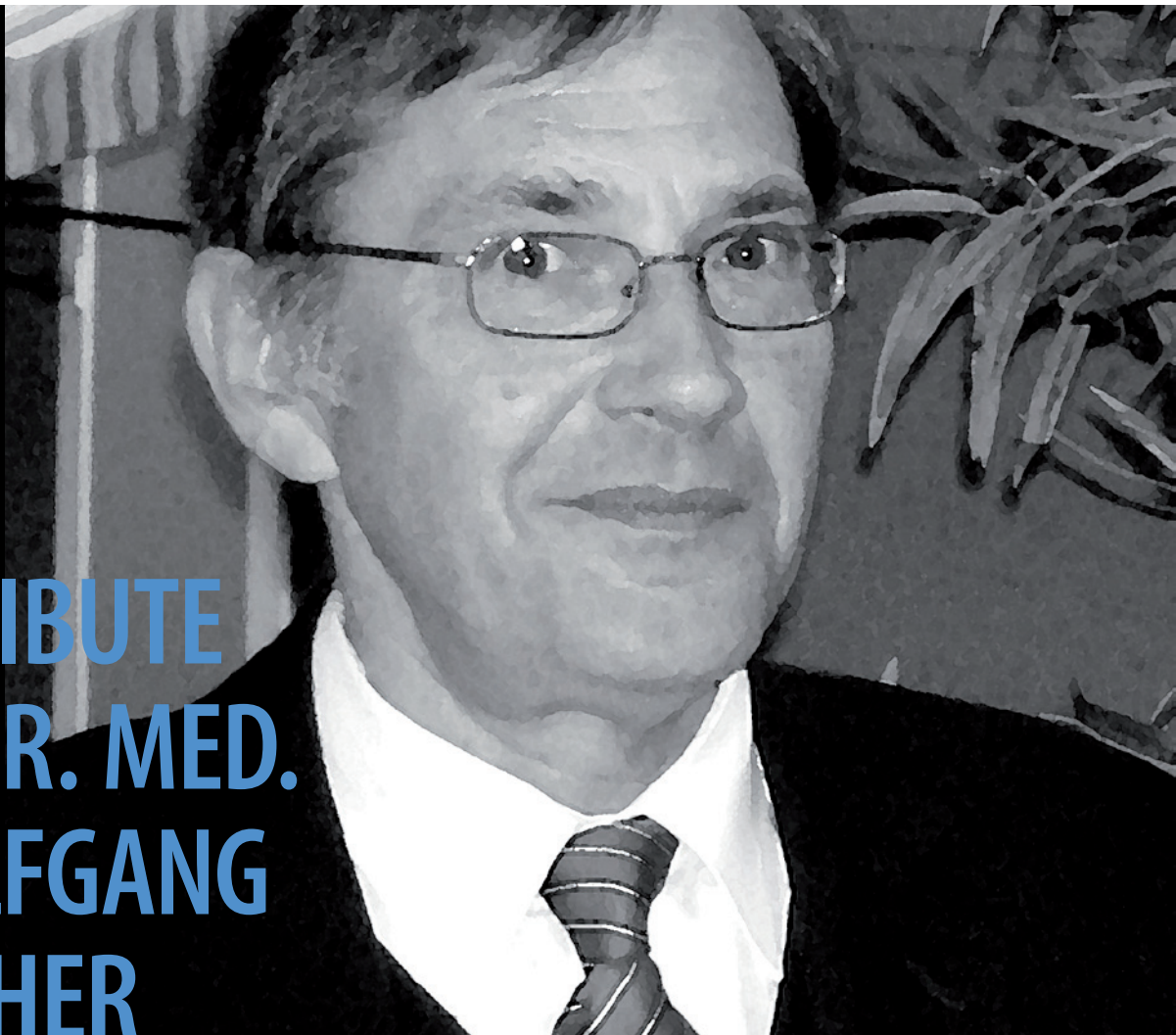
filtration chromatography analysis (used sephadex "Sigma" of the G-50-150 brand), a diffusion method in an agar for determination of antibacterial activity.

At creation of the nanostructured medicines it is necessary to consider influence of high-molecular and low-molecular components on activity of peroxidase. The optimum compositions of gel and cream including nanostructure (peroxidase, β -cyclodextrins and gentamycin) and excipients were developed. It is known that from stressful influences the vegetable organism is protected high-molecular (enzymes antioxidants, in particular peroxidase) and low-molecular antioxidants. Enzymes antioxidants eliminate active forms of oxygen in a cage: peroxidase catalyzes reaction of restoration of hydrogen peroxide to water, neutralizing this oxidizer. Gentamycin treats

aminoglycoside antibiotics of a broad spectrum of activity. In a complex with peroxidase gentamycin promotes increase in activity of enzyme and expansion of its range of action. The received gel and cream have antioxidant and antibacterial effect. Results of experiments on a comparative assessment of safety of activity of enzyme of peroxidase in solution and in the received samples of gel and cream showed that at introduction of nanostructure to composition of gel and cream during the term of supervision of peroxydase don't change the activity.

CONCLUSION: developed optimum compositions of the nanostructured medicines, received trial samples. Carrying out preclinical researches is planned. The received samples are advanced for creation of new ready dosage forms.

A TRIBUTE TO DR. MED. WOLFGANG FISCHER



It was with great sadness that we learned of the sudden death of Dr. Wolfgang Fischer in the last days of August 2014. Dr. Wolfgang Fischer was a well-known German neurologist and a friend and colleague who contributed a lot to development of our journal and the conference "Euromedica-Hannover".

Doctor Fischer worked as a Deputy Director and Chief of the Division at the neurological rehabilitation clinic Beelitz-Heilstätten, where he was highly appreciated for his professionalism and personality by patients and colleagues. Beside his work as neurologist, Dr. Fischer was actively involved in scientific and educational activities and was a prominent speaker at various medical conferences.

From 2010 he was a constant medical advisor and co-organizer of our medical conference "Euromedica - Hannover" where he conducted a state-of-art neurological section with participation of leading neurologists and other specialists.

Dr. Fischer was also the Vice-Director of the Editorial Board of the journal "Archiv Euromedica". Due to his efforts, a great number of outstanding medical researchers contributed their articles to our journal.

Wolfgang Fischer was a man who saved lives and health of the patients not only in Germany but also in other countries. He did his best helping patients to overcome their serious illnesses and their social problems as well.

Being an extraordinary doctor and personality Wolfgang Fischer managed not only to keep friends of his youth; all his life he was able to make new friends that loved and respected him. He was remarkable for his optimism, kindness and generosity. Until his last days, he was vividly interested in a wide range of topics and had lots of professional plans and ideas.

We are expressing our condolences to Dr. Fischer's wife, his large and wonderful family. He will be very much missed by all that used to know him as the doctor, scientist and friend.



Medizinisches Kompetenzzentrum in Neurologie und Rehabilitation



- Neurologische Rehabilitationsklinik
- Fachkrankenhaus für neurologische Frührehabilitation
- Neurologisches Fachkrankenhaus für Bewegungsstörungen/Parkinson

Leistungsangebote

- **Neurologische Frührehabilitation** (einschließlich beatmungspflichtiger Patienten)
Referenzklinik für Guillain-Barré-Syndrom-Patienten
- **Neurologische Spätrehabilitation** aller neurologischer Krankheitsbilder,
Anschlussheilbehandlung
- Spezialabteilungen:**
 - Brandenburgisches Zentrum für Querschnittgelähmte* (Rehabilitation einschließlich beatmungspflichtiger Patienten)
 - Epilepsie-Zentrum Berlin-Brandenburg*
 - Rehabilitation neuroimmunologischer Erkrankungen* in Kooperation mit der Charité - Universitätsmedizin Berlin, Campus Mitte
 - Schwerpunkt Dystonie und Spastik* im Funktionsbereich Neuroorthopädie mit individuellen spezifischen Therapieangeboten
- **Akutbehandlung von Patienten mit Parkinson-Erkrankungen und Bewegungsstörungen**

Indikationen

Zustand nach Schädel-Hirn-Trauma, Hirninfarkt oder intrakranieller Blutung, Operation von Hirntumor, Nervenverletzung, entzündliche Hirn- oder Rückenmarkerkrankung, Querschnittslähmung, Parkinson, Dystonie, hypoxische Hirnschädigung, chronisches Guillain-Barré-Syndrom/Polyneuritis/Polyneuropathie, Multiple Sklerose, Epilepsie, degenerative Hirn- und Rückenmarkerkrankung mit akuten Veränderungen



Therapieangebote

Physio-, Ergo-, Musik-, Sport-, Hippo-, Physikalische Therapie, Logopädie, Psychologie/Neuropsychologie, Redression, Snoezelen, Diätetik, Seelsorge, Bewegungsbad, Sozialdienst



Ambulanzen

Ermächtigungsambulanz für klinische Neurophysiologie, Institutsambulanz (Physikalische Therapie), Spezialsprechstunden Botulinumtoxin und Parkinson



Unterbringung

Die Kliniken befinden sich in modern rekonstruierten, historischen Gebäuden eines einzigartig architektonischen Ensembles von Gebäude- und Landschaftsarchitektur. Helle und freundliche, durchgehend barrierefreie Zimmer sowie ein aufmerksames, fachlich hochkompetentes Team von Ärzten, Pflegekräften, Therapeuten, Service- und Verwaltungsmitarbeitern sorgen für Ihren angenehmen Aufenthalt. Unser Personal spricht englisch und teilweise russisch; internationale Gäste sind also willkommen.



Lage

Beelitz-Heilstätten liegt in unmittelbarer Nähe zu Potsdam und im Nahverkehrsbereich Berlin. Mit stündlicher Zuganbindung ist das Stadtzentrum Berlins in 45 Minuten erreicht. Die Mittelmark mit Wald- und Seenreichtum hat einen hohen Erholungs- und Freizeitwert und zeichnet sich durch Ruhe und naturbelassene Landschaften aus. Eigener Regionalverkehrsbahnhof und eigene Ausfahrt an der BAB 9 direkt vor dem Berliner Ring sorgen für eine hervorragende Verkehrsbindung. Die internationalen Flughäfen Berlin-Tegel und Berlin-Schönefeld sind in kürzester Zeit erreichbar.



Kontakt

Kliniken Beelitz GmbH, Paracelsusring 6 a, 14547 Beelitz-Heilstätten
Telefon: (033204) 200, E-Mail: info@kliniken-beelitz.de, Internet: www.kliniken-beelitz.de



Noventalis
Institut für systemische
BioKorrektur

Die individuelle systemische BioKorrektur

Eine begleitende Behandlung des metabolischen Syndroms speziell des Diabetes mellitus Typ II durch moderate körperliche Belastung unter erhöhter Sauerstoffkonzentration in der Umgebungsluft.



Anwendungsgebiete der BioKorrektur sind

- Metabolisches Syndrom
 - Diabetes Typ II
 - Adipositas (besonders abdominelle Fettleibigkeit)
 - Fettstoffwechselstörung
 - Bluthochdruck

außerdem bei

- Tinnitus
- chronische Lungenkrankheiten
- chronische Herzkrankheiten
- Verschlechterung der Leistungsfähigkeiten
- Depression, Schlafstörungen



Fragen Sie uns! Besuchen Sie uns!

ICP HealthCare GmbH
Robert-Rössle-Strasse 10,
Haus D79
D-13125 Berlin

Ansprechpartner: Frau Sabine Buchwitz
Tel.: +49 (0)30-94893174
Fax.: +49(0)30-94893167
E-Mail: s.buchwitz@icp-healthcare.de



HEALTH CARE

Innovative Forschung aus Berlin-Buch

Die ICP HealthCare GmbH entwickelt Diätetische Lebensmittel der Serie

nanovit®
für besondere medizinische Zwecke.

Die besonderen medizinischen Zwecke bestehen in der adjuvanten Behandlung von:

- Metabolischem Syndrom, speziell Diabetes mellitus Typ II
 - Erhöhter Infektfälligkeit
 - Schuppenflechte und Neurodermitis
 - Vitalitätsverlust im Alter
- Alters-und krankheitsbedingter Muskelschwund



Pharmazentral-
nummer 10525844

Für die fünf links abgebildeten Produkte werden die erstaunlichen enzymartigen Eigenschaften des pulverisierten Naturstoffs Zeoaktiv genutzt.

Zeoaktiv kann:

- Krankheitserreger so zerlegen, dass sie vom Immunsystem des Körpers besser abgewehrt werden,
- den Stoffwechsel von Diabetikern entlasten, indem es Glukose in Fruktose umwandelt,
- freie Radikale entschärfen und Schadstoffe aus dem Körper ausleiten,
- und darüber hinaus noch einiges mehr.

Fragen Sie uns! Besuchen Sie uns!

ICP HealthCare GmbH
Robert-Rössle-Strasse 10,
Haus D79
D-13125 Berlin

Ansprechpartner: Frau Sabine Buchwitz
Tel.: +49 (0)30-94893174
Fax.: +49 (0)30-94893167
E-Mail: s.buchwitz@icp-healthcare.de



Medizinische Hochschule
Hannover



Fachklinik für Rehabilitation

Durch unsere Partnerschaft mit der Medizinischen Hochschule (MHH) können wir allen Patienten eine effiziente Behandlung auf höchsten Niveau in fast allen Fachgebieten anbieten. Wir überprüfen gemeinsam mit der MHH die Behandlungsmöglichkeiten und führen die notwendigen Voruntersuchungen durch. Zur Operationen werden die Patienten in der MHH stationär aufgenommen und sobald wie möglich wieder zurück in die Klinik Fallingbostel verlegt.

Die Klinik Fallingbostel ist ein Zentrum für spezialisierte Rehabilitation aller Herz- und Gefäßkrankheiten, der postoperativen Nachsorge mit Wundbehandlung und der Rehabilitation chronischer Krankheiten z.B. durch orthopädische oder neurologische Krankheiten.

Die Rehabilitationsbehandlung wird aus einem breiten, modernen Angebot von anerkannten Therapieverfahren individuell auf die Bedürfnisse und Fähigkeiten des einzelnen Patienten abgestimmt. Alle Patienten erhalten täglich 5-6 Behandlungen, jeweils 20-30 Minuten. Der Sonntag steht den Patienten zur freien Verfügung.

Die Patienten werden vom Flughafen oder vom Hauptbahnhof (Hannover, Hamburg oder Bremen) direkt abgeholt. Wir haben englisch und russisch sprechende Ärzte und Fachpersonal und bieten eine rund-um-die-Uhr Versorgung d.h. auch nachts und am Wochenende.

Unterbringung

In unserem barrierefreien Haus wohnen die Patienten in hellen und freundlich eingerichteten Zimmern. Es kann zwischen unterschiedlich großen Einzelzimmern bis zum 4-Raum-Appartement mit Balkon, Dusche, WC, Safe, Telefon, russisches Fernsehen und Internetanschluss gewählt werden.

Selbstverständlich können Angehörige und Betreuer den Patienten begleiten und auch auf Wunsch im Zimmer oder Appartement des Patienten wohnen oder ein extra Zimmer in der Nähe erhalten.

Unsere Klinik befindet sich am Rande der Kleinstadt Bad Fallingbostel in Norddeutschland (zwischen Hamburg, Hannover und Bremen) und liegt am Rande des Kurparks mit kurzen Wegen zum Ortszentrum. Der Ort ist sicher und ruhig und es gibt ausreichend Geschäfte für den täglichen Bedarf.

Weitere Informationen über uns und unsere Möglichkeiten können über unser Aufnahmebüro unter 05162/44-605 erfragt werden. Gerne schicken wir auch Informationsmaterial zu. Auch im Internet unter www.klinik-fallingbostel.de würden wir uns über einen Besuch freuen.



Fachklinik für Rehabilitation

- Kardiologie
- Angiologie
- Pneumologie
- Nephrologie
- Transplantations-Rehabilitation
- Internationale Rehabilitation

Kolkweg 1
D-29683 Bad Fallingbostel

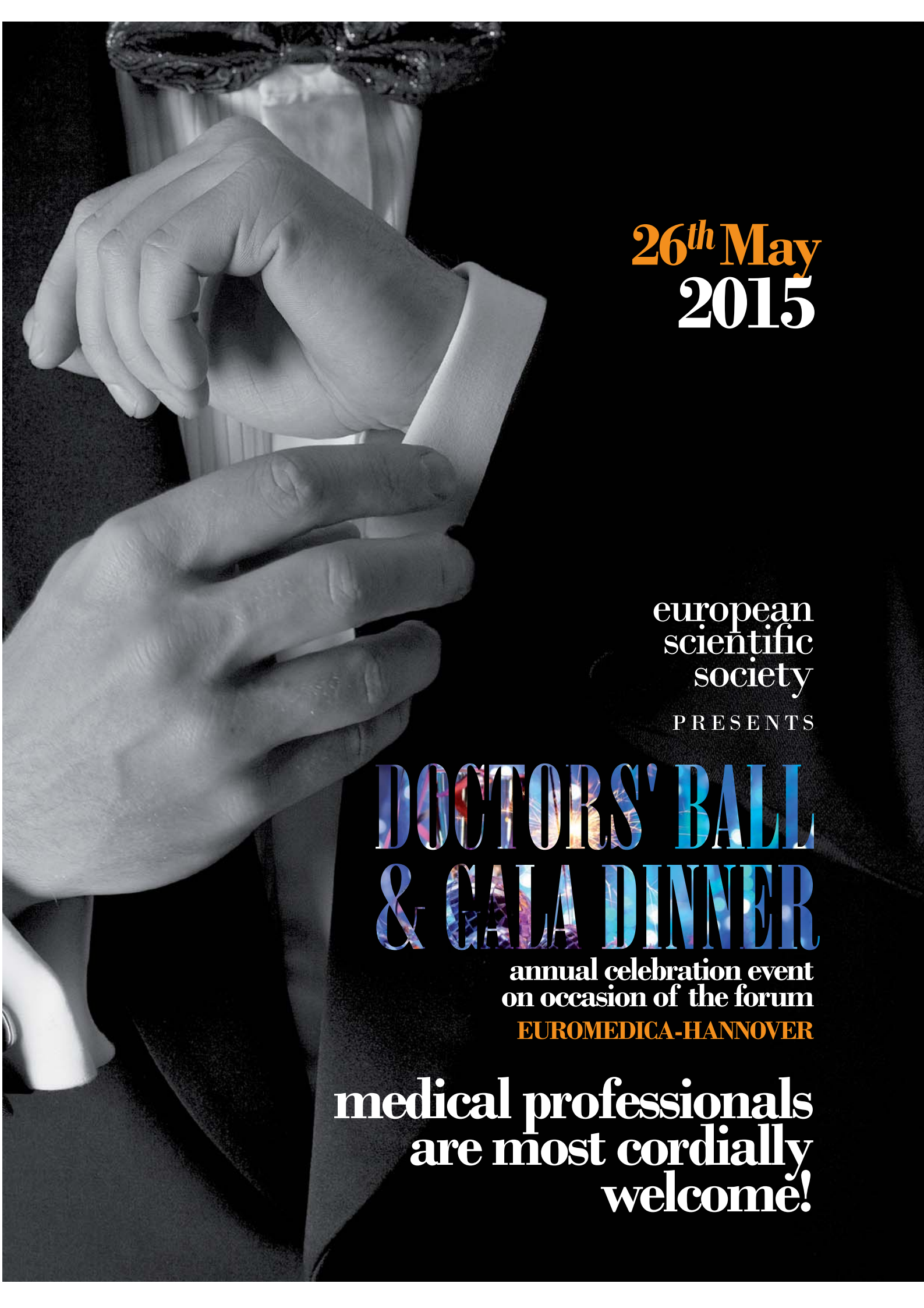
Aufnahme

Tel.: +49 5162 44-605

Fax.: +49 5162 44-400

www.klinik-fallingbostel.de
international@klinik-fallingbostel.de





**26th May
2015**

european
scientific
society

P R E S E N T S

DOCTORS' BALL & GALA DINNER

annual celebration event
on occasion of the forum

EUROMEDICA-HANNOVER

**medical professionals
are most cordially
welcome!**



www.congress-euromedica.de

May, 26–27

EUROMEDICA HANNOVER 2015

International Expo & Congress

The congress highlights up-to-date theoretical and practical aspects of the internal medicine, neurology, surgery and related fields that will bring together experts of the scientific research with clinical practitioners through a range of interactive sessions.

Venue:
Hanover
Congress Center,
Andor
Hotel Plaza

May, 26–27

Please contact:
Georg Tyminski, MD,
Olga Tyminski, MBA
Tel.: + 49 (0) 511 390 80 88,
Fax: + 49 (0) 511 390 64 54
info@eu-eco.eu, info@eanw.de